ADVANCES IN SHEET MOLDING COMPOUNDS FOR AUTOMOTIVE APPLICATIONS

A Dissertation
Presented to
The Academic Faculty

by

Ferdinand Baaij

In Partial Fulfillment
of the Requirements for the Degree
Master of Science in Mechanical Engineering
in the
George W. Woodruff School of Mechanical Engineering

Georgia Institute of Technology
August 2017

ADVANCES IN SHEET MOLDING COMPOUNDS FOR AUTOMOTIVE APPLICATIONS

Approved by:

Dr. Kyriaki Kalaitzidou
School of Mechanical Engineering
Georgia Institute of Technology

Dr. Oliver Sawodny
Institute for System Dynamics
University of Stuttgart

Dr. Robert Moon
School of Material Science and Engineering
Georgia Institute of Technology

Dr. Christina Tarín
Institute for System Dynamics
University of Stuttgart

Date Approved: August 01, 2017

ACKNOWLEDGEMENTS

First and foremost, I owe sincere gratitude to my advisor, Dr. Kyriaki Kalaitzidou, for her great mentorship, guidance and support during my time at Georgia Tech. I would also like to thank Dr. Christina Tarín, Dr. Robert Moon and Dr. Oliver Sawodny for their assistance as members of my thesis committee. I owe special thanks to Dr. Oliver Sawodny and Dr. Paul Neitzel for their efforts in creating this special program between the University of Stuttgart and the Georgia Institute of Technology and their valuable advices before and throughout my participation in this program. I thank Dr. Jonathan Colton for providing me full access to his laboratories and equipment which were essential for the success of this research. I would like to thank Tae Joong Jeong for performing the contact angle measurements for me. My colleague Dr. Amir Asadi deserves special recognition for his assistance and consultations during the whole research project. He was working with me on this project and helped a lot with assisting in the manufacturing and mechanical testing and with performing the fracture surface analysis. Finally, I would like to thank my family and friends for their tireless support during my whole course of study.

TABLE OF CONTENTS

ACKNOWLEDGEMENTS **iv**

LIST OF TABLES **vii**

LIST OF FIGURES **viii**

LIST OF SYMBOLS AND ABBREVIATIONS **x**

SUMMARY **xi**

CHAPTER 1. Introduction **1**
1.1 Light-weighting in the automotive industry **1**
1.1.1 Importance of light-weighting 1
1.1.2 General techniques for light-weighting 4
1.1.3 Material substitution in automobiles 5
1.2 Polymer matrix composites (PMC) in automotive industry **6**
1.2.1 Fiber and matrix types used in automotive composites 7
1.2.2 Thermoplastic matrix composites 9
1.2.3 Thermoset matrix composites 10
1.3 Sheet Molding Compound (SMC) Technology **13**
1.3.1 General SMC process 13
1.3.2 Resins used in SMC composites 14
1.3.3 Reinforcements used in SMC composites 15
1.3.4 Applications of SMC composites 17
1.4 Goal and Objectives **18**

CHAPTER 2. Materials and Methods **21**
2.1 Materials **21**
2.1.1 Epoxy 21
2.1.2 Reinforcements 21
2.1.3 Cellulose nano-crystals 23
2.2 Fabrication techniques **24**
2.2.1 Resin preparation 24
2.2.2 Sheet molding compounding process 26
2.2.3 Compression molding process 28
2.2.4 Testing coupon preparation 30
2.3 Characterization techniques **32**
2.3.1 Single-fiber fragmentation test (SFF) 32
2.3.2 Microscopy 35
2.3.3 Differential scanning calorimetry (DSC) 35
2.3.4 Specific density, fiber fraction and void content 35
2.3.5 Dynamic mechanical analysis (DMA) 37
2.3.6 Mechanical testing 37
2.3.7 Contact angle measurement 38

CHAPTER 3. Feasibility study of using basalt fibers as an alternative to glass fibers in sheet molding compounds (SMC) 40
3.1 Interfacial shear strength (IFSS) 40
3.2 Curing behavior 43
3.3 Density and void content 45
3.4 Thermomechanical properties 46
3.5 Mechanical properties 47
3.5.1 Tensile and flexural properties 47
3.5.2 Impact properties 52
3.6 Fracture surface morphology 53
3.7 Conclusions 55

CHAPTER 4. Light-weighting of high fiber content Composites by Addition of Cellulose Nano-Crystals 57
4.1 Methodology 57
4.2 Contact angle 60
4.3 Density and void content 61
4.4 Mechanical properties 63
4.4.1 Determination of the maximum fiber content 63
4.4.2 Light-weighting study 66
4.5 Fracture surface morphology 74
4.6 Conclusions 78

CHAPTER 5. Conclusions and future work 79

APPENDIX A Calibration of the SMC line 82

APPENDIX B Process integration of CNC fiber coating in the sheet molding compounds production line 98

APPENDIX C Publications Based on this Research Work 106

REFERENCES 107

LIST OF TABLES

Table 1.1: Fiber types used in PMCs for automotive applications according to [3]. 8
Table 2.1: Properties of basalt and glass fiber single filaments. 22
Table 2.2: Properties of cellulose nanocrystals according to [33]. 23
Table 3.1: Curing characteristics for 25BF/epoxy and 25GF/epoxy. 44
Table 3.2: Experimental and theoretical density and void content of 25BF/epoxy and 25GF/epoxy composites. 45
Table 3.3: Theoretical and experimental tensile moduli for 25BF/epoxy and 25GF/epoxy SMC composites. 48
Table 4.1: Density and modulus for different CNC-epoxy mixtures [53]. 58
Table 4.2: Fiber and CNC concentrations of the manufactured SMC composites. 59
Table 4.3: Moduli and densities of the manufactured SMC composites for light-weighting. 60
Table 4.4: Contact angle results for BF and GF rovings with neat epoxy and CNC-epoxy. 60
Table 4.5: Theoretical and experimental densities and void contents of the manufactured SMC composites. 62
Table 4.6: ANOVA test results for mechanical performance between specific properties of 60GF/epoxy and *n*GF/*m*CNC-epoxy SMC composites. 70

LIST OF FIGURES

Figure 1.1: General manufacturing process of SMC composites. 14
Figure 1.2: Different SMC types depending on fiber length and orientation adapted from [22]. 17
Figure 2.1: Sheet molding compound (SMC) production line used in this work. 26
Figure 2.2: Schematic of the sheet molding compound (SMC) process..... 27
Figure 2.3: Temperature profile for the curing process of the low fiber content SMC. ... 29
Figure 2.4: Temperature profile for the curing process of the high fiber content SMC. .. 30
Figure 2.5: Labelling and distribution of testing specimens in a cut SMC plate (dog bones for tensile testing, big rectangles for flexural testing, small rectangles for impact testing). 31
Figure 2.6: Schematic presentation of the SFF process with increasing number of fiber cracks caused by increased strain in the matrix (left) and the corresponding stress in the fiber (right) with zero stress points coinciding with the positions of the fiber cracks [46]. 33
Figure 3.1: SEM images of individual basalt and glass fiber filaments (scale bar is 60 microns in both images). 41
Figure 3.2: Polarized microscopy image of post-tested SFF sample with a single BF and three fracture events. 42
Figure 3.3: SFF test results (Average fragment length and IFFS) for BF and GF with epoxy. 42
Figure 3.4: Curing curves for 25BF/epoxy and 25GF/epoxy SMC composites. 43
Figure 3.5: Thermomechanical properties of 25BF/epoxy and 25GF/epoxy composites and neat epoxy. 47
Figure 3.6: Tensile and flexural properties of 25BF/epoxy and 25GF/epoxy SMC composites..... 50
Figure 3.7: Specific tensile and flexural moduli and strength values of 25BF/epoxy and 25GF/epoxy SMC composites. 51
Figure 3.8: Impact energy of 25BF/epoxy SMC composites compared to 25GF/epoxy composites..... 52
Figure 3.9: Cavity traces and pulled out fibers on the fracture surface of 25BF/epoxy (a),(c) and 25GF/epoxy (b),(d) SMC composites 54
Figure 3.10: Fiber breakage and matrix cracking in (a) 25BF/epoxy and (b) 25GF/epoxy SMC composites 55
Figure 4.1: (a) Tensile, (b) flexural and (c) impact properties of GF/epoxy and BF/epoxy SMC composites made for the determination of the maximum fiber content. 64
Figure 4.2: Specific (a) tensile, (b) flexural and (c) impact properties of GF/epoxy and BF/epoxy SMC composites made for the determination of the maximum fiber content. 65
Figure 4.3: (a) Tensile, (b) flexural and (c) impact properties of GF/CNC-epoxy and BF/CNC-epoxy SMC composites in the light-weighting study. 67
Figure 4.4: Specific (a) tensile, (b) flexural and (c) impact properties of GF/CNC-epoxy and BF/CNC-epoxy SMC composites in the light-weighting study. 68

Figure 4.5: Composite selection plot for GF and BF SMC composites with and without CNC. 74
Figure 4.6: SEM images for tensile fracture surface of (a)-(b) 60GF/epoxy, (c)-(d) 60GF/0.6CNC-epoxy, and (e)-(f) 48GF/0.9CNC-epoxy SMC composites. 75
Figure 4.7: SEM images for tensile fracture surface of (a)-(b) 60BF/epoxy, (c)-(d) 60BF/0.6CNC-epoxy, and (e)-(f) 48BF/0.9CNC-epoxy SMC composites. 77

LIST OF SYMBOLS AND ABBREVIATIONS

AHSS	Advanced high-strength steel
ASTM	American Society for Testing and Materials
BF	Basalt fiber
CAFE	Corporate Average Fuel Economy
CMC	Ceramic matrix composites
CNC	Cellulose nanocrystals
DMA	Dynamic mechanical analysis
DSC	Differential scanning calorimetry
GF	Glass fiber
GMT	Glass mat thermoplastics
HSS	High-strength steel
IFSS	Interfacial shear strength
ISO	International Organization for Standardization
LFT	Long fiber thermoplastics
MMC	Metal matrix composite
PMC	Polymer matrix composite
SEM	Scanning electron microscope
SFF	Single fiber fragmentation
SFT	Short fiber thermoplastics
SMC	Sheet molding compound
TEX	Unit of measure for the linear mass density of fibers, rovings, etc. It is defined as the mass in grams per 1000 meters.

SUMMARY

This master thesis addresses new approaches in the manufacturing of lightweight composites for the automotive industry. Governmental regulatory and customer requirements force car manufacturers to reduce the weight of new car models on an ongoing basis. Therefore, the goal of this thesis was to find new techniques to create lightweight sheet molding compound (SMC) composites for automotive applications. Two general approaches were chosen: 1) Investigating basalt fibers as an alternative reinforcement to the commonly used glass fibers and 2) light-weighting of SMC composites by replacing a portion of the heavy reinforcing fibers with a small amount of cellulose nano-crystals (CNC). An SMC production line similar to the ones used in industry was used to make the various SMC sheets. The composites were then made by compression molding of the SMC and were characterized using various characterization techniques, e.g. single fiber fragmentation test, differential scanning calorimetry, thermo-/mechanical testing and microscopy. In the first part of the study, it was found that SMC composites made with basalt fibers show overall similar properties to those made with glass fiber reinforced composites. The advantage of basalt fibers is that they are an ecofriendly and lower cost alternative to glass fibers. The second part of the study showed that adding small amounts of CNC can enhance the mechanical properties of glass fiber reinforced SMC composites significantly, allowing to reduce the fiber content leading thus to a weight reduction of 11%.

CHAPTER 1. INTRODUCTION

This introductory chapter conveys the theoretical background of this study. First, the role and different techniques of light-weighting in the automotive industry are described. The second section focuses on polymer composites in automotive applications. In the third section, the sheet molding compound technology as major composite manufacturing technology for composites used in the automotive industry and as the basic technology used in this research is described in detail. Based on the theoretical background, the goals and objectives of this study are described in the last section of this chapter.

1.1 Light-weighting in the automotive industry

The first section highlights the importance of light-weighting for automotive applications. Additionally, different techniques to reduce the weight of automobiles are outlined focusing on material substitution.

1.1.1 Importance of light-weighting

A clear trend towards weight reduction in the automotive vehicles was seen in the recent years. The key drivers for this development are diverse and guarantee that this trend will constantly continue throughout the next generations of cars [1]. Governmental regulations as well as societal pressures related to the vehicles' fuel efficiency and emission controls as well as customers' preferences about their vehicles' performances, force car manufacturers to continuously find new ways to reduce the weight of their new models.

Fuel economy standards were implemented in many regions around the globe and have shown high effectiveness in reducing the oil demand and greenhouse gas emissions of automotive vehicles [2]. In the USA, the Corporate Average Fuel Economy (CAFE) program forces car manufactures to keep the average sales-weighted fuel efficiency of their new car models above a certain level. Starting with an initial fuel efficiency of 18 mpg in 1978, the CAFE standard was increased to 28.5 mpg for 2012 and is further increased to 54.5 mpg in 2025 [3, 4]. Governmental standards in other regions, i.e. Japan or the European Union, tend to be even more stringent than the ones in the USA [2]. Reducing a car's weight, reduces its rolling resistance and the energy needed to accelerate it and keep it at a certain speed [5]. Therefore, light-weighting is one of the major techniques to enable car manufacturers to adhere to the stringent fuel economy regulations.

In addition to governmental regulations, societal pressure forces car manufacturers towards the design and manufacturing of lightweight vehicles. Especially residents in cities complain about high greenhouse gas emissions to a large extent caused by cars and demand drastic improvements. A vehicle weight reduction of 100 kg saves up to 12.5 g of CO2 emissions every kilometer [3]. In other words, every kilogram in car weight reduction can save 20 kg greenhouse gas emissions throughout the lifetime of a car [6]. Furthermore, volatile and gradually increasing gas prices lead to a higher demand for lightweight cars with higher fuel efficiency [7]. Also, customers frequently require better performance when buying a new car. Reducing the weight of the car can realize both customer requirements mentioned above. Lightweight cars require less energy to fulfil certain performance requirements. Therefore, either the performance (acceleration, top speed) and/or the fuel

economy can be increased. Previous studies revealed that in average a 5 % to 8 % better fuel efficiency can be achieved by reducing the vehicle weight by 10 % [8, 9].

Apart from combustion vehicles, the emerging market of electric and hybrid vehicles grew additional attention on vehicle light-weighting [8]. One major challenge in the development of electric vehicles is to increase their range. By reducing the vehicles weight, the required energy is reduced, making the batteries last longer. Furthermore, the weight of the heavy batteries has to be compensated through weight reduction in other parts of the car.

Light-weighting of automobiles shows a couple of additional benefits. As mentioned above, the reduced weight of the car requires less power for accelerating and less force for breaking. As a consequence, engines, transmissions and break systems can be dimensioned smaller leading to so called secondary weight savings. For every kilogram saved with primary weight savings additional 0.23 – 1.5 kg can be saved through secondary weight savings [10]. Furthermore, the weight reduction of selected parts allows to balance the weight distribution between front and rear axles and to lower the car's center of gravity, which both lead to a better handling of the car. In the recent BMW M6 model, the steel roof panel was replaced by a 5.5 kg lighter carbon fiber epoxy composite, lowering the car's center of gravity and thus increasing its stability [3]. Possible drawbacks going along with the weight reduction are downturns in safety and ride comfort which, however, can be prevented by an appropriate design and material selection [11]. Different approaches to reduce the weight of a vehicle are pointed out in the next subsection.

1.1.2 General techniques for light-weighting

There are two general approaches to reduce the weight of new car models. The first option is downsizing and the second option is reducing component weights part-by-part. Downsizing while providing great potential for significant weight reductions is not a universal option since the customer base will still require large cars [3]. Reducing the weight of components, however, can be applied on large and small cars in the same way. To reduce the weight of vehicle components car manufacturers can either optimize the component designs or substitute heavy materials through new materials with higher strength-to-weight ratios [5].

Design optimizations can be diverse, i.e. a maximized engine efficiency allows to reduce the size and/or the number of propulsion components and a structurally efficient body design requires less and/or thinner and thus lighter parts [8]. Through parts consolidation less weight adding connections as screws or welding seams are needed anymore, which reduces the weight of body and chassis components. With a share of 60% of a vehicle's total weight, the body and chassis components provide the greatest potential for light-weighting [3].

Especially the body and chassis components were traditionally made out of conventional steel. In the future, these steel parts will be substituted by new materials with either higher strength and/or lower density than steel to reduce the weight of the components. The modern lightweight vehicle therefore consists of a mix of different materials as high strength steels, aluminum, magnesium and titanium alloys as well as fiber reinforced

composites [3]. The lightweight materials considered in automotive applications are described in the next subsection.

1.1.3 Material substitution in automobiles

Due to its low cost, high modulus, great formability and weldability as well as its recyclability steel is the predominating material in automotive vehicles [3]. Furthermore, new alloys and processing technologies lead to the development of so called high-strength steels (HSS) and advanced high-strength steels (AHSS) with increased mechanical properties providing a wide range of different steel types which can be chosen according to the formability and strength requirements of different car components. HSS and AHHS are mainly used for structural parts and panels. In addition to weight reduction, HSS and AHHS significantly improve the crashworthiness of car bodies [12].

Other lightweight metals are alloys from aluminum, magnesium and titanium. Cast aluminum parts substitute more and more cast iron components, stamped aluminum replaces stamped steel components, magnesium alloys are considered for powertrain applications and titanium alloys are used in spring coils or engine and exhaust system parts [5]. It is expected, that the weight of sheet metals for automotive applications can be reduced by 35 - 50% by using aluminum and even up to 60% by using magnesium [13]. The significant weight reduction is enabled by considerably lower densities of titanium (4.43 g/cm^3), aluminum (2.7 g/cm^3) and magnesium (1.74 g/cm^3) compared to that of steel (7.87 g/cm^3). Major downsides of these alloys with respect to steel are the increased cost for the materials themselves as well as the cost for new processes and new required equipment [13].

Composites constitute additional lightweight materials suitable for material substitution. For the near future, it is expected that today's average 900 kg of steel and other metals can be lowered to 600 kg per car through substitution by composites and hybrid solutions [7]. Composites are materials made of different materials that combine the positive effects of each constituent material. Generally, composites consist of a matrix material which is reinforced by incorporation of fibers. At the top-most-level, composites can be categorized in metal matrix composites (MMC), ceramic matrix composites (CMC) and polymer matrix composites (PMC). MMC used in automobiles usually consist of short fibers or ceramic particles as silicon carbide (SiC) or aluminum oxide (Al_2O_3) mixed into one of the low-density titanium, aluminum or magnesium alloys mentioned before [3]. MMC have a high strength-to-weight ratio even at elevated temperatures. They show a high resistance against creep, fatigue and wear. Therefore, MMC are ideal lightweight substitution materials for cast iron or other materials in engine and brake parts as pistons, cylinder liners, connecting rods, valves and brake drums and rotors [14, 15]. As this thesis addresses advances in sheet molding compounds, a specific type of PMC, the next section focuses more detailed on PMC for automotive applications.

1.2 Polymer matrix composites (PMC) in automotive industry

This section first describes different reinforcements and matrix materials used in automotive composites. Then, different manufacturing techniques for thermoplastic and thermoset matrix composites are outlined.

1.2.1 Fiber and matrix types used in automotive composites

The most popular fibers used as reinforcement in polymer matrix composites for automotive applications are glass, carbon and kevlar fibers [3]. Due to low costs, high strength, good insulation and chemical resistance, glass fibers (GF) represent the most commonly used fiber type. However, GF have multiple downsides with respect to carbon fibers (CF). Carbon fibers, mainly used in aerospace applications, show higher strength and modulus values and have lower densities compared to glass fibers. Therefore, composites using carbon fibers have significantly higher modulus-to-density and strength-to-density ratios and hence show a much greater weight saving potential in automotive applications than glass fiber reinforced composites. Impediments for the comprehensive use of carbon fibers in automotive industry is a lack of suitable high-volume manufacturing processes of carbon fiber composite parts and more important the high costs for carbon fibers [3]. However, carbon fiber prices recently decreased to a level which is sufficiently low enough for car manufactures to use it [16]. First carbon fiber reinforced composites were used in sports cars where competitive performance overweighs cost decisions. Recently, the application of carbon fiber composites became also popular in luxury models and electric cars.

In addition to the fiber types mentioned above, natural fibers i.e. jute, kenaf are used in automotive applications though limited to interior trim components due to their lower mechanical properties and hydrophilicity [3]. The different fiber types used in PMCs for automotive applications along with their densities and mechanical properties are listed in Table 1.1 according to [3].

Table 1.1: Fiber types used in PMCs for automotive applications according to [3].

Fiber type	Density (g/cm^3)	Tensile Modulus (GPa)	Tensile Strength (MPa)	Elongation (%)
Glass fibers	2.49-2.54	72.5-85.6	3445-4585	4.88-5.7
Carbon fibers	1.76-2.20	230-930	1520-3600	0.25-2.5
Aramid (Kevlar)	1.45	131	3620	2.8
Natural fibers (Hemp, flax, kenaf, coir, sisal, jute)	1.25-1.48	6-80	220-1500	1.2-25

PMC in automotive applications do not only differ in fiber types but also in the method fibers are incorporated in the polymer matrix and in the polymer type used as matrix material. The fibers in PMC can be continuous or discontinuous and their orientation within the matrix can be either random, unidirectional, bidirectional or a combination of them [11]. Also, single fiber filaments are very fragile due to their tiny diameters (less than 20 µm) which is why they are bundled in form of rovings or tows, a form that also allows for better handling.

The load between the fibers is transferred by the matrix which also keeps the fibers in place. The matrix fulfils multiple other functions in a composite for example it provides the compressive and shear strength, fracture resistance and energy absorption capability of the composite [3]. Furthermore, the matrix protects the reinforcements from environmental influences such as chemicals, moisture or mechanical degradation. Depending on the matrix material, PMC are subdivided in thermoplastic matrix composites and thermoset matrix composites. Both general PMC types and corresponding manufacturing techniques are outlined in the following two subsections.

1.2.2 Thermoplastic matrix composites

Thermoplastic matrix composites for automotive applications usually use thermoplastic polymers such as polypropylene (PP), polyamide (PA), polybutylene terephthalate (PBT) and acrylonitrile butadiene styrene (ABS) as matrix combined with randomly oriented discontinuous glass fibers as reinforcements. Thermoplastic composites distinguish from thermoset ones through higher ductility and impact resistance as well as a significantly lower processing time since no time-consuming polymerization and crosslinking reactions are taken place. Further advantages of thermoplastic composites are their high damage resistance, weldability and recyclability. Major disadvantage of thermoplastic composites is the high viscosity of the polymer impeding sufficient impregnation of fiber bundles, especially in case of continuous fibers.

Thermoplastics and hence thermoplastic composites become soft or even melt upon heating. This allows different processing possibilities such as thermoforming, blow molding, injection molding and even welding. In many cases, these processes can be carried out repeatedly, allowing easy recycling of old parts into new ones [3].

Injection molding is the major manufacturing method used for thermoplastic matrix composites in automotive applications as it enables to manufacture complex parts with a high dimensional accuracy and class A surface finish at high production rates. The injection molding process for thermoplastic composites does not differ from the process for neat thermoplastic parts. However, the pellets fed into the injection molding machine already contain fibers.

In the case of short fiber thermoplastics (SFT), chopped fibers with a length less than 1 mm are impregnated with the thermoplastic polymer in a compounding extruder and chopped into pallets which are subsequently used in conventional injection molding machines to manufacture semi-structural and functional car components as water pump housings or electrical switches [3].

Long fiber thermoplastics (LFT) contain longer fibers (up to 50 mm) leading to higher tensile modulus and strength and higher impact strength compared to SFT. LFT car components as door modules, dashboard carriers, front end modules or bumper beams are manufactured using either injection molding, compression molding or injection-compression molding. Pellets for injection molding processes are made using pultrusion-compounding where continuous fibers are impregnated by pulling them through an extrusion process of liquid thermoplastic polymers [3]. Another technique for making LFT parts is compounding fiber and matrix in-line during the compression molding process.

Compression molding is also used to make glass mat thermoplastic (GMT) parts. GMT are sheets with glass fiber mats (randomly discontinuous or uni-/bi-directional continuous fiber mats) impregnated in thermoplastic polymers. Less complex shapes of GMT parts can also be made using thermostamping which requires less pressure, heat and processing time. Other types of thermoplastic matrix composites are glass fabric thermoplastics, laminated thermoplastic prepreg composites and self-reinforced thermoplastics.

1.2.3 Thermoset matrix composites

In thermoset matrix composites, polyester, vinyl ester and epoxy are the commonly used polymers. Polyester and vinyl ester have shorter curing cycles and cost advantages with

respect to epoxy. Epoxy, however, has better mechanical properties and thus is suitable for more advanced applications. A major advantage of thermoset resins is the lower viscosity compared to thermoplastics allowing easier fiber wetting. Thus, thermosets are the prevailed matrix for long and continuous fiber composites which provide higher strengths and moduli appropriate for structural components. Other advantages of thermoset composites are a higher heat and chemical resistance and lower creep deformation. Downsides of thermoset matrix composites compared to thermoplastic matrix composites are the long curing cycles (up to several hours) and the fact that melting and hence direct reuse of the material is not possible. Different manufacturing techniques for incorporation of the fibers into the thermoset resin and the polymerization and curing of the resin are described below.

In the resin transfer molding (RTM) process, liquid resin is injected into a closed mold cavity in which dry fiber layers of prefroms are placed in advance. Applied pressure ensures that the resin fills the whole mold including the spaces between the fibers, thus all fibers get impregnated and air is pushed out through vents. Subsequently, the resin is cured at ambient or elevated temperature depending on the resin system before the final part is demolded. RTM allows manufacturing of parts with complex shapes and geometries. The tooling costs are relatively low making it a suitable process for the production of low- and mid-volume components (5000-50000 parts per year) [3]. Instead of injecting the resin into the dry fiber preform in the mold cavity, vacuum can be used to pull the resin into the cavity as applied in the vacuum assisted resin transfer molding (VARTM) or SCRIMP method.

In structural reaction injection molding (SRIM) method also a liquid resin is injected into a mold cavity which contains a dry fiber preform. However, the injection is performed at much higher speeds. The resin consists of two highly reactive components (based on polyurethane or polyuria) which are mixed immediately before the injection because of the very short curing time. The processing time of SRIM (around 1 min.) is much shorter than the one of RTM (around 5 min). SRIM parts however have lower moduli and hardness than RIM parts. SRIM is used to manufacture large parts as a pick-up truck cargo box [3].

In the filament winding process continuous fiber rovings are pulled through a thermoset resin bath and then wrapped around a shaping kernel, called mandrel, until the desired part thickness is achieved. Then, the part is cured in an oven. Afterwards, the mandrel can either be removed to create a hollow part or kept inside for different purposes such as sealing for gas tanks. Filament winding is used for the manufacturing of drive shafts, leaf springs and tanks [3].

The last and most common manufacturing method for thermoset matrix composites for automotive applications is compression molding, because it can produce complex parts with excellent surface finish highly automated in a short time. Pre-impregnated fibers, usually in form of sheet molding compound (SMC) sheets, are placed in a mold cavity. Then, external pressure (2 to 25 MPa) is applied to distribute the uncured fiber-resin compound in the cavity, to completely wet the fibers, to consolidate multiple sheet layers and to push out trapped air. Removing air from the compound is very important as voids are the most critical defect in the final composite parts. Thus, usually vacuum is applied during the compression molding process [11]. After the mold is closed, external heat is applied to start and complete the curing of the thermoset resin. Finally, the part is removed

from the mold. As described before, starting materials for the compression molding process are usually SMC sheets. Advances in the manufacturing of these SMC sheets are the topic of this thesis. Therefore, the next section describes the SMC technology in detail.

1.3 Sheet Molding Compound (SMC) Technology

This section first describes the general procedure to manufacture SMC parts. Then, different matrix materials and reinforcements used for SMC are described. Finally, different applications of SMC are outlined.

1.3.1 General SMC process

Sheet-molding compound (SMC) technology is a technique to incorporate reinforcing fibers into a polymer matrix. In general, SMC are thin sheets consisting of fibers and thermoset resin which are subsequently cut and cured in a compression molding process to create composite parts [17, 18]. The general SMC process starts with metering and mixing of the resin ingredients, followed by the introduction and wetting of reinforcing fibers before the compound material is rolled up as a continuous sheet. This sheet matures under certain temperature and humidity conditions until it achieves an ideal viscosity for the further processing, e.g. cutting and compression molding. In the compression molding process, single or multiple SMC sheets are shaped and cured through application of heat and pressure in a mold. A general overview of the SMC manufacturing procedure is shown in Figure 1.1. A more detailed description of the SMC process as it was used in this study is given in section 2.2.2.

Figure 1.1: General manufacturing process of SMC composites.

1.3.2 Resins used in SMC composites

Usually, thermoset resins are used as matrix material for SMC composites due to their low initial viscosity compared to thermoplastics. This ensures a better fiber impregnation and easier removal of trapped air during the compaction stage before the curing reaction starts. Polyester and vinyl esters are the most commonly used resins for SMC composites in automotive industry because of their lower curing times and costs compared to epoxy resins [3]. However, epoxy resins are suitable matrix materials for advanced applications due to their moisture resistance and higher mechanical properties [15], which is why epoxy resins are commonly used for composites in aerospace industries. Besides these three resin systems, resins made from soybean oil have been tested as a sustainable resin alternative in SMC composites [19].

Additional materials can be added to the resin mixture to enhance either the performance and/or the processibility of the material [18]. Low profile additives are added to reduce shrinkage during the cross-linking process. Another way to reduce polymerization shrinkage is adding filler materials into the resin. Fillers also support a more homogenous fiber distribution and reduce the cost of the composite. Catalysts or initiators are added to start the polymerization reaction at high temperatures. As a counterpart, inhibitors are added to avoid the starting of the curing process before it is desired, i.e. during the mixing of the resin. Thickening agents increase the viscosity of the uncured resin. Consequently,

the whole compound has a higher viscosity, which enables easier handling of the uncured SMC sheets before they are used in the subsequent compression molding process. The tradeoff for the easy handling is that the higher viscosity restrains the impregnation of the fibers. Therefore, some thickening agents reverse their thickening effect under the influence of heat in the compression molding process, reducing the viscosity and thus enabling a good fiber wet-out during compression molding [11]. Furthermore, mold release agents are added to reduce the friction between a cured composite part and the mold cavity for easy demolding. They can be either mixed into the resin or directly sprayed onto the mold surface.

1.3.3 Reinforcements used in SMC composites

Due to the higher modulus and strength of the fibers compared to the matrix, the fibers' major role is to carry the load in the composite. Fiber type, fiber content, fiber length and fiber distribution directly impact tensile and compressive strength and modulus of a composite as well as its thermal and electrical conductivity, its density and its cost [11].

The most common fiber type used in SMC manufacturing are glass fibers. In general, however, all of the fibers for automotive applications mentioned in section 1.2.1 can be used in SMC composites. Carbon fibers or natural fibers for instance were used in SMC composites to achieve different properties as increased modulus and strength or fire retardancy [20, 21].

The fiber content of SMC composites usually varies between 25-60 wt%. At higher fiber concentrations, it is difficult to ensure complete fiber wetting. The determination of the fiber ratio depends on performance, processability and cost requirements. In general,

increasing the fiber content increases the modulus and the strength of the composite. However, the higher densities and costs of the fibers compared to the resins lead to a heavier and costlier composite. In addition, higher fiber contents can limit the processibility of the SMC materials. In automotive applications, higher fiber contents are preferred in structural parts as radiator supports which carry higher loads. For semi- and non-structural parts as grille opening panels lower fiber contents are sufficient [3].

There are different ways to introduce the fibers in the thermoset matrix of SMC composites. Variations in fiber length and orientation lead to basically four different types of SMC composites which are displayed in Figure 1.2. The most common SMC composites are SMC-R sheets in which the fibers are usually chopped to a length of 25.4 mm (1 in) and randomly distributed between the two resin layers in the SMC machine. Different lengths of chopped fibers (0.5 in, 2 in, etc.) are possible. In general, the composite strength and modulus increase with an increased fiber length [20]. The randomly oriented chopped fibers lead to isotropic properties in all directions of the composites' plane sheet. In contrast to that, SMC-C composites use continuous and unidirectional oriented fibers to provide higher modulus and strength in one direction of the composite. In SMC-CR composites, randomly dispersed chopped fibers are combined with continuous unidirectional fibers. That way, the final composite part has reinforcements in all directions but especially increased strength or stiffness in a single direction as it is required in structural applications as cross members [3]. A fourth SMC type are XMC composites. They also contain continuous fibers, but instead of being unidirectional oriented in this case the fibers are arranged in an X-pattern with an angle of 5° to 7°. They can contain additional chopped randomly oriented fibers.

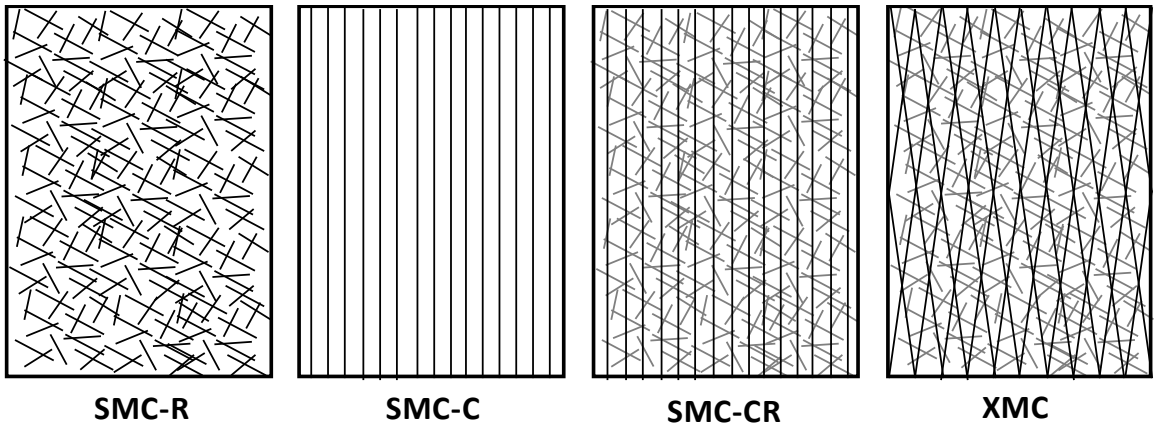

Figure 1.2: Different SMC types depending on fiber length and orientation adapted from [22].

When the fibers are incorporated and final SMC sheets are matured and cut in preparation for the compression molding process, multiple possibilities for placing the SMC sheets in the mold cavity exist. One can place just a single sheet of one of the SMC types just described in the mold. Usually, however, multiple layers of SMC sheets are stacked on top of each other either to increase the thickness of the final composite part or to orient multiple unidirectional sheets (i.e. SMC-C or SMC-CR) in different directions to get a more isotropic composite.

1.3.4 Applications of SMC composites

The SMC and compression molding manufacturing processes can be highly automated. Therefore, the SMC technique is faster and less labor-intensive compared to other composite manufacturing processes, i.e. hand lay-up technique. Hence, SMC composites are mainly used for medium and large products with high production volumes [18]. The high production rate and good automation capacity, the ability to manufacture large parts and the fact that complex shapes with class A surface finish can be created by the

compression molding at significantly lower tooling costs compared to similar sized steel parts make the SMC process a major technology in the manufacturing of thermoset composites for automotive applications [20]. Automotive parts made using SMC and compression molding technique are hoods, deck lids, fenders, radiator supports, bumper beams, roof frames, door frames, engine valve covers, timing chain covers, oil pans, exterior and interior body panels, seats, trunk covers, lift gates, cargo boxes, radiator supports, cross members [3].

In addition to automotive applications, SMC materials are used in truck and aerospace industries, agricultural, rail and marine systems as well as electrical and industrial products and many other fields [22-24]. The industries in which SMC technology is applied, especially the automotive sector, require continuous innovations in SMC technology to reduce costs, improve the quality and further decrease the weight of the SMC parts. Therefore, research has to address this needs and develop lighter, stronger, cheaper and ecofriendly SMC composites [7]. How this thesis contributes to these needs is described in the next section.

1.4 Goal and Objectives

As described above, car manufacturers require ongoing progress in the manufacturing of lightweight materials to further reduce the weight of their new models to meet governmental fuel efficiency regulations and customer requirements. SMC manufacturing is the most common technology in the manufacturing of lightweight composites in the automotive industry and thus advances in SMC technology have great potential to deliver a major contribution towards the light-weighting of automobiles. Therefore, the goal of

this thesis is to create lightweight SMC composites for automotive applications. To accomplish this goal two approaches are chosen.

The first objective is to determine whether basalt fibers can serve as an alternative for the commonly used glass fibers in SMC production to reduce the weight of the composites by comparing the properties of SMC composites made with basalt fibers to SMC composites made with glass fibers.

The second objective is applying nanotechnology, specifically addition cellulose nano-crystals in the SMC matrix to increase the properties of the SMC composites. Increased properties allow to either reduce the material thickness of composite parts or to reduce the fiber content in the composites, both leading to the desired weight reduction.

The structure of the thesis is the following:

CHAPTER 2 outlines the different materials, manufacturing processes and characterization techniques used in this study.

CHAPTER 3 addresses the feasibility study of using basalt fibers as an alternative for glass fibers in SMC manufacturing.

CHAPTER 4 describes the results of the lightweight approach using nanotechnology.

Fehler! Verweisquelle konnte nicht gefunden werden. concludes the results of both o bjectives and provides an overview of future work in this field of study.

APPENDIX A provides a comprehensive guideline for the calibration and proper set up of the SMC production line used in this study.

APPENDIX B describes a second approach of using nanotechnology to lightweight SMC composites by integrating a fiber coating process in the SMC production line.

CHAPTER 2. MATERIALS AND METHODS

2.1 Materials

2.1.1 Epoxy

The resin used in the SMC process was a bi-component thick epoxy resin system supplied by US Composites (West Palm Beach, FL). The main components were the 150 thick epoxy (diglycidyl ether of Bisphenol-A epoxy) and the 556 slow polyamide hardener which were mixed in a 2:1 ratio. Additionally, fumed silica (Aerosil-Cabosil supplied by US composites) was added as thickening agent. The density of the resin was 1.15 g/cm^3.

2.1.2 Reinforcements

Glass fibers (GF) are currently the predominant reinforcement used in SMC composites for automotive applications [25]. However, research has recently focused on the use of natural fibers (extracted from plants) or fibers from mineral origin due to more stringent environmental requirements [26]. Basalt fibers, extruded from molten volcanic basalt rock, are produced in a very energy efficient and much simpler process than that of competing fiber types, e.g. glass fiber and carbon fiber (CF) [27]. Due to advantages in the manufacturing technology, neither precursor nor additives are required in the production process of BF, leading to a reduction in cost and environmental impact [28]. Therefore, the cost for industrial production of BF is not only lower compared to the corresponding cost of CF, but also at the same level or even lower than the cost for GF manufacturing [29]. Furthermore, BF have good chemical resistance [30, 31]. Also, composites with BF reinforcements show a high temperature resistance and fire-redundant properties, which is

an additional advantage BF can bring in automotive applications [27, 32]. In addition, the mechanical properties of BF are similar or higher compared to those of GF as shown in the comparison of the fibers used in this study provided in Table 2.1.

Table 2.1: Properties of basalt and glass fiber single filaments.

	Basalt fibers	Glass fibers
Density (g/cm^3)	2.75*	2.54*
Filament diameter (μm)	10±1	10±1
Elastic modulus (GPa)	87*	75*
Tensile strength (MPa)	4500±400	4100±300

*Data provided by suppliers

Because BF have better mechanical properties and at least equal costs compared to GF, BF were investigated as a potential lightweight alternative to GF in SMC composites. Multi-end roving basalt fibers BARA4800 were provided by Mafic Ireland (Kells, County Meath, Ireland) and multi-end roving glass fibers ME1510 were received from Owens Corning (Oak Brook, IL, US). For both fiber types the linear mass density of the rovings was 4800 tex. They were used in the SMC line as received and chopped to an average length of 25±0.5 mm.

2.1.3 Cellulose nano-crystals

Cellulose nano-crystals (CNC) are rod-like or whisker shaped particles (0.05-0.5µm x 3-5 nm x 3-5 nm) extracted from the crystalline regions of cellulose micro-fibrils, a parallel stacking of multiple cellulose chains [33]. Trees, plants, tunicate, algae and bacteria are the sources from which the cellulose can be extracted. Based on the different cellulose sources, extraction methods and modifications of the surface chemistry, a large variety of cellulose nanomaterials with different properties evolved and is currently developing [34]. CNC is one type of cellulose nanomaterials and its mechanical properties as reviewed in [33] are shown in Table 2.2.

Table 2.2: Properties of cellulose nanocrystals according to [33].

Density (g/cm^3)	1.6
Tensile strength (GPa)	7.5 – 7.7
Elastic modulus in axial direction (GPa)	110 – 220
Elastic modulus in transverse direction (GPa)	10 – 50

Introducing CNC in the polymer matrix of composites to enhance their mechanical properties is one of the most promising applications of CNC [35], and for the same reason it was used in this study. Previous studies showed that the introduction of nanomaterials in polymer resins can improve the mechanical properties of the resin and consequently of the composites [36-39]. Therefore, car manufacturers like Ford [7] and Volkswagen see great light-weighting potential in this nanotechnology as the enhancement of the matrix'

properties allows to either reduce the material thickness of the composite parts or to reduce the fiber content in the composite parts, both leading to a weight reduction. As described above, CNC is one type of nanomaterials which can be used for this purpose. It has been successfully applied to enhance the properties of fiberglass SMC composites in a lab scale method [40]. In this study, it was investigated whether the positive effect of CNC in the epoxy matrix can be also seen in high fiber content SMC composites manufactured on an industrial SMC production line (see CHAPTER 4).

Not only introducing CNC to the matrix can enhance the composites' mechanical properties, but also the coating of the reinforcing fibers with CNC showed significant improvements in the mechanical properties of SMC composites [41]. Therefore, it was investigated whether the CNC coating process of fibers can be integrated in the SMC production line process (see APPENDIX B).

In this study, Cellulose nanocrystals (CNC) sourced from the USDA Forest Products Laboratory (FPL) (Madison, WI, USA) were used in the form of freeze-dried powder. The CNC have a length of 138 ± 22 nm and a width of 6.4 ± 0.6 nm [42].

2.2 Fabrication techniques

2.2.1 Resin preparation

The SMC resin was prepared in a two-step process. First, the thickening agent was mixed in the epoxy resin. Second, the hardener was added to the thickening agent-epoxy-solution and mixed until a homogeneous solution was achieved. The epoxy-hardener weight ratio was 2:1. The thickening agent made up 4 wt% of the total SMC resin mixture. Depending

on how many SMC plates had to be manufactured, either two batches of 780 g resin (500 g epoxy, 250 g hardener, 30 g thickening agent) or two batches of 520 g resin (333 g epoxy, 167 g hardener, 20 g thickening agent) were prepared. A paint-mixer with a diameter of 2 in connected to a cordless electric screwdriver was used to stir mix the resin until the resulted solution looked homogeneous. Mixing the thickening agent in the epoxy took about 10 minutes for each batch. Adding the hardener and mixing it to the final SMC resin took another 5 minutes for each batch. The cordless screwdriver was run in low speed mode to avoid too high internal friction leading to heat generation and early curing in the resin.

For the second part of this study, CNC was added to the resin. In these cases, the procedure for the resin preparation was slightly different. Before the hardener was mixed with the thickening agent-epoxy-solution, the CNC was dispersed in the hardener. Therefore, 14.8 g or 21.2 g of CNC were mixed into 333.3 g of hardener little by little to achieve a share of 1.4 wt% or 2 wt% respectively in the total resin mixture. While adding the CNC to the hardener, the mixer was stirred continuously to avoid the formation of big agglomerates. Afterwards, the CNC-hardener dispersion was sonicated (UIP500hd Heilscher ultrasonic processor, 34 mm probe diameter, amplitude of 70) for 5 minutes to break down existing agglomerates. An ice water bath was used to keep the solution below 40 °C during sonication and to cool it down to room temperature afterwards. Finally, the CNC-hardener-suspension was then added to the thickening agent-epoxy-solution in the same way as described above for the procedure without the use of CNC.

2.2.2 Sheet molding compounding process

The SMC materials were manufactured on a Finn and Fram SMC line which is similar to heavy duty industrial machines. The main difference is the smaller width of the produced materials (0.3 m vs. 0.9-1.5 m in industry). However, the processing-structure-properties of the manufactured composites are the same compared to those produced on the wider industrial machines. Therefore, the results and the knowledge gained in this study can be reliably transferred to industrial applications. The SMC line is displayed in Figure 2.1.

Figure 2.1: Sheet molding compound (SMC) production line used in this work.

SMC materials with different fiber types (GF and BF), different fiber concentrations (from 25% up to 70%) and different resin mixtures (with and without CNC) were manufactured.

Therefore, the SMC set-up parameters differed between the different production runs. A SMC set-up template to easily calculate the set-up parameters for each run has been designed. Additionally, a detailed description of how to set up the SMC line is given in **Fehler! Verweisquelle konnte nicht gefunden werden.** The following section, however, focuses on the SMC run itself as it was used in this study. The different set-up parameters for each manufactured material are given along with the corresponding results in 0 and 0 respectively.

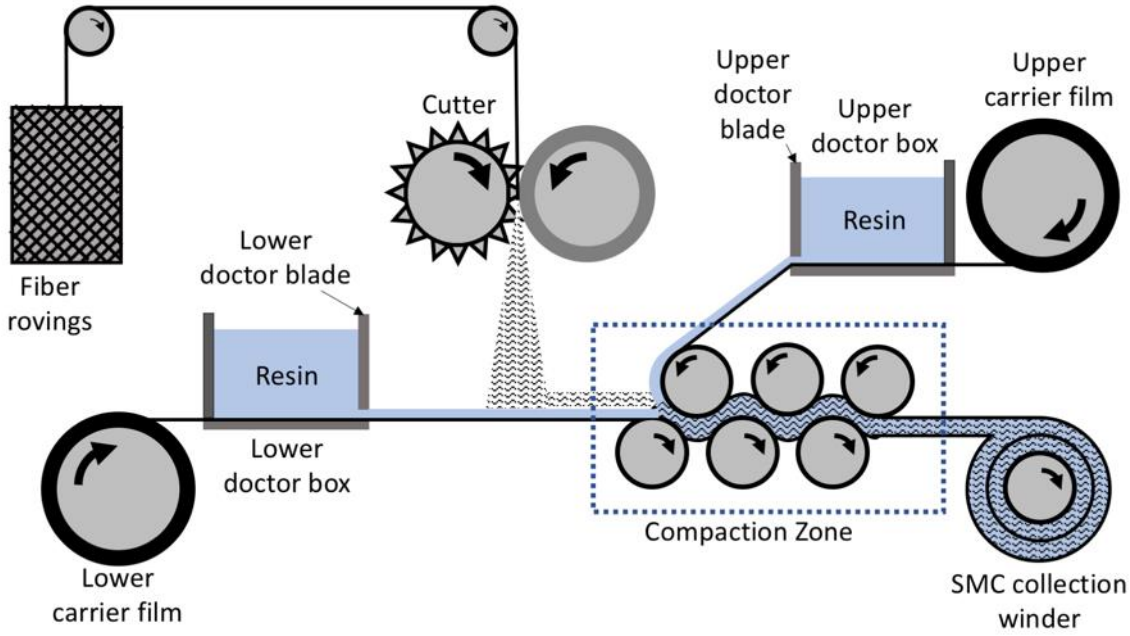

Figure 2.2: Schematic of the sheet molding compound (SMC) process.

A schematic of the process is displayed in Figure 2.2. The SMC line pulled either 4 or 6 rovings of GF or BF through a rotating set of cutters and chopped them to 25.4 mm long bundles which were subsequently dropped randomly on the lower resin layer. The resin layer was constantly carried forward by a polyethylene carrier film on a conveyor belt. A second resin layer (upper) covered the chopped fibers and the resin/fiber/resin sandwich

compound entered the compaction zone. In the compaction zone, consisting of a set of rollers, trapped air was removed and the resin was pressed in-between the fibers to achieve good impregnation. When all the resin in the doctor boxes was depleted, the cutter was stopped manually. The conveyor belt continued running until all the material passed the compaction zone. Finally, the material was collected as a continuous sheet on a winder.

The amount of resin was controlled by the height of the doctor blades, the width of the side blades of the resin reservoirs (defining the cross section of the resin film) and the speed of the conveyor belt. The amount of the chopped fibers was controlled by the number of rovings and the rotational speed of the cutter. To achieve the desired fiber contents these parameters were combined and adjusted accordingly.

Each SMC run lasted around 10 min. The final SMC materials were ~1.8-3 m long, 254 mm wide and ~2-8 mm thick. Before continuing with the compression molding process, the SMC materials were conditioned at room temperature. Compounds with lower fiber content (higher resin fraction) needed 1.5 h to allow the compound viscosity to reach a state where it was sufficiently high enough to remove the carrier films without destroying the material. However, too long preconditioning time made molding more difficult and prevented good fiber wetting especially for compounds with high fiber content, which is why a much shorter conditioning time was applied in these cases.

2.2.3 Compression molding process

The continuous SMC materials were cut into plates and subsequently stacked on top of each other, before they were put into a mold. For the lower fiber contents, a two-layer and a three-layer plate with the dimensions of 292x254x5.5 (and 3.5) mm^3 were made for each

batch. Producing plates of two different thicknesses allowed to analyze the effect of the thickness on the materials' mechanical properties. Aluminum plate tools were used as open molds. The two- and three-layer compounds were put between the aluminum plates and hot-pressed for 3 h at 124 kPa using a Carver 4122 manual heated press. First, they were cured at 100 °C for 1 h before the temperature was increased to 120 °C for another 2 h for post-curing. Since the plates were relatively thin, it was not expected that the closing speed of the mold affects the resin flow pattern significantly [11] and therefore would not relevantly impact the properties of the manufactured composites. However, the maximum closing speed of the hot-press (7 mm/s) was applied to minimize any potential effects. Figure 2.3 displays the temperature profile of the above-mentioned curing process.

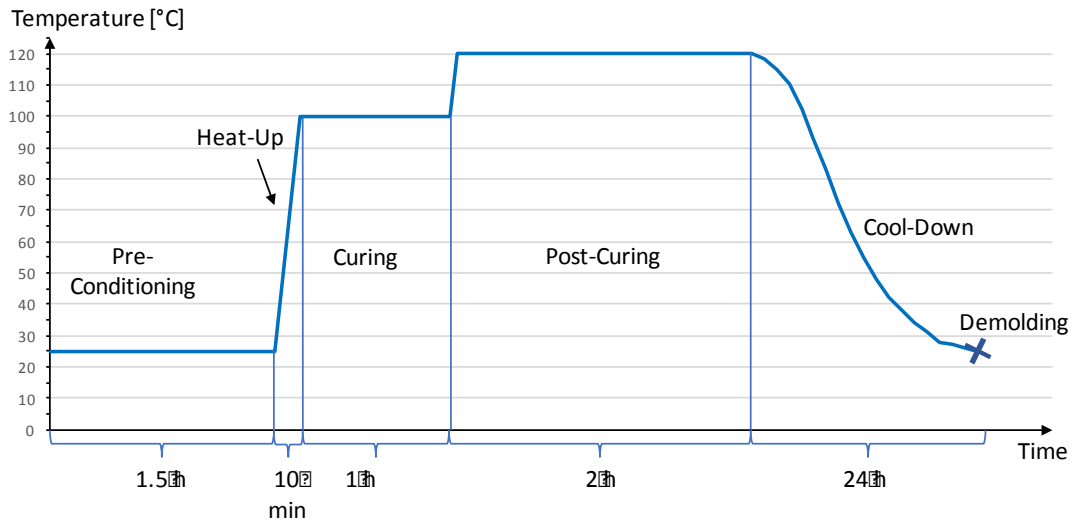

Figure 2.3: Temperature profile for the curing process of the low fiber content SMC.

For the higher fiber concentrations, no extra pre-conditioning time at ambient temperature was applied since the compound viscosity was high enough immediately after the SMC run. Also, the compression molding process was modified to decrease the void content

and to improve the surface finish of the compounds. A closed aluminum mold with a length of 419 mm length, a width of 279 mm and a cavity depth of 0-10 mm was used instead of the simple aluminum tool plates. This allowed using higher pressures up to 430 kPa without squeezing-out all the resin. In addition, vacuum was applied during the curing at 100°C for 1 h. Post-curing was operated at 120 °C for 2 h. Then, the mold including the material was cooled down to 35 °C for demolding. Spacers were used in each run to close the mold always up to a constant material thickness of 5.7 mm. The modified curing process was carried out using a hydraulic hot-press (Model V50-1818-2TMX, Wabash Metal Products Inc.). Figure 2.1 displays the modified curing cycle for the SMC composites with higher fiber content.

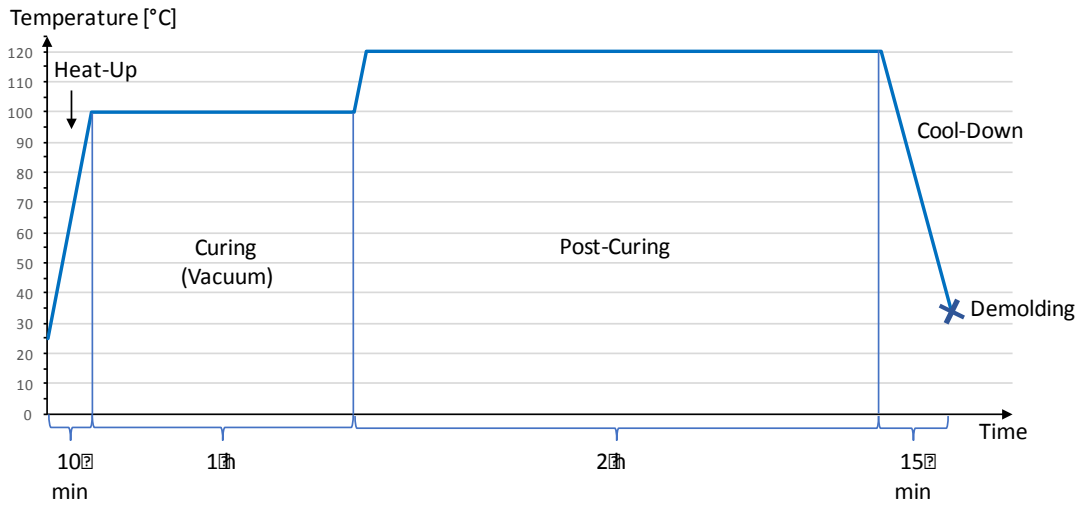

Figure 2.4: Temperature profile for the curing process of the high fiber content SMC.

2.2.4 Testing coupon preparation

Prior to the cutting of the testing coupons, the SMC composite plates were stored at ambient temperature for at least 48 h to avoid any potential plastic deformation caused by the cutting

or handling of the plates. The cutting of the testing specimens was carried out using a waterjet (MAXIEM 1515). The different testing coupon types (tensile, flexural and impact) were evenly distributed across the SMC plates to get realistic average results of the whole plate and not just of certain regions of the plate. After the cutting, the testing coupons were quickly dried using air pressure and subsequently remained at ambient temperature for at least 48 h to completely dry. Additionally, every testing coupon of each plate was labelled and captured in a picture, so that the position of every specimen within the plates could be traced back. This allowed to investigate potential property variation across the SMC plates. Figure 2.5 shows an exemplary SMC plate with the labelling of the testing coupons and their even distribution throughout the plate.

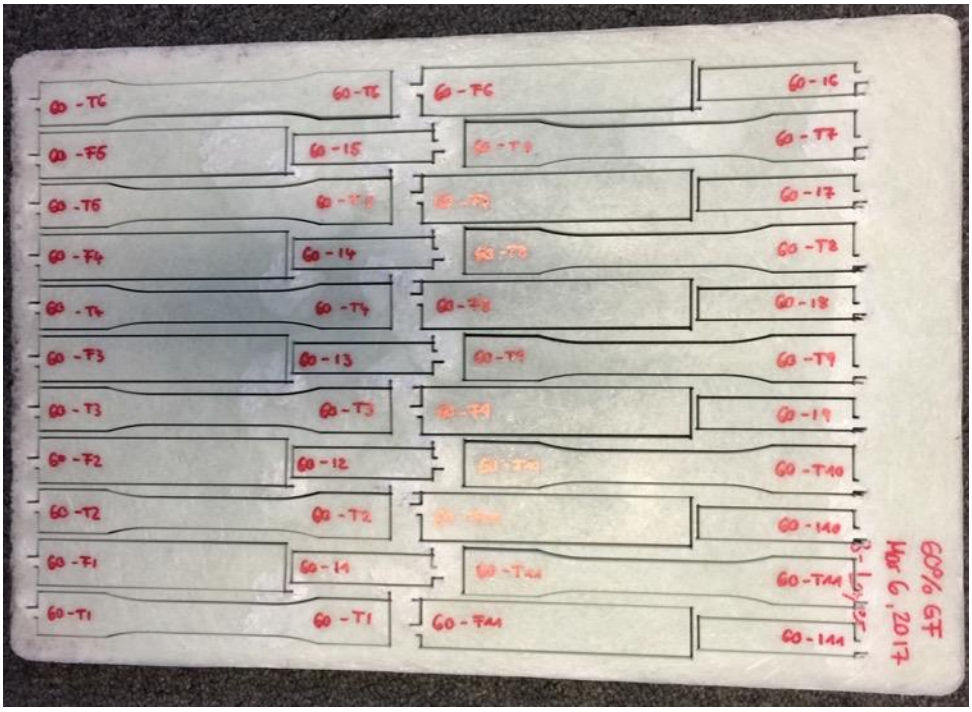

Figure 2.5: Labelling and distribution of testing specimens in a cut SMC plate (dog bones for tensile testing, big rectangles for flexural testing, small rectangles for impact testing).

2.3 Characterization techniques

2.3.1 Single-fiber fragmentation test (SFF)

The efficiency of the stress transfer between fiber and matrix was evaluated through quantification of the interfacial shear strength (IFSS) for both fiber types, i.e. GF and BF. Therefore, single fiber fragmentation (SFF) tests were carried out following the procedure of Hunston et al. [43].

In the SFF test, dogbone specimens containing a single fiber filament in the center of the polymer matrix are elongated in tensile tests. When the matrix is elongated sufficiently, the shear forces will break the fiber into fragments [44]. At the fiber`s break points, the axial stress drops to zero. The shear forces in the matrix, however, transfer further load into the fragments leading to linearly increasing tensile stress from the fragments' ends to a stress plateau in long fragments [45]. Higher axial strain of the testing coupons leads to higher shear forces which further break down the fragments. However, at some point a critical length is reached, which does not transfer enough stress for further breaking down the fragments. Based on this critical fragment length, the IFSS can be calculated as described later in this section. The process described above is visualized in Figure 2.6.

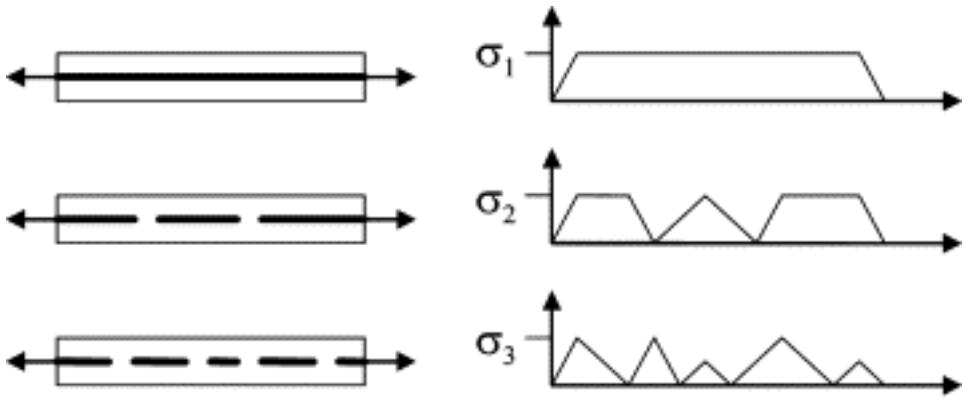

Figure 2.6: Schematic presentation of the SFF process with increasing number of fiber cracks caused by increased strain in the matrix (left) and the corresponding stress in the fiber (right) with zero stress points coinciding with the positions of the fiber cracks [46].

The preparation of the SFF test specimens started with the separation of individual GF (BF) filaments form the multifilament rovings. Individual fibers with a length of ~120 mm were gently pulled off from the respective rovings and placed in the center of a dogbone shaped rubber mold. The mold dimensions were as described in the above mentioned test protocol [43], i.e. a gauge length of 25 mm long, width of 3 mm and a depth of 2 mm, with an overall length and width of 80 and 10 mm respectively. To keep the single filaments under tension during pouring and curing of the epoxy, the ends of the filaments were pre-strained and taped down using high temperature tape.

Next, the resin was prepared similar to the protocol described in chapter 2.2.1. For the sake of transparency, which was required to measure the fiber fragments under the optical microscope, no fumed silica was added to the resin. Also, thin epoxy was used instead of thick epoxy for clear and sharp visibility. The curing cycle was 1 h at 100 °C followed by 2 h at 120 °C as used in the fabrication of actual SMCs, but without any pressure.

The tensile tests of the SFF samples were performed on an Instron 33R 4466 equipped with a 500 N load cell at a displacement rate of 1 mm/min. It was expected that saturation in the filament fragmentation already set in, when the epoxy had reached its strain to failure since the filaments were pre-strained. Therefore, the tests were stopped after the load passed its peak and dropped to 95% of its maximum. This ensured that no further fiber fragmentation could occur. At the same time, breakage of the test specimens was prevented which would restrict the recording of the fragment lengths.

The tested samples were subsequently inspected under a Leica DM2500 polarized light optical microscope to measure the fragment lengths of the single fibers in the center of the testing samples. Finally, the IFSS was determined using the Kelley and Tyson model [47] given in Eq. (1),

$$\tau_i = \frac{d_f \sigma_f(l_c)}{2l_c} = \frac{3d_f \sigma_f(l_c)}{8\bar{l}} \quad (1)$$

where τ_i is the IFSS, d_f is the fiber diameter, $\bar{l}$ is the average length of fiber fragmentation segments, l_c is the fiber critical fragmentation length (l_c=4$\bar{l}$/3) and $\sigma_f(l_c)$ is the fiber strength at the critical length. Aside from the fiber fragment lengths also the fiber diameters were measured using the polarized microscopy. A minimum of seven samples was analyzed for each fiber type. The fiber strengths of the GF and BF respectively were determined by tensile testing (ASTM D3822) with a displacement rate of 1 mm/min using the same Instron. To grab the single filaments with the grips of the Instron, they were affixed onto paper tabs with a gage length of 25.4 mm. The single glass and basalt fiber strength values are the average of at least seven measurements.

2.3.2 Microscopy

In addition to the optical microscope used for the fragment measurements in the SFF tests, a Phenom G2 Pro (Phenom-World BV) scanning electron microscope (SEM) at an acceleration of 5 kV was used to examine the fracture surface of the tested SMC composites. The aim of the fracture surface examination was to identify the various failure modes of the manufactured composites. To minimize the charging effect a gold coating was applied on the surface of the testing samples using a plasma sputter (Ted Pella Inc.).

2.3.3 Differential scanning calorimetry (DSC)

DSC tests were performed on a modulated DSC Q2000 (TA Instruments) to determine the effect of the different fiber types, i.e. BF and GF, on the curing behavior of the corresponding composites. 5 mg samples of epoxy with 25 wt% fiber content were heated at a rate of 10 °C/min from 25 °C to 160 °C. For both fiber types a minimum of 4 samples was tested. DSC tests were also performed with samples from the manufactured SMC composites to confirm that the curing process was completed.

2.3.4 Specific density, fiber fraction and void content

Water displacement method was used to determine the specific density of the manufactured SMC composites according to ASTM D-792. For each manufactured SMC composite type, at least 10 samples were tested to measure the density.

To quantify the volumetric void content of the SMC composites the following equation according to ASTM D2734-16 was used in the first part of the study,

$$V_{void} = 100 \times \frac{\left(\rho_{theoretical} - \rho_{\exp}\right)}{\rho_{theoretical}} \quad (2)$$

where ρ_{exp} is the measured density using ASTM D-792 and $\rho_{theoretical}$ is the theoretical density calculated by the rule of mixtures, as given in Eq. (3).

$$\rho_{theoretical} = \frac{1}{\left(w_f/\rho_f\right) + \left(w_m/\rho_m\right)} \quad (3)$$

where w_f and w_m are mass fraction, and ρ_f and ρ_m are density of the fiber and resin matrix respectively. For the first part of this study, the values for w_f and w_m were taken as they were defined by the set-up values of the parameters in the SMC production line assuming a high accuracy of the manufacturing process. Also, the squeeze-out of resin during the molding process which is increasing the fiber fraction w_f in relation to the matrix fraction w_m was neglected at that time.

For the second part of the study in which the maximum fiber content was examined and light-weighting was pursued, it was crucial to determine the exact fiber fractions and void contents of the composites made in the different SMC runs. Therefore, acid digestion method according to ASTM D3171 was used to measure the fiber fractions and calculate the exact void contents instead of estimating them based on the pre-set values of the SMC parameters. To dissolve the epoxy matrix, the samples were put into nitric acid (70%) for 24 h at 80 °C. Subsequently, the remained fibers were washed with distilled water, dried at 50˚C for 6 h and weighed to measure the fiber mass fraction. Finally, the void contents of the composites were calculated using the following equation

$$V_{void} = 100 \times \frac{\left(\rho_{exp,wd} - \rho_{\mathrm{exp,ad}}\right)}{\rho_{exp,wd}} \quad (4)$$

where $\rho_{exp,wd}$ and $\rho_{exp,ad}$ are the measured densities from water displacement and acid digestion method respectively. $\rho_{exp,ad}$ is determined by substituting the measured fiber mass fraction and the known densities of the fiber and matrix in Eq. (3). Each void data is a representative of at least six samples.

2.3.5 Dynamic mechanical analysis (DMA)

Dynamic mechanical thermal analyses were carried out in three-point bending mode to determine the storage and rubbery moduli as well as the glass transition temperature. The tests were performed in a temperature range from 25 °C to 160 °C at a heating rate of 5 °C/min and 1 Hz using a DMA Q800 (TA Instruments). A load of 0.01 N was pre-set and a maximum strain of 0.05% was applied. The support span was 50 mm and the testing samples were 12.7 mm wide and ~5 mm thick. For each fiber type, a minimum of five specimens was tested.

2.3.6 Mechanical testing

Tensile, flexural and impact tests were carried out to obtain a holistic characterization of the mechanical properties of the manufactured composites. The tensile properties were measured on an Instron 5982 equipped with a 100 kN load cell according to ASTM D638. The dogbone samples had a gauge length of 57 mm, a width of 13.1 mm and different thicknesses reaching from 3 mm to 6 mm. The axial strain was measured by an Instron 2630-106 extensometer with a gauge length of 25 mm.

The flexural tests were carried out in three-point bending mode (ASTM D790-02) using an Instron 33R 4466 with a support span of 80 mm at a displacement rate of 2.15 mm/min. The test specimens had a width of 20 mm and different thicknesses reaching from 3 mm to 6 mm. For both test methods, i.e. tensile and flexural testing, the moduli were calculated between the strain values of 0.05% and 0.2%.

The impact strength was determined using the Charpy test method on an Instron SI series pendulum impact tester with a maximum impact head of 406.7 J (300 ft-lbf) according to ISO179 and a support span of 43 mm. The non-notched rectangular samples had a width of 12.7 mm and thickness of 3-6 mm. For each composite type at least 10 samples were tested in each of the three mechanical test methods, i.e. tensile, flexural and impact testing.

In addition, statistical analysis using one-way analysis of variance (ANOVA) with a level of significance of 5% (i.e. 95% level of confidence) was carried out to analyze the effect of CNC addition on the mechanical properties of the SMC composites in the second part of the study.

2.3.7 Contact angle measurement

Contact angle measurement was performed on a Ramé-Hart Goniometer following ASTM D7334-08 to determine the wettability between the fibers, e.g. BF and GF, and the epoxy resins, e.g. with and without CNC. As the measurement procedure requires a flat surface, glass slides with small water droplets on their surface were used to hold the fibers stacked flat. Eight fiber strains were stacked alongside each other to provide a wide enough surface for the measurement. A 250 µL Teflon tip from DuPont was used as deposition material. The epoxy droplets were precisely set as 4 µL and deposited onto the fibers using a Ramé-

Hart pressure controller. Finally, the images were captured with a high definition camera and the contact angles were analysed using DROPimageAdvanced software.

CHAPTER 3. FEASIBILITY STUDY OF USING BASALT FIBERS AS AN ALTERNATIVE TO GLASS FIBERS IN SHEET MOLDING COMPOUNDS (SMC)

This chapter addresses the first objective of the thesis: investigating the use of basalt fibers as an alternative to glass fibers in sheet molding compounds. Therefore, SMC composites with 25 wt% short chopped basalt fibers in an epoxy matrix (25BF/epoxy) were compared to the equivalent composites containing 25 wt% short chopped glass fibers (25BF/epoxy). First, basic differences in interfacial properties and curing behavior were investigated using lab-scale techniques. Then, composite plates were manufactured using SMC production line and compression molding to study the (thermo-)mechanical and rheological properties of both composite types. The results are presented in the following sections along with the assessment of the interfacial properties.

3.1 Interfacial shear strength (IFSS)

The analysis of the interfacial strength (IFSS) was conducted as initial study to determine the general suitability of using basalt fibers in epoxy matrix composites. Therefore, single fiber fragmentation (SFF) tests were carried out as described in section 2.3.1 for both fiber types. The single fiber filaments were extracted from the BF and GF rovings respectively and are displayed in Figure 3.1.

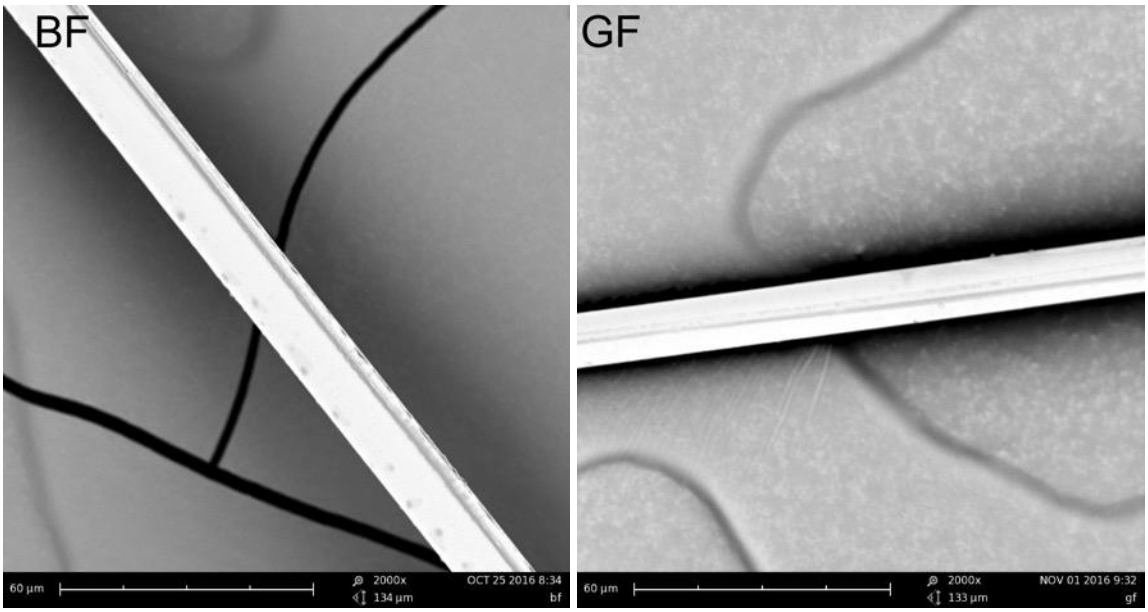

Figure 3.1: SEM images of individual basalt and glass fiber filaments (scale bar is 60 microns in both images).

The average strength values for these BF and GF filaments are 4.5±0.4 and 4.1±0.3 GPa respectively as determined using tensile testing. Subsequently, the Weibull moduli, derived from the strength data, are 4.79 and 4.13 for BF and GF respectively using the Weibull distribution [48]. Based on these values the BF and GF fiber strength was extrapolated to get the fiber strength at the critical fragment length ($\sigma_f(l_c)$).

The critical fiber lengths (taken as 4/3 of the average fiber fragment lengths) were derived from the average fiber fragment lengths which were measured using polarized microscopy. Figure 3.2 displays a post-tested SFF sample with three fracture events, black spots along the fiber, in the single BF filament. The distance between the fracture events represents the fiber fragment length. The resulting critical fiber length as well as the calculated IFSS are shown for both fiber types in Figure 3.3.

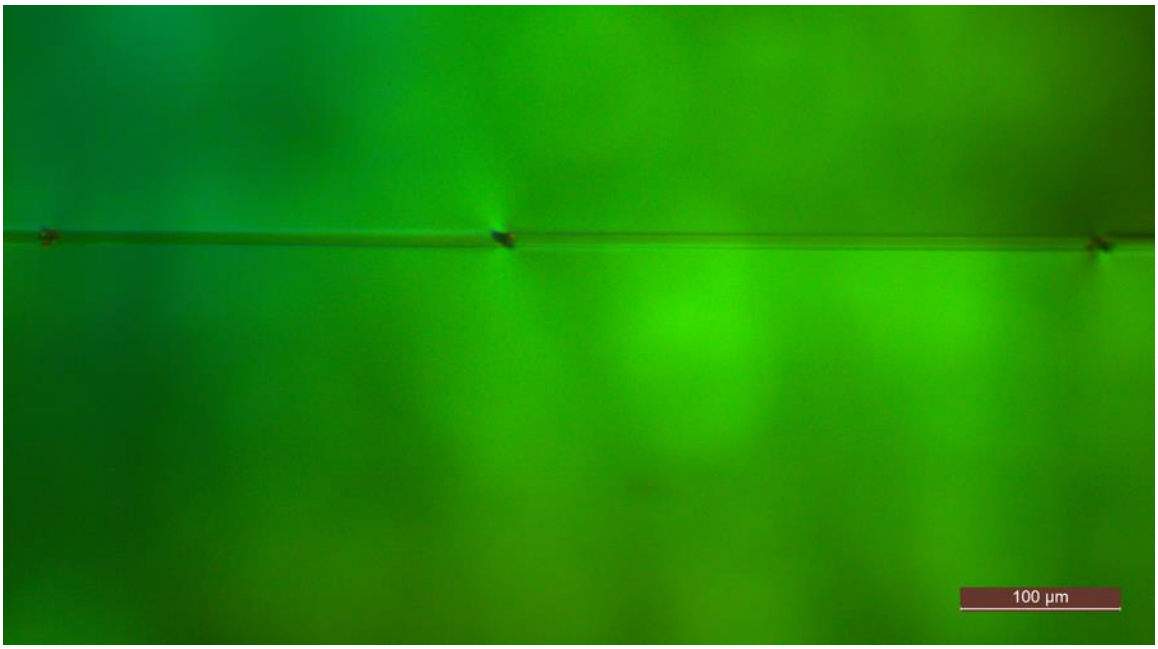

Figure 3.2: Polarized microscopy image of post-tested SFF sample with a single BF and three fracture events.

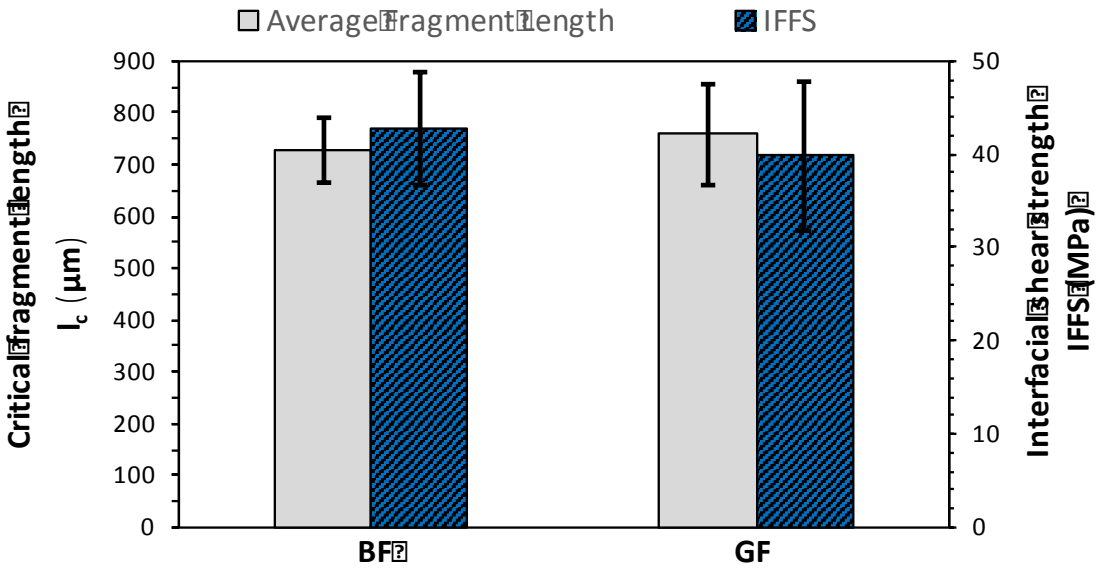

Figure 3.3: SFF test results (Average fragment length and IFFS) for BF and GF with epoxy.

The critical fragment lengths for the BF/epoxy samples (729.7±62.4 μm) were in the same statistical range with those of the GF/epoxy samples (758.0±98.9 μm). Similarly, the IFFS results for both fiber types are within the same range and any observed differences are not statistically significant i.e., the IFFS is 42.7±6.1 MPa and 39.8±8.1 MPa for BF/epoxy and GF/epoxy respectively. These results indicate similar interfacial properties between both fiber types and the epoxy matrix. Therefore, the study was continued towards making composite plates using the SMC production line and compression molding.

3.2 Curing behavior

To confirm that the proven curing cycle for GF/epoxy can be also applied to the BF/epoxy composites DSC tests were performed. The curing behavior is shown in Figure 3.4. The overall curves of the 25BF/epoxy samples were quite similar compared to the ones of the 25GF/epoxy samples.

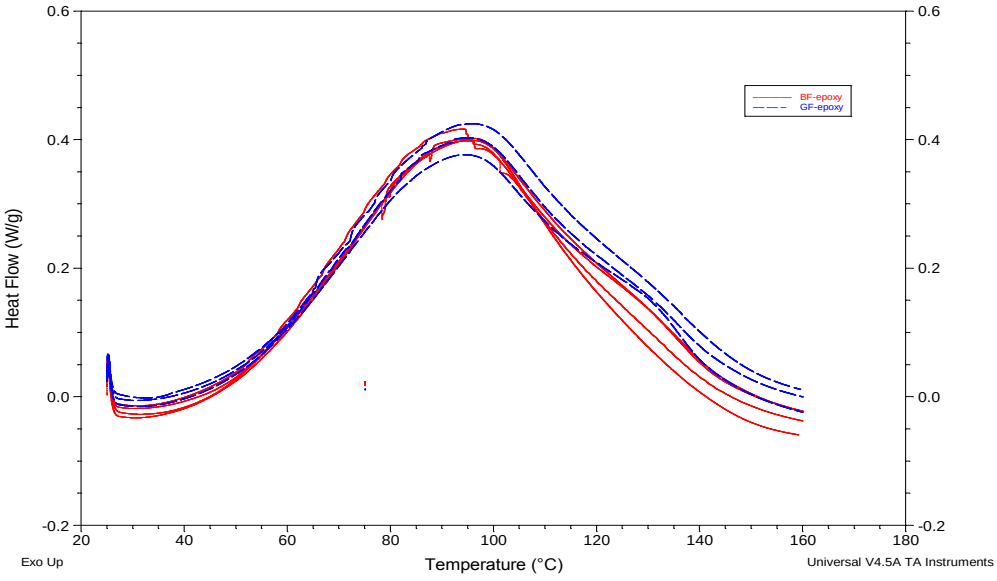

Figure 3.4: Curing curves for 25BF/epoxy and 25GF/epoxy SMC composites.

The curing temperature and time (determined at the exothermic peak) were not affected by the fiber type. Slight differences were, however, determined in the maximum heat flow and the heat of reaction. The maximum heat flow of 25BF/epoxy was a little bit higher compared to 25GF/epoxy. Also, the heat of reaction which is the area under the heat flow curve was slightly higher for the 25BF/epoxy with respect to 25GF/epoxy. Overall, the same degree of curing was determined for both composite types. The data recorded in the DSC test is presented in Table 3.1.

Table 3.1: Curing characteristics for 25BF/epoxy and 25GF/epoxy.

	25BF/epoxy	**25GF/epoxy**
Max. heat flow (W/g-sample)	0.41±0.01	0.39±0.03
Max. heat flow (W/g-epoxy)	0.81±0.03	0.77±0.06
Heat of reaction (ΔH, J/g-sample)	278.4±14.7	274.3±17.7
Heat of reaction (ΔH, J/g-epoxy)	556.7±29.4	548.6±35.4
Cure temperature (˚C)	94.4±0.3	94.4±1.4
Cure time (min)	14±0.1	14±0.3

As no significant differences in the curing behavior of GF/epoxy and BF/epoxy were observed, the same manufacturing process as specified in section 0 could be applied for both types of composites. Therefore, two batches (each with a two and a three SMC-sheet)

with 25 wt% fiber content were manufactured for each fiber type, i.e. BF and GF. The first curing cycle (for low fiber content) as described in chapter 2.2.3 was applied at this point.

Performing additional DSC tests on samples from the post-cured SMC composites showed no residual exothermic heat confirming that the cross-linking of the epoxy was completed during compression molding.

3.3 Density and void content

Table 3.2 shows the experimental density measured with the water displacement method, the theoretical density calculated with equation (3) (based on the fiber and resin density and a fiber fraction of 25 wt%) and the volumetric void content calculated with equation (2). The equations are listed in section 2.3.4 on page 35.

Table 3.2: Experimental and theoretical density and void content of 25BF/epoxy and 25GF/epoxy composites.

	25BF/epoxy	**25GF/epoxy**
ρ_{exp} (g/cm^3)	1.29±0.04	1.25±0.01
$\rho_{theoretical}$ (g/cm^3)	1.35	1.31
Void content (%)	5±1	5±1

As BF (2.75 g/cm^3) have a higher density compared to GF (2.55 g/cm^3), the theoretical density of the 25BF/epoxy composites (1.35 g/cm^3) is also higher than that of 25GF/epoxy (1.31 g/cm^3). The same trend holds for the average measured density with a 3% higher value for the composites containing 25 wt% BF (1.29±0.04 g/cm^3) with respect to the ones

with GF (1.25±0.01 g/cm^3). The differences between the experimental and theoretical density were caused by the void content of 5 vol% in both types of composites.

3.4 Thermomechanical properties

The thermomechanical properties of both composite types and the neat epoxy are shown in Figure 3.5 below. The use of BF and GF did not show a significant effect on the glass transition temperature of the neat epoxy. Differences were, however, noticed in the storage modulus at 25 °C (below T_g). The storage modulus of 25BF/epoxy SMC composites was 5.6±0.6 GPa and thereby 22 % higher than that of 25GF/epoxy SMC composites (4.6±0.6 GPa). When thermoset materials are heated up above glass transition temperature, their stiffness drops to a much lower value than the storage modulus which is known as rubbery modulus [49]. In this study, the rubbery modulus was measured at 115 °C. The 25BF/epoxy SMC composites showed a 15 % higher average rubbery modulus (199.8±28 MPa) compared to that of 25GF/epoxy SMC composites (173.5±59 MPa). However, taking into account the overlap of the standard deviations of the results it is concluded that this difference is not statistically significant. The average value of tan δ for 25BF/epoxy SMC composites (0.51±0.01) was slightly lower compared to that of 25GF/epoxy SMC composites (0.54±0.01). This indicated a lower energy dissipation of the 25BF/epoxy SMC composites which might also lead to a possible reduction in the impact strength.

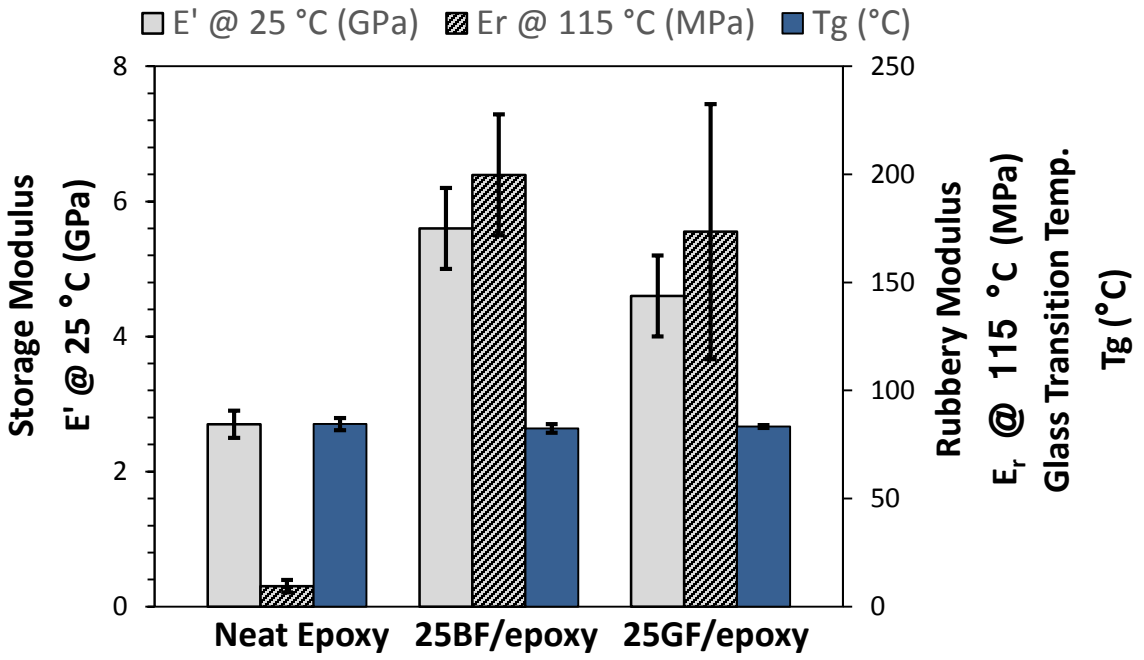

Figure 3.5: Thermomechanical properties of 25BF/epoxy and 25GF/epoxy composites and neat epoxy.

3.5 Mechanical properties

3.5.1 Tensile and flexural properties

The tensile and flexural properties of the 25BF/epoxy and 25GF/epoxy SMC composites are contrasted in Figure 3.6. A 13 % higher average tensile modulus and a 15 % higher average flexural modulus were recorded for the 25BF/epoxy SMC composites. Higher moduli were the consequence of the higher modulus of BF (87 GPa) compared to that of GF (75 GPa) and thus were expected. One needs to consider the higher density of the BF itself and consequently of the 25BF/epoxy SMC composite. Thus, the specific tensile and flexural moduli (moduli divided by measured density) of the 25BF/epoxy SMC composites

were determined and found to be 10% higher in average values than the ones of the 25GF/epoxy SMC composites.

Table 3.3: Theoretical and experimental tensile moduli for 25BF/epoxy and 25GF/epoxy SMC composites.

	25BF/epoxy	**25GF/epoxy**
$E_{c,theoretical}$ (GPa)	6.4	6.3
$E_{c,exp}$ (GPa)	7.0± 1.5	6.2± 0.9
$E_{specific,theoretical}$	4.7	4.7
$E_{specific,exp}$	5.5±1.1	4.9±0.7

Table 3.3 shows the experimental results for the elastic modulus for 25BF/epoxy and 25GF/epoxy SMC composites. Considering the statistical variations of the experimental results the measured Young's moduli were matching with their theoretical values for both composite types, whereas the experimental specific moduli were larger than the theoretical values in both cases. This is a consequence of the 5 vol% void content, which resulted in densities lower than the theoretical ones calculated using the rule of mixtures. The theoretical moduli were calculated using the micromechanical model developed for short fiber reinforced composites [50] as given in equation (5).

$$E_{Composite} = \frac{3}{8}E_{11} + \frac{5}{8}E_{22} \quad (5)$$

where,

$$E_{11} = E_m \frac{\left(1 + 2\frac{l_f}{d_f}\eta_L v_f\right)}{(1 - \eta_L v_f)} \tag{6}$$

$$E_{22} = E_m \frac{\left(1 + 2\eta_L v_f\right)}{(1 - \eta_L v_f)} \tag{7}$$

$$\eta_L = \frac{\left(\frac{E_f}{E_m} - 1\right)}{\left(\frac{E_f}{E_m} + 2\frac{l_f}{d_f}\right)} \tag{8}$$

$$\eta_T = \frac{\left(\frac{E_f}{E_m} - 1\right)}{\left(\frac{E_f}{E_m} + 2\right)} \tag{9}$$

where l_f is fiber length, d_f is fiber diameter, v_f is fiber volume fraction, and E_f and E_m are the fiber and matrix moduli. v_f is calculated using equation (10).

$$v_f = \frac{w_f/\rho_f}{\left(w_f/\rho_f\right) + \left(w_m/\rho_m\right)} \tag{10}$$

with the mass fractions w_f and w_m and densities ρ_f and ρ_m of the fiber and matrix respectively.

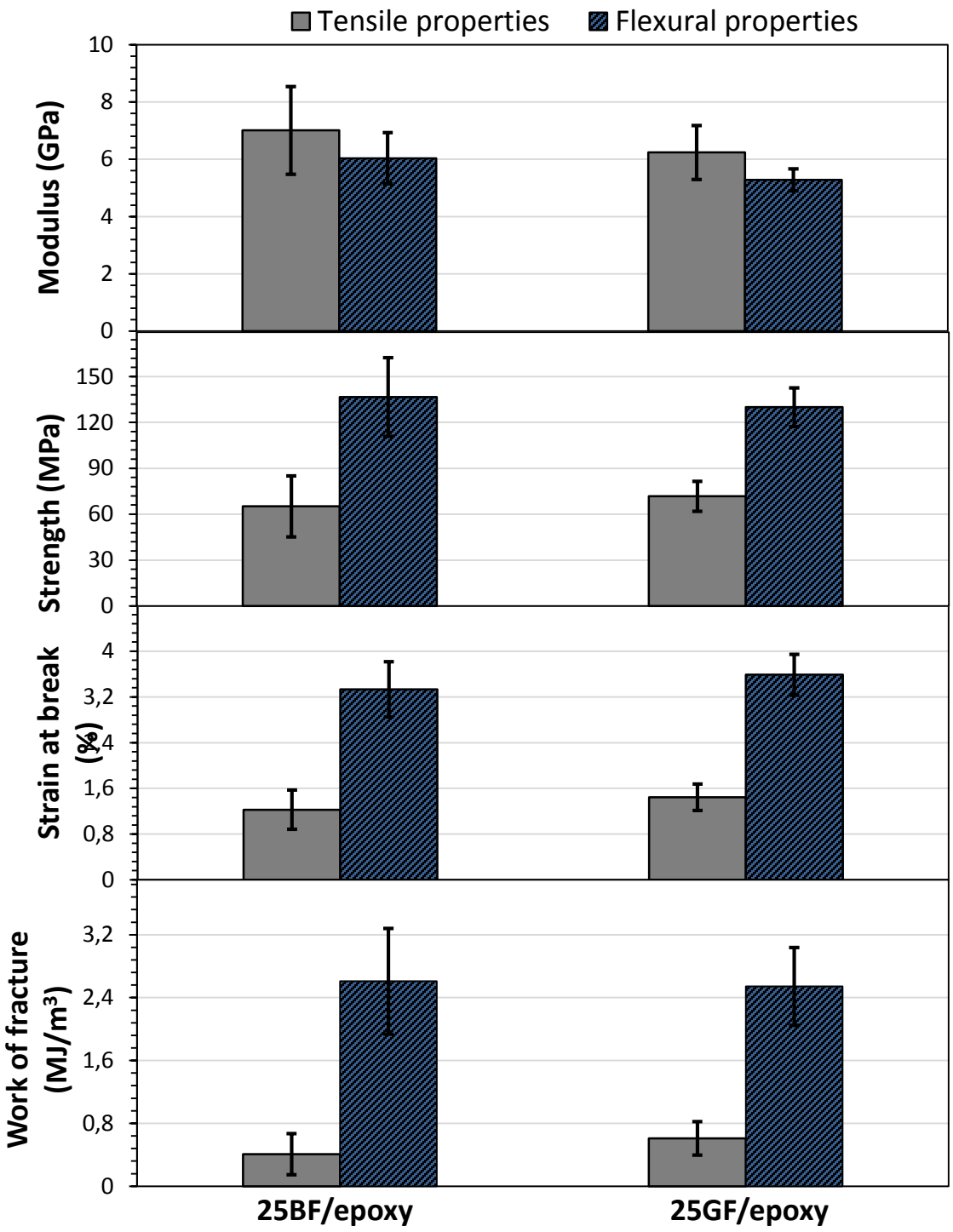

Figure 3.6: Tensile and flexural properties of 25BF/epoxy and 25GF/epoxy SMC composites.

The average flexural strength of the 25BF/epoxy composites was about 5% higher with respect to the 25GF/epoxy ones whereas the average tensile strength was about 9% lower. However, as seen in Figure 3.6 there is significant overlap of the standard deviations of the strength values indicating that the observed differences are not statistically significant. The same holds for the specific strength values as displayed in Figure 3.7. In addition, the strain at break values for both types of composites as well as the tensile and flexural fracture toughness (the area under stress-strain curve) are in the same experimental range as shown in Figure 3.6.

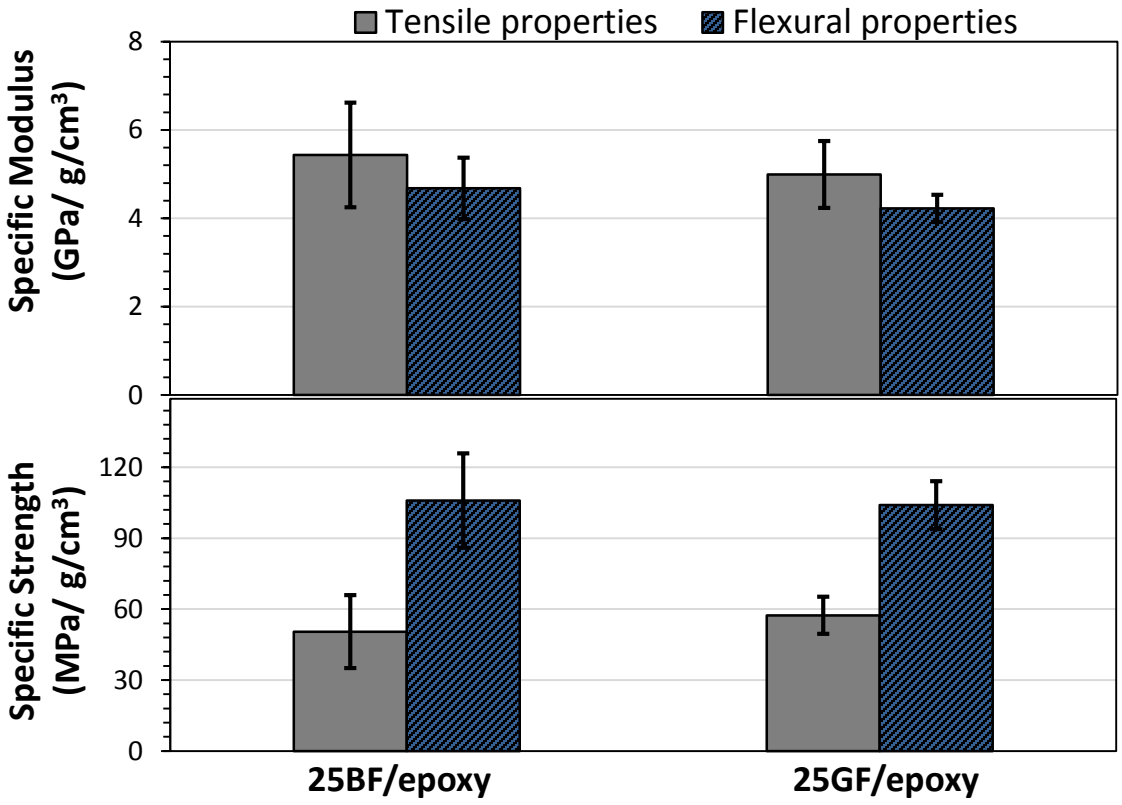

Figure 3.7: Specific tensile and flexural moduli and strength values of 25BF/epoxy and 25GF/epoxy SMC composites.

3.5.2 Impact properties

The impact energy of 25BF/epoxy and 25GF/epoxy SMC composites are displayed in Figure 3.8. The 25BF/epoxy SMC composites show a slightly lower average impact strength (by 6%) compared to the 25GF/epoxy SMC composites, but because of the statistical variation the impact strength of both composite types can be considered the same.

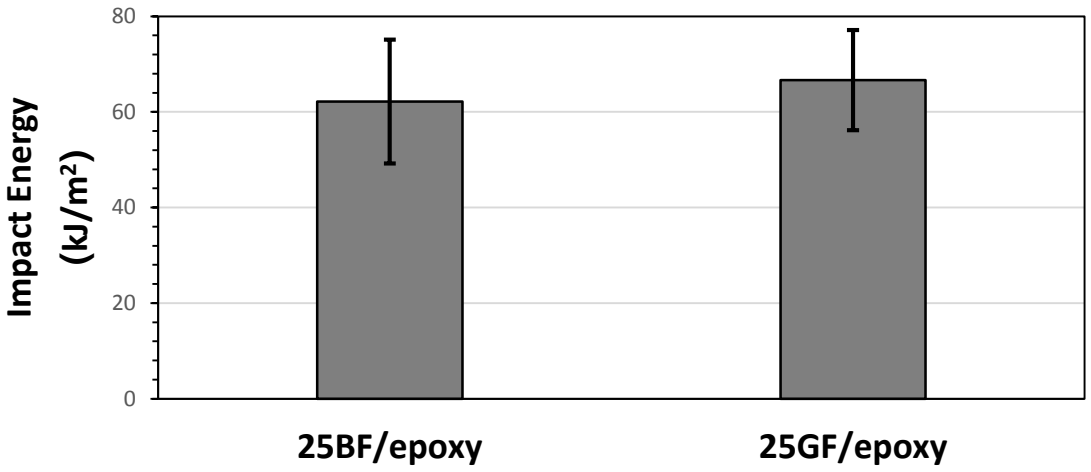

Figure 3.8: Impact energy of 25BF/epoxy SMC composites compared to 25GF/epoxy composites.

In conclusion, the mechanical properties of 25BF/epoxy SMC composites are equal or slightly better than those of 25GF/epoxy SMC. Some results, however, showed high statistical variation. Most likely reasons for the variation in the results are voids and varying fiber contents in the testing samples. Voids in the composites create defects leading to premature failure. During the SMC and compression molding process inhomogeneity in the fiber distribution can occur, e.g. the pressing leads to an outward flow of resin resulting in fiber rich regions in the center and a higher resin fraction at the edges. The formation

and consequences of fiber concentrated regions within an SMC plate are discussed more detailed in [40].

3.6 Fracture surface morphology

The failure modes of the tensile testing coupons of the 25BF/epoxy and 25GF/epoxy SMC composites were studied using SEM. Overall, the fiber type did not impact the fracture surface morphology. For both composite types, the main failure mechanism was interfacial debonding as shown by the smooth and clean cavity traces of the pulled out fibers and the clean pulled out fibers themselves in Figure 3.9 (a) and (c) for BF and in Figure 3.9 (b) and (d) for GF respectively. The smooth cavity traces as well as the clean pulled out fibers in both types of composites indicated that the interfacial adhesion of fiber and matrix is similar for 25BF/epoxy and 25GF/epoxy, which confirmed the IFSS results of the SFF test presented in section 3.1.

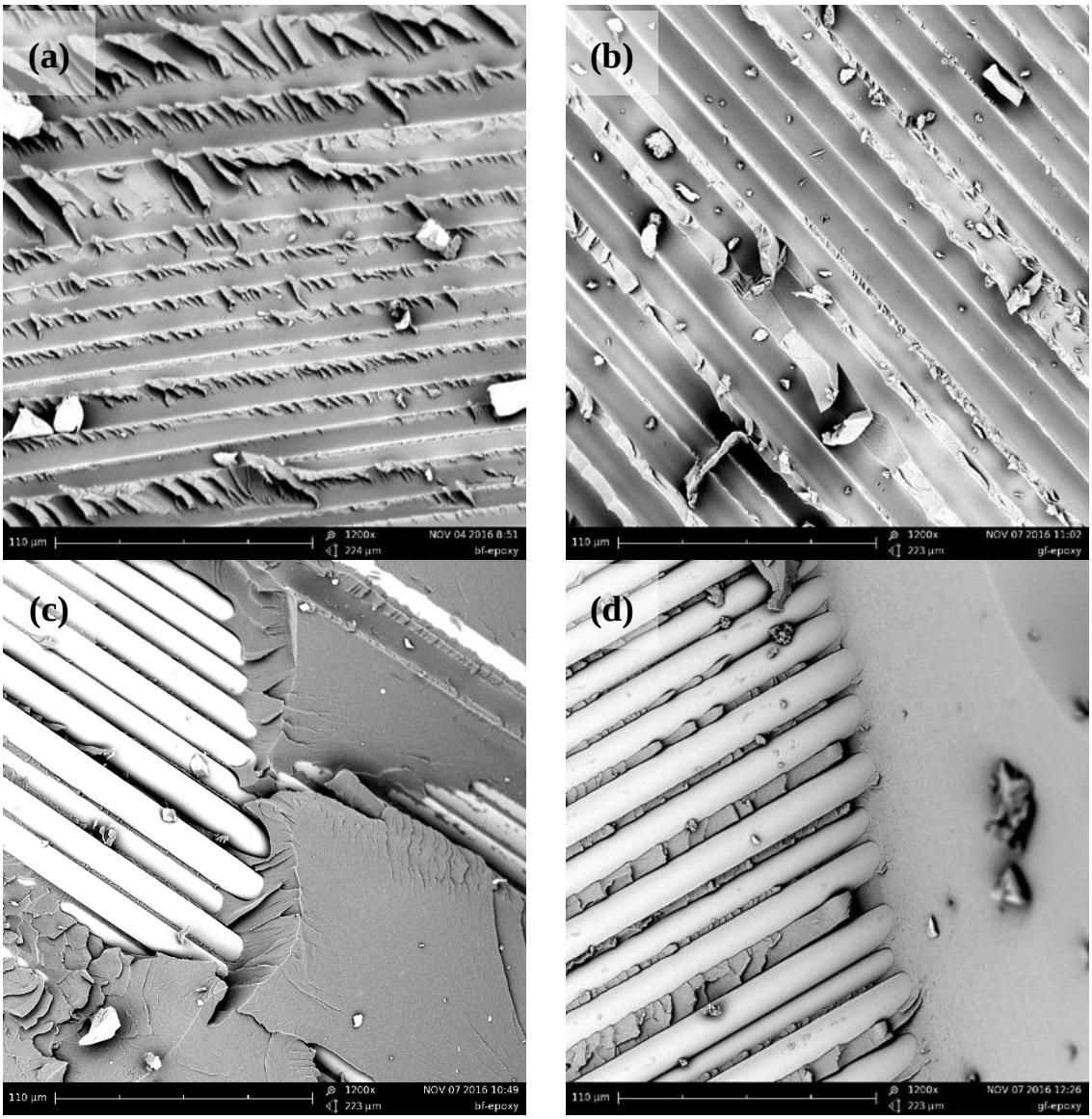

Figure 3.9: Cavity traces and pulled out fibers on the fracture surface of 25BF/epoxy (a),(c) and 25GF/epoxy (b),(d) SMC composites

Similarities were also found for the size of the shear cusps in the fracture surfaces. This indicated a similar crack growth leading to a similar mechanical strength [51] for both composite types which was confirmed by the mechanical testing results as described in section 3.5. Further damage mechanisms, i.e. fiber breakage and matrix cracking, occurred in the same extend in the BF25/epoxy and 25GF/epoxy SMC composites as represented in Figure 3.10.

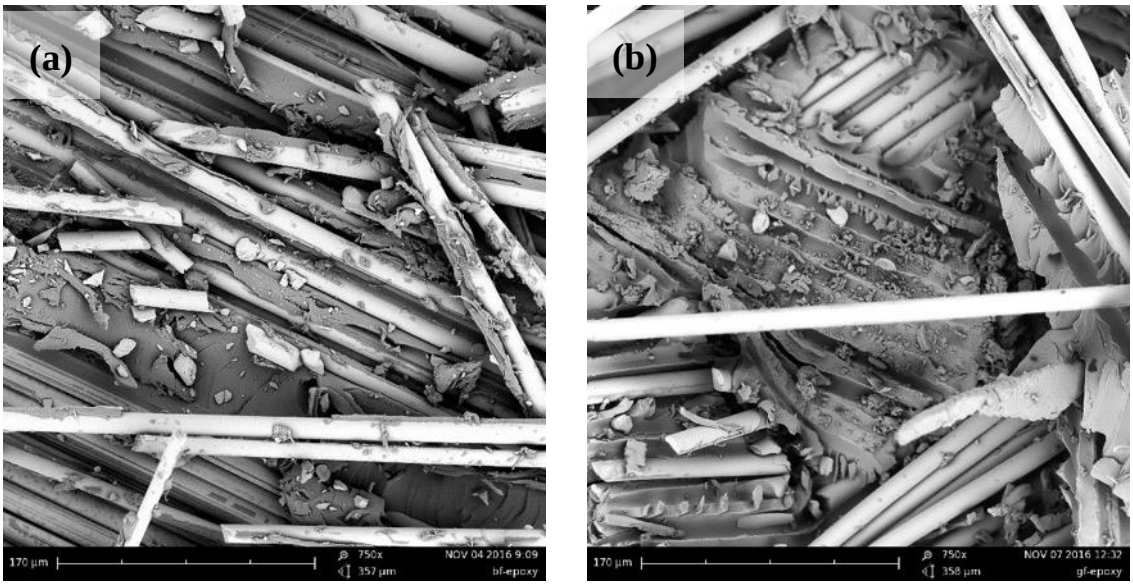

Figure 3.10: Fiber breakage and matrix cracking in (a) 25BF/epoxy and (b) 25GF/epoxy SMC composites

3.7 Conclusions

BF were investigated as an alternative to GF as reinforcement in SMC composites. BF showed a similar interfacial shear strength as GF in the used epoxy matrix which indicated that the interfacial adhesion and therefore the stress transfer ability between fiber and matrix is similar for BF/epoxy and GF/epoxy composites. Additionally, no significant differences between 25BF/epoxy and 25GF/epoxy were determined in the curing behavior of both composite types. At room temperature, the 25BF/epoxy composites had a higher storage modulus than the 25BF/epoxy composites, whereas the rubbery moduli above glass transition temperature were similar. The characteristic values of the tensile, flexural and impact testing were also similar for both composite types. Furthermore, the analysis of the fracture surface morphology showed the same failure mechanisms for 25BF/epoxy SMC composites as compared to the 25GF/epoxy SMC composites. These results verify the ability of BF to be used as an alternative to GF in the production of SMC composites,

especially considering that the BF can easily be used in the SMC production line and the eco friendliness and the potential cost advantages of BF.

CHAPTER 4. LIGHT-WEIGHTING OF HIGH FIBER CONTENT COMPOSITES BY ADDITION OF CELLULOSE NANO-CRYSTALS

In this chapter, it was investigated whether lightweight GF/epoxy and BF/epoxy SMC composites can be produced by replacing a portion of the reinforcing fibers with CNC. In the first stage, the maximum GF and BF content in the SMC materials was experimentally determined. Then, CNC were introduced in the SMC manufacturing line as a dispersion within the epoxy resin (abbreviated as CNC-epoxy) of SMC composites. The maximum fiber content was used for light-weighting to provide more tangible results. Then, the effect of 1.4-2 wt% CNC content in the epoxy matrix on the mechanical performance of both GF/epoxy and BF/epoxy SMC composites was investigated based on the fiber type, i.e. GF and BF, and compared with those of composites with no CNC. The first section of this chapter describes the methodology followed to lightweight SMC composites. In the second section, the effect of fiber type and CNC on the fiber wettability with the epoxy matrix is described. The third section focuses on the densities and void contents of the manufactured composites. Section 4 compares the mechanical properties of the manufactured SMC composites. In section 5, the fracture surfaces of post-tested samples are analyzed and the final section contains the conclusions of the determined results.

4.1 Methodology

The approach used for making lightweight SMC composites is to replace a portion of GF or BF with CNC without compromising the mechanical performance. To determine the

amount of GF or BF that can be removed and the amount of CNC to be added in the SMC composites a design criterion based on specific modulus (e.g. modulus divided by density) was applied. Specificially, both SMC composite with and without CNC should have the same specific modulus. Two CNC concentrations of 1.4 and 2 wt% in the epoxy resin were used, as the density and modulus of the resulting CNC-epoxy concentrations were experimentally known from a previous study [52] as presented in Table 4.1.

Table 4.1: Density and modulus for different CNC-epoxy mixtures [53].

Material	**ρ (g/cm^3)**	**E (GPa)**
Epoxy	1.15	3.0±0.3
1.4CNC-epoxy	1.15	4.4±0.5
2CNC-epoxy	1.15	4.7±0.3

Based on that, the reduced amount of GF or BF was calculated using and iteration approach, i.e. the modulus of the neat epoxy was substituted with that of the CNC-epoxy and then the amount of fibers was determined so that the theoretical specific modulus of the lightweight composite was equal to that of the standard composite. The moduli of the corresponding composites were calculated using equations (5) to (10) as provided in section 3.5.1. E_m is the elastic modulus of the matrix. So, in this part of the study it was either the modulus of the neat epoxy or of the CNC-epoxy mixtures as provided in Table 4.1. These calculations were used as guidance to make lighter SMC composites eliminating a costly, time inefficient and random "trial and error" approach.

Table 4.2 shows the different fiber and CNC concentrations of the produced GF/epoxy and BF/epoxy SMC composites. The naming scheme for the GF(BF)/epoxy SMC composites is *n*GF(BF)/*m*CNC-epoxy, where *n* is the fiber wt% and *m* is the CNC wt% in the composite. In the determination of the maximum fiber content, SMC composites with 50, 60, 65 and 70 wt% GF or BF were produced. In the second phase, GF and BF SMC composites with 60 wt% was chosen for light-weighting study and then 1.4CNC-epoxy and 2CNC-epoxy were added. 60 wt% content was selected as the maximum fiber content as dry spots were seen in SMC composites with higher fiber content, i.e. 65 and 70 wt%. Thus, the SMC composites with 60 wt% fiber content were used as reference for the light-weighting study. SMC composites with 44 wt% and 48 wt% fiber content were used based on the approach explained above (same specific modulus) as presented in Table 4.3.

Table 4.2: Fiber and CNC concentrations of the manufactured SMC composites.

	Maximum fiber content				**Lightweight**		
Fiber content	50	60	65	70	60	48	44
CNC content in resin	0	0	0	0	1.4	1.4	2.0
CNC content in composite	0	0	0	0	0.6	0.9	1.1

Table 4.3: Moduli and densities of the manufactured SMC composites for light-weighting.

Composite	E_{theor} (GPa)	ρ (g/cm^3)	$E_{specific,theor}$
60GF/epoxy	14.38	1.71	8.40
48GF/0.9CNC-epoxy	13.23	1.56	8.48
44GF/1.1CNC-epoxy	12.73	1.51	8.41
60BF/epoxy	14.99	1.76	8.48
48BF/0.9CNC-epoxy	13.41	1.58	8.47
44BF/1.1CNC-epoxy	13.17	1.54	8.52

4.2 Contact angle

Table 4.4: Contact angle results for BF and GF rovings with neat epoxy and CNC-epoxy.

Material	BF	GF
Neat Epoxy	34.16	29.2
2CNC-epoxy	40.68	36.36

Table 4.4 summarizes the results of the contact angle measurement between the CNC-epoxy and GF and BF rovings. The neat epoxy and 2CNC-epoxy have better wettability for GF compared to BF that possibly lead to a better adhesion between GF and CNC-epoxy compared to that of BF and CNC-epoxy.

4.3 Density and void content

The theoretical density, measured density and void content for SMC composites with various contents of GF (BF) and CNC are shown in Table 4.5. The theoretical density is calculated using equation (3) in section 2.3.4 assuming that the fiber content of the SMC composites is the same as the desired value set in the SMC machine. The actual value of the fiber content is measured using acid digestion method as presented in Table 4.5 using equation (4). It is noted that $\rho_{exp,ad}$ is the measured density from acid digestion calculated from the actual fiber content using equation (3).

In general, the void content in BF/epoxy is higher than that of GF/epoxy composites. Especially, for lower content BF composites, i.e. 44 wt% and 48 wt%, where CNC is also present in the matrix, the void content increases as shown in Table 4.5. In addition, the void content in BF/epoxy SMC composites containing CNC, is higher than that of corresponding GF/epoxy composite with CNC content. According to the contact angle measurement results in Table 4.4, the presence of CNC in the epoxy decreases the wetting ability of the epoxy and BF more than that of GF and CNC-epoxy, resulting in higher void content in BF SMC composites containing CNC.

Table 4.5: Theoretical and experimental densities and void contents of the manufactured SMC composites.

Composite	$\rho_{c,theoretical}$ (g/cm^3)	$\rho_{exp,wd}$ (g/cm^3)	Fiber (wt%, by acid digestion)	$\rho_{exp,ad}$ (g/cm^3)	Void content (%)
70GF/epoxy	1.86	1.86±0.07	-	-	-
65GF/epoxy	1.78	1.72±0.04	0.69±0.04	1.85±0.06	7
60GF/epoxy	1.71	1.67±0.06	0.69±0.08	1.85±0.07	9
50GF/epoxy	1.58	1.41±0.07	-	-	-
60GF/0.6CNC-epoxy	1.71	1.74±0.06	0.66±0.05	1.80±0.08	3
48GF/0.9CNC-epoxy	1.56	1.51±0.03	0.56±0.05	1.66±0.06	9
44GF/1.1CNC-epoxy	1.51	1.49±0.05	0.52±0.06	1.61±0.07	8
65BF/epoxy	1.85	1.82±0.07	0.72±0.04	1.97±0.07	8
60BF/epoxy	1.77	1.75±0.07	0.72±0.03	1.97±0.07	12
50BF/epoxy	1.62	1.35±0.09	-	-	-
60BF/0.6CNC-epoxy	1.77	1.73±0.05	0.71±0.08	1.96±0.1	13
48BF/0.9CNC-epoxy	1.59	1.48±0.05	0.55±0.05	1.69±0.07	14
44BF/1.1CNC-epoxy	1.55	1.39±0.06	0.53±0.08	1.66±0.1	19

4.4 Mechanical properties

In this section, the effect of GF (BF) and CNC content on the tensile, flexural and impact properties of the SMC composites is presented. First, the results of the determination of the maximum fiber content are discussed. Then, the results of the light-weighting study are presented. In addition to the measurement of the mechanical properties, a single factor (CNC effect) ANOVA was carried out to determine whether the enhancement of properties in presence of CNC is significant. The ANOVA test compared the specific properties of CNC-enhanced GF (BF) composites with those of 60GF (BF)/epoxy with no CNC. When the *P* value is larger than 0.001 and the *F* ratio ($F/F_{Critical}$) less than 1, the difference between the mean values is considered negligible.

4.4.1 Determination of the maximum fiber content

Figure 4.1 and Figure 4.2 show the absolute and specific properties of SMC composites made for the determination of the maximum fiber content. As expected, the average values for the modulus, strength and impact energy of both GF/epoxy and BF/epoxy SMC composites increase with the increase of the fiber content for both tensile and flexural properties. However, considering the statistical standard deviation, the difference between properties of SMC composites containing 60 wt%, 65 wt% and 70 wt% GF (BF) is not significant. Especially, for the specific values, the differences between the properties of composites with 60 wt%, 65 wt% and 70 wt% GF (BF) decreased even more compared to the absolute values. Therefore, 60 wt% was selected as the SMC composites with the maximum GF (BF) content for the light-weighting study.

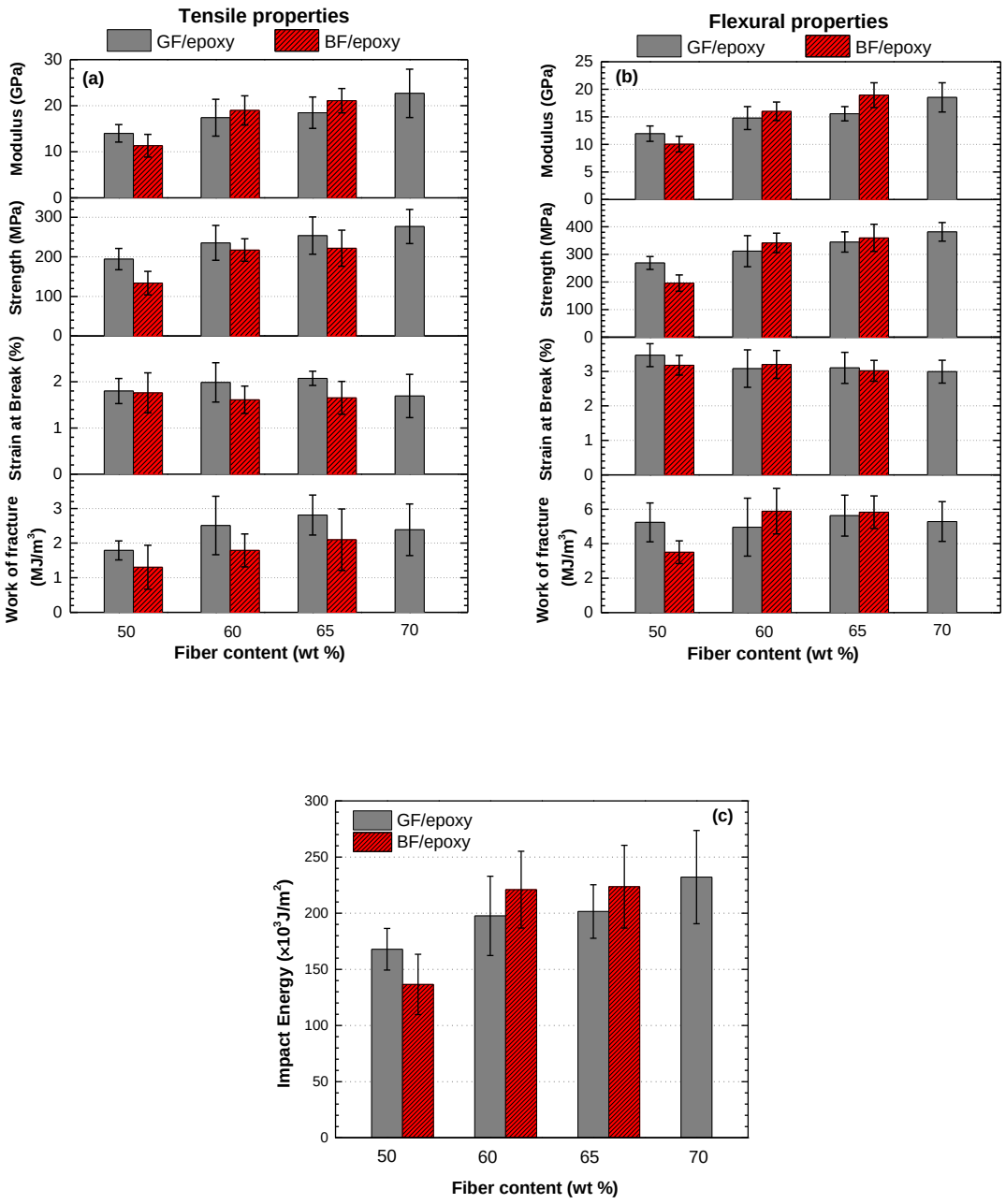

Figure 4.1: (a) Tensile, (b) flexural and (c) impact properties of GF/epoxy and BF/epoxy SMC composites made for the determination of the maximum fiber content.

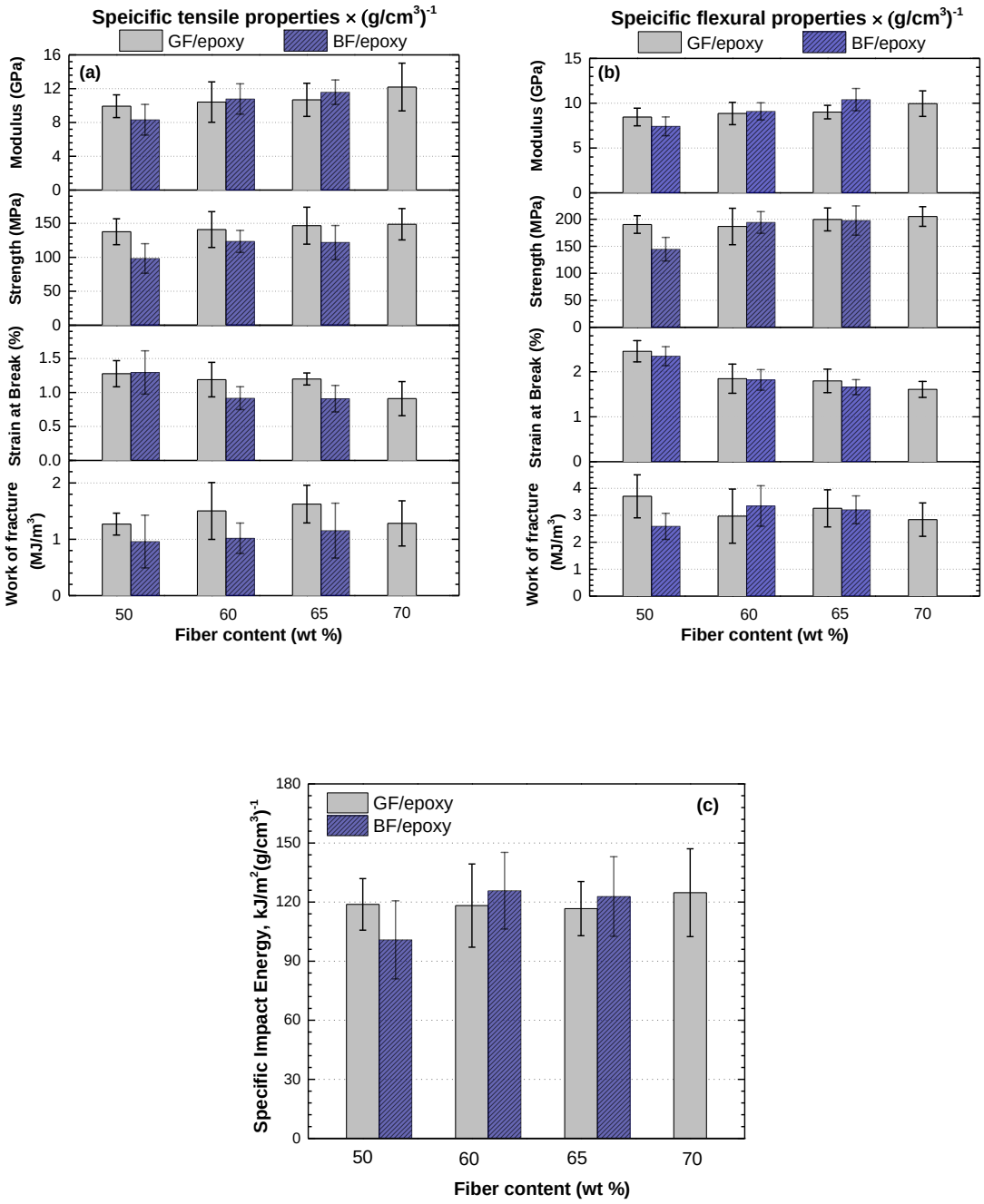

Figure 4.2: Specific (a) tensile, (b) flexural and (c) impact properties of GF/epoxy and BF/epoxy SMC composites made for the determination of the maximum fiber content.

4.4.2 Light-weighting study

The effect of the CNC content on absolute and specific properties of the SMC composites is presented in Figure 4.3 and Figure 4.4 respectively. The tensile, flexural and impact properties of the 60GF/0.6CNC-epoxy SMC composites are similar to those of 60GF/epoxy with no CNC considering the standard deviation, indicating that for the SMC composites with maximum fiber content, adding CNC does not significantly improve the properties. The tensile modulus of 48GF/0.9CNC-epoxy and 44GF/1.1CNC-epoxy SMC composites are both in a same range and ~20% lower than that of 60GF/epoxy as shown in Figure 4.3. In addition, the tensile strength of both composites with CNC is in the same level and ~9% lower than that of 60GF/epoxy. The work of fracture in tensile mode for all of the composites are similar. A similar trend is observed for the flexural and impact properties where for the composites with CNC the flexural modulus is ~23%, the flexural strength is ~10% and the impact is 11% lower than the corresponding values of 60GF/epoxy with no CNC.

Although a similar trend to that of GF/epoxy can be seen for BF/epoxy SMC composites as shown in Figure 4.3, the properties decrease more dramatically for 48BF/0.9CNC-epoxy and 44BF/CNC-epoxy SMC composites compared to the GF/epoxy corresponding composites. For example, a decrease of ~58% for the tensile modulus, ~46% for the tensile strength, ~37-45% for the flexural modulus, ~30-34% for the flexural strength were observed for 48BF/epoxy and 44BF/epoxy composites containing CNC compared with those of 60BF/epoxy with no CNC. The impact strength of BF composites containing CNC were also 47-59% lower than that of 60BF/epoxy composites with no CNC which is much lower compared to corresponding differences in GF/epoxy composites. A possible culprit

is the higher void content of BF/epoxy (14-19%) compared to that of GF/epoxy composites (9%), as presented in Table 4.5.

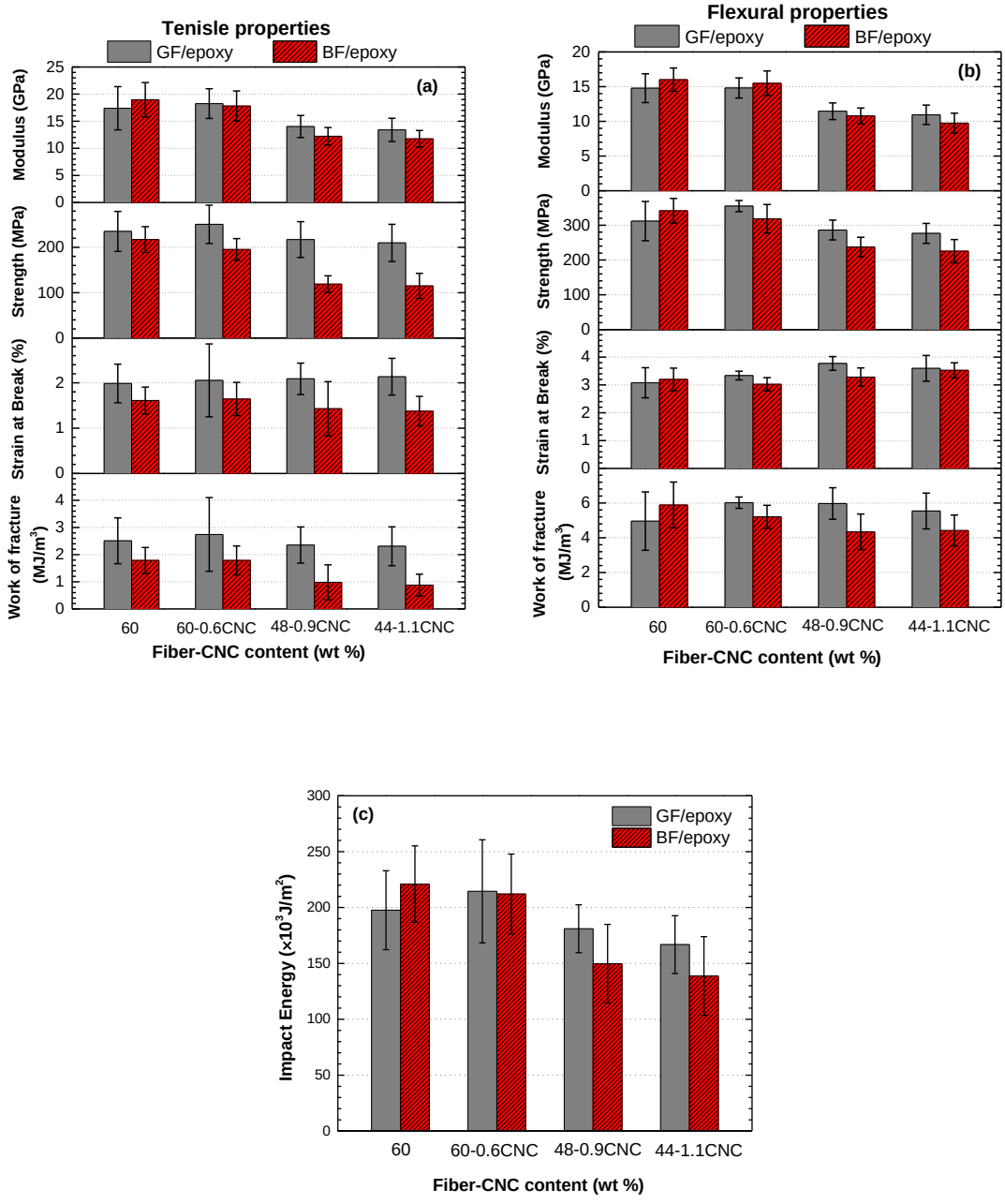

Figure 4.3: (a) Tensile, (b) flexural and (c) impact properties of GF/CNC-epoxy and BF/CNC-epoxy SMC composites in the light-weighting study.

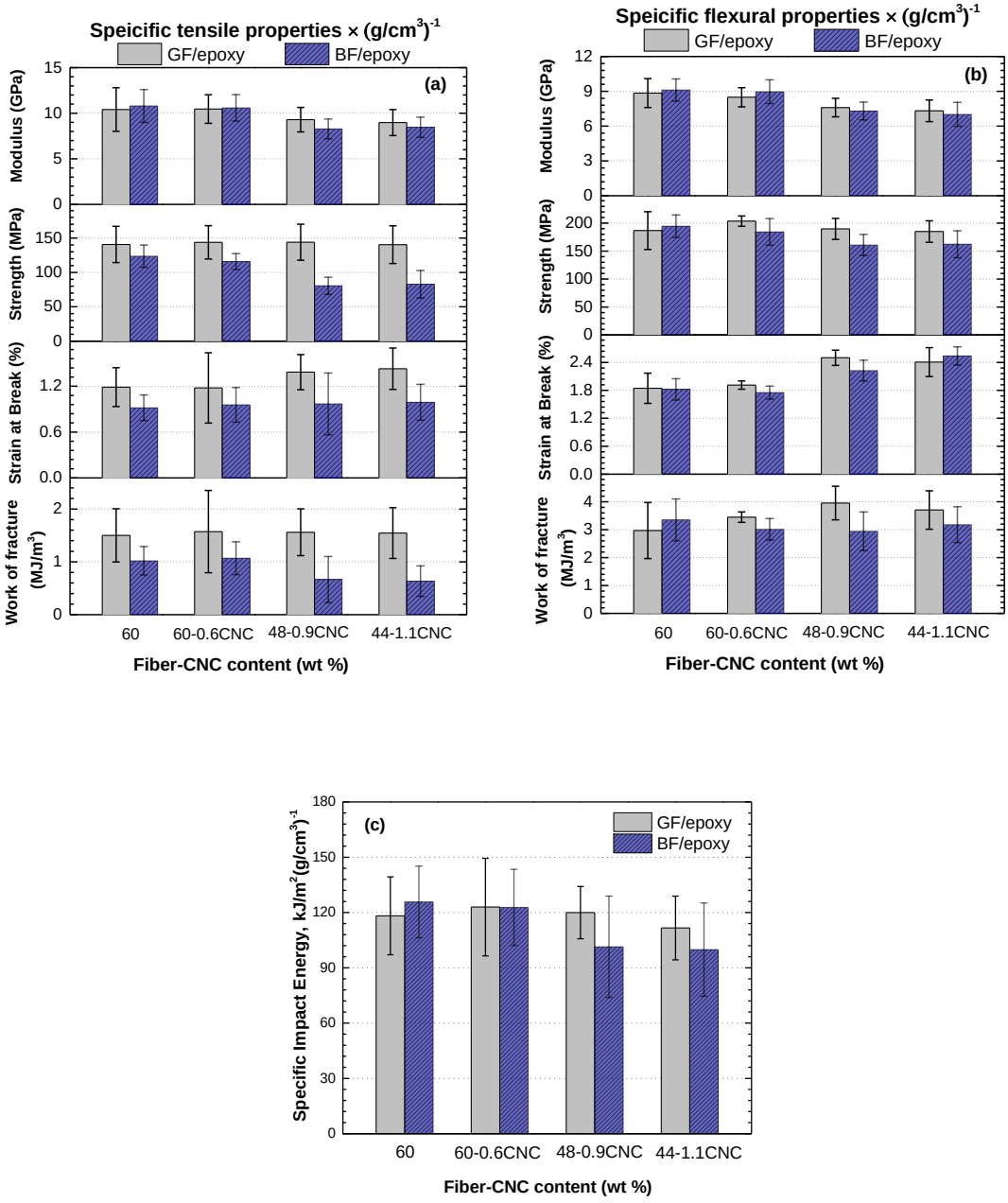

Figure 4.4: Specific (a) tensile, (b) flexural and (c) impact properties of GF/CNC-epoxy and BF/CNC-epoxy SMC composites in the light-weighting study.

According to Figure 4.4, the difference between the specific modulus and strength for tensile and flexural properties as well as the impact energy of the GF/epoxy composites containing CNC is not significant with those of 60GF/epoxy with no CNC considering the statistical deviation. Particularly, the specific strength and impact strength values of 48GF/0.9CNC-epoxy and 44GF/1.1CNC-epoxy (1.51±0.03 and 1.49±0.05 g/cm^3 respectively) are similar to those of 60GF/epoxy composites with no CNC (1.67±0.06 g/cm^3). This implies that the mechanical performance of ~11% lighter SMC composites containing ~ 1 wt% CNC reach the level of heavier composites, i.e. 60GF/epoxy, owing to the enhancement by CNC. This is also confirmed by the ANOVA results presented in

Table 4.6, where *P* value > 0.001, indicating that the difference between the specific values of all composites are not significant. The similar trend was also observed for the specific values of elongation at break and work of fracture for GF/epoxy composited with and without CNC.

Table 4.6: ANOVA test results for mechanical performance between specific properties of 60GF/epoxy and *n*GF/*m*CNC-epoxy SMC composites.

Sample	Sum of squares	P value	F ratio	Sum of squares	P value	F ratio
	Tensile modulus			**Tensile strength**		
60GF/0.6CNC-epoxy	0.01	> 0.001	6.5×10^{-4}	36.16	> 0.001	0.01
48GF/0.9CNC-epoxy	4.78	> 0.001	0.33	43.11	> 0.001	0.01
44GF/1.1CNC-epoxy	7.68	> 0.001	0.49	0.27	> 0.001	8×10^{-5}
	Flexural modulus			**Flexural strength**		
60GF/0.6CNC-epoxy	0.59	> 0.001	0.12	1392.33	> 0.001	0.59
48GF/0.9CNC-epoxy	11.46	> 0.001	2.21	9.65	> 0.001	3×10^{-3}
44GF/1.1CNC-epoxy	11.46	> 0.001	2.21	9.65	> 0.001	3×10^{-3}
	Impact energy					
60GF/0.6CNC-epoxy	118.65	> 0.001	0.04			
48GF/0.9CNC-epoxy	16.33	> 0.001	0.01			
44GF/1.1CNC-epoxy	226.4	> 0.001	0.14			

Table 4.6 continued.

Sample	Sum of squares	*P* value	*F* ratio	Sum of squares	*P* value	*F* ratio
	Tensile modulus			**Tensile strength**		
60BF/0.6CNC-epoxy	0.19	> 0.001	0.01	285.81	> 0.001	0.31
48BF/0.9CNC-epoxy	31.85	= 0.001	3.25	9247.26	< 0.001	10.08
44BF/1.1CNC-epoxy	27.37	= 0.002	2.78	8326.03	< 0.001	5.71
	Flexural modulus			**Flexural strength**		
60BF/0.6CNC-epoxy	0.10	> 0.001	0.02	482.66	> 0.001	0.22
48BF/0.9CNC-epoxy	14.72	< 0.001	4.36	5081.43	= 0.002	2.96
44BF/1.1CNC-epoxy	19.75	< 0.001	4.44	4660	= 0.005	2.12
	Impact Energy					
60BF/0.6CNC-epoxy	48.93	> 0.001	0.03			
48BF/0.9CNC-epoxy	3254.38	> 0.001	1.32			
44BF/1.1CNC-epoxy	3514.49	> 0.001	1.59			

The enhancement of the modulus of CNC-contained GF/epoxy composites is expected to be the result of the increase in the apparent modulus of the matrix (CNC-epoxy) due to the stiffening effect of the CNC. The increase in the strength of composites containing CNC is possibly a result of stronger GF-matrix adhesion and hence, a better stress transfer efficiency across the GF/CNC-epoxy [54]. This hypothesis cannot be validated in this study due to lack of relevant experiments (e.g. fiber pull out test or atomic force microscopy); however, the observed trend in specific tensile and flexural strength values of GF/CNC-epoxy composites and SEM imaging can qualitatively suggest the increase of adhesion between the GF and epoxy in presence of CNC.

In contrast with GF/CNC-epoxy composites, the specific values for BF/epoxy composites containing CNC did not reach the level of performance of 60BF/epoxy with no CNC. The ANOVA results presented in Table 4.6 also indicates that the difference between tensile and flexural modulus and strength as well as impact strength of 48BF/0.9CNC-epoxy and 44BF/1.1CNC-epoxy SMC composites with the corresponding properties of 60BF/epoxy composites is significant ($F_{Critical} < 1$ and P value < 0.001 or very close to 0.001). As discussed earlier, the void content of 44BF/0.9CNC-epoxy and 44BF/1.1CNC-epoxy are higher (14-19%) compared to that of corresponding GF/CNC-epoxy composites (9%), as presented in Table 4.5. It is also plausible that the adhesion between CNC-epoxy matrix and BF does not improve as suggested by the lower wettability of BF and CNC-epoxy matrix in contrast with that of GF as shown in Table 4.4.

The high-observed statistical standard deviation in the results is likely due to inhomogeneous dispersion of CNC and aggregates of different size in the matrix. Moreover, fiber rich regions at the center of the SMC materials due the outward flow of

the resin because of pressure during the compaction in SMC manufacturing process and/or the compression molding process [40].

Figure 4.5 presents an Ashby plot comparing the specific properties of the lightweight GF and BF-SMC composites containing CNC with the composites with no CNC. Overall, the mechanical properties of the lightweight GF-SMC composites (i.e. 48 wt% and 44 wt% GF content) containing CNC overlaps with that of 60GF/epoxy composites with no CNC, indicating that light weighting has been achieved for GF composites with CNC. However, the properties of the lightweight BF-SMC composites with CNC, i.e. 48BF/0.9CNC-epoxy and 48BF/1.1CNC-epoxy, does not superpose with that of heavier 60GF/epoxy composite with no CNC. This implies that the presence of CNC does not increase the performance of the BF composites to the level of the 60BF/epoxy composites possibly due to the higher void content and lower wettability as previously discussed. It is plausible that modification of the sizing of BF will improve the wettability and hence the adhesion between BF and CNC-epoxy leading to lower void content and higher macroscopic mechanical properties.

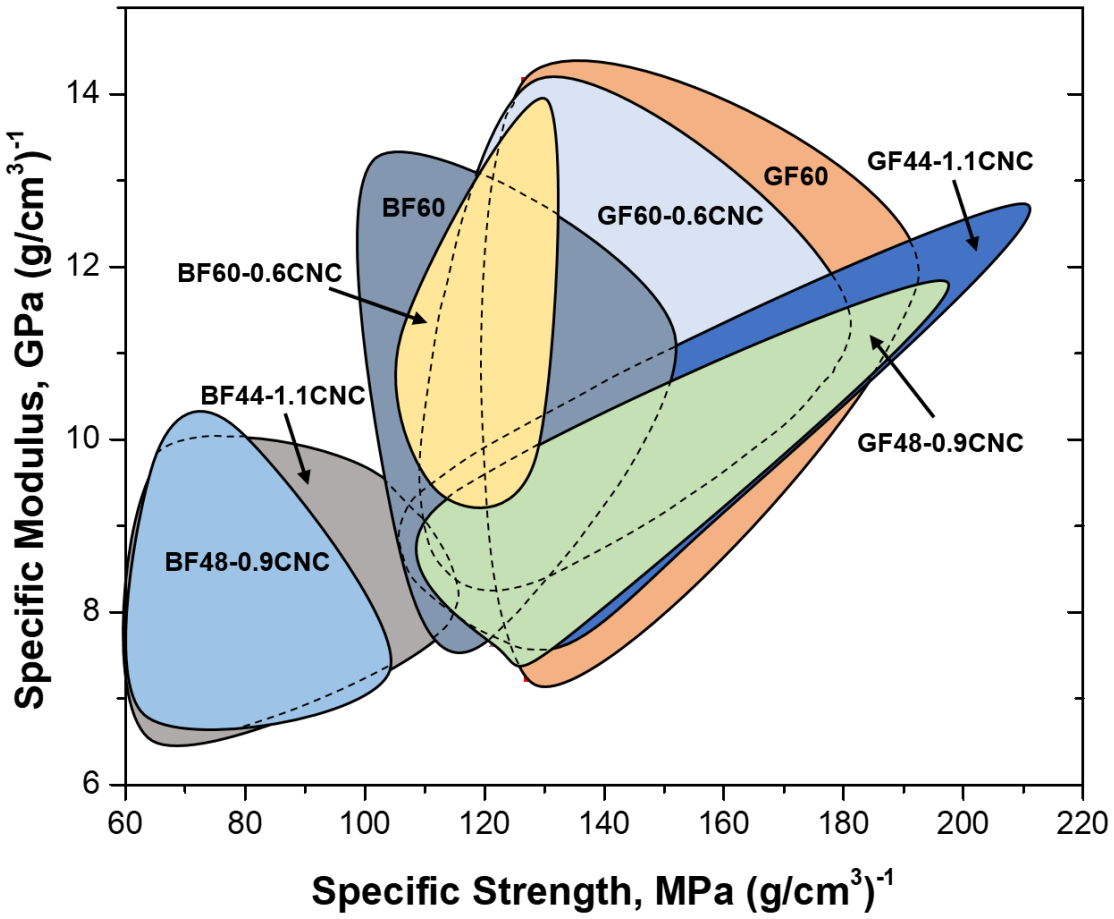

Figure 4.5: Composite selection plot for GF and BF SMC composites with and without CNC.

4.5 Fracture surface morphology

Figure 4.6 and Figure 4.7 show the morphology of the tensile fracture surface of the GF/epoxy and BF/epoxy SMC composites respectively. In general, addition of CNC in the epoxy matrix of GF/epoxy composites results in rougher fracture surfaces as compared in Figure 4.6 (a), (c) and (e). Although the main failure mode is fiber debonding in GF/epoxy composites with and without CNC, it appears that the presence of CNC increases the fiber/matrix adhesion resulting in more matrix residues on the fibers as shown in Figure 4.6 (b), (d) and (f).

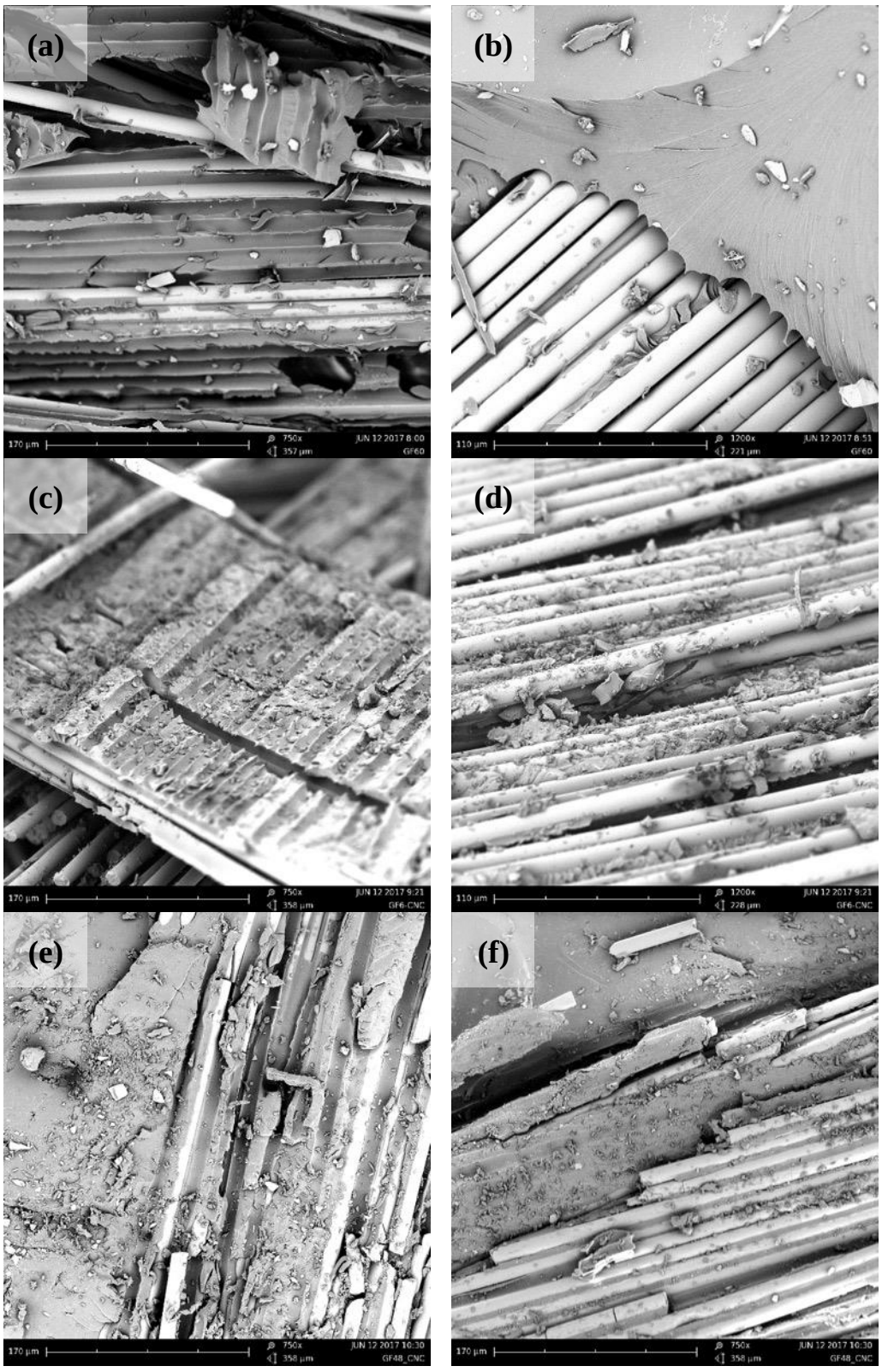

Figure 4.6: SEM images for tensile fracture surface of (a)-(b) 60GF/epoxy, (c)-(d) 60GF/0.6CNC-epoxy, and (e)-(f) 48GF/0.9CNC-epoxy SMC composites.

Clean cavity traces of the pulled out fibers in the matrix of the composites with no CNC in contrast with those with rough texture in composites containing CNC also implies a better interfacial adhesion between fiber and matrix in the presence of CNC as compared in Figure 4.6 (a) and (c). Higher interfacial adhesion results in a better load transfer from matrix to fiber and hence, increases the macroscopic strength. It is plausible that the presence of CNC in the polymer matrix increases the friction between fiber and matrix and thus more energy is required to debond fiber from matrix [55]. Toughening mechanisms such as interlocking mechanism restricting GF debonding at the GF/matrix interphase and interfacial crack bridging [56] in the presence of CNC can also be legitimate reasons for better adhesion between GF and matrix. These mechanisms lead to an increase in the absorbed energy in fracture and thus, improvement in mechanical properties.

The presence of CNC in BF/epoxy SMC composites slightly alters the texture towards a rougher surface as compared in Figure 4.7 (b) and (d). In contrast with GF/epoxy composites, presence of CNC appears not to improve the adhesion between BF and matrix as suggested by i) smooth fracture surface, ii) clean cavity traces and iii) pulled out fibers devoid of matrix in BF/epoxy composites with and without CNC as shown in Figure 4.7 (b), (c) and (e). It is noted that the interfacial shear strength between BF and neat epoxy is similar to that of GF with neat epoxy as seen in section 3.1. Also, similar to GF/epoxy SMC composites, the main failure mode is fiber pull out as seen in Figure 4.7 (a) and (f).

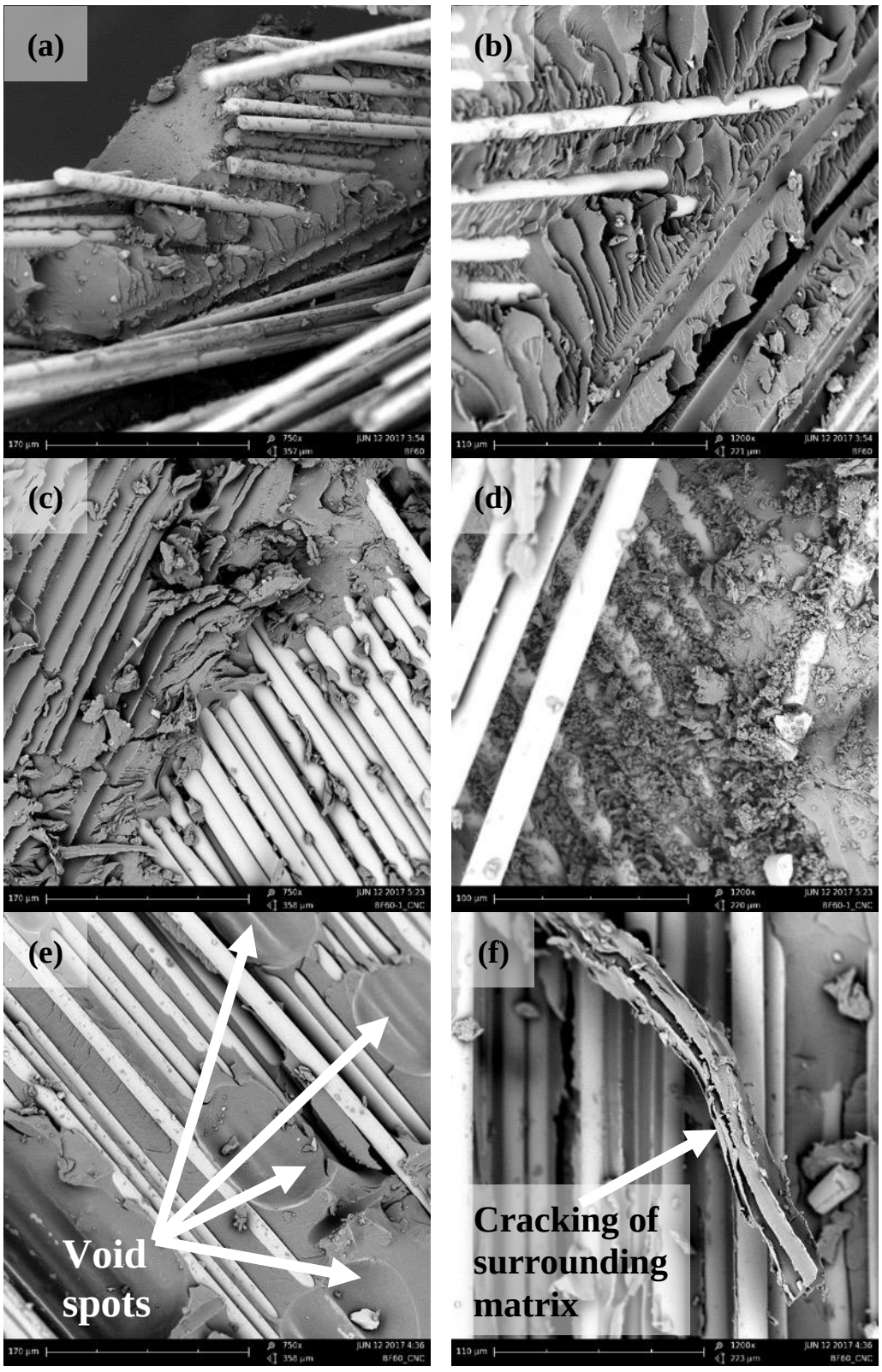

Figure 4.7: SEM images for tensile fracture surface of (a)-(b) 60BF/epoxy, (c)-(d) 60BF/0.6CNC-epoxy, and (e)-(f) 48BF/0.9CNC-epoxy SMC composites.

In addition, both 60BF/epoxy and 60BF/0.6CNC-epoxy composites have almost similar smooth texture of the matrix in fracture surface shown in Figure 4.7 (a) and (c) indicating a same fracture toughness independent of CNC content. Shear cusps also seem to be smooth and similar in size as shown in Figure 4.7 (b) and (c) suggesting a similar crack growth in BF/epoxy composites with and without CNC.

The number of void spots in BF/epoxy composites containing CNC appear to be qualitatively more than that of corresponding GF composites, as seen Figure 4.7 (c). In addition, in the presence of CNC, it seems that during the fiber pull out, the surrounding matrix easily cracks, shown in Figure 4.7 (d), which can potentially result in lower macroscopic strength values. All these observations may imply that addition of CNC does not significantly improve the mechanical properties of BF/epoxy SMC composites.

4.6 Conclusions

Producing lightweight GF (BF)/epoxy SMC composites through replacing 12-16 wt% with 1.4-2 wt% CNC was investigated. It was shown that presence of ~1 wt% CNC in SMC composites with 44-48 wt% GF content, increased their specific tensile, flexural and impact properties to the level of composites with maximum GF content, i.e. 60 wt%, resulting in 11% lighter composites with no penalty on mechanical performance. However, the specific properties of the BF/epoxy SMC composites containing CNC did not meet those of 60BF/epoxy composites possibly due to the high void content and lower wettability compared to that of GF and CNC-epoxy. The results of this study conclude that that producing high volume lightweight SMC composites is feasible through using cellulose nanomaterials once the wettability and void content issues are addressed.

CHAPTER 5. CONCLUSIONS AND FUTURE WORK

The goal of this thesis was to create lightweight SMC composites for automotive applications. In CHAPTER 1, the importance of light-weighting in the automotive sector was described. Governmental regulations for fuel efficiency and greenhouse gas emissions as well as customers' increasing demand for ecofriendly cars without compromises in performance were determined as the key drivers for the car manufacturers' endeavors towards light-weighting. Different materials for light-weighting in automotive applications with special focus on polymer matrix composites were described. Sheet molding compound technology as major composite technology used in automotive industry and basic manufacturing process used in this study was explained in detail.

In CHAPTER 2, the different materials used in this study were outlined. Basalt fibers were described as they were investigated as potential alternative for glass fibers as reinforcement in SMC composites. Also, cellulose nano-crystals were characterized as they were investigated as a tool for the light-weighting of SMC composites. Additionally, the exact fabrication procedures as well as the characterization techniques used in this study were outlined in CHAPTER 2.

CHAPTER 3 described the feasibility study of using basalt fibers as an alternative to glass fibers in sheet molding compounds. It was found that epoxy-based SMC composites with 25 wt% basalt fibers and 25 wt% glass fibers show overall similar mechanical and thermo-mechanical properties. Therefore, basalt fibers represent an ecofriendly alternative to glass fibers in sheet molding compounds with potential cost advantages.

In CHAPTER 4, it was investigated whether lightweight GF/epoxy and BF/epoxy SMC composites can be produced by replacing a portion of reinforcing fibers with CNC. It was shown that by adding ~1 wt% CNC in SMC composites with 44-48 wt% GF content their specific tensile, flexural and impact properties are equal to composites with 60 wt% GF content. As a result, a weight reduction of 11% without drawbacks in mechanical performance was achieved for GF reinforced SMC composites. For BF reinforced SMC composites, adding CNC was not an effective light-weighting method. The SMC composites with 44-48 wt% BF and ~1 wt% CNC could not meet the specific mechanical properties of BF60/epoxy SMC composites. High void contents and bad wettability in the BF/epoxy composites are the most likely reasons for that.

The results described above indicate that the initial goal of this thesis, creating lightweight SMC composites for automotive applications, has been reached. Although BF did not show any light-weighting or performance advantages in SMC composites compared to GF, BF reinforced SMC composites still represent a suitable light-weight material for automotive applications. They show no performance disadvantages compared to common GF reinforced SMC composites either and BF can easily replace GF in the SMC manufacturing process. Also, BF are ecofriendly and they show potential cost advantages compared to GF as high-volume production is reached. Low cost and eco-friendliness can be significant drivers for the use of BF reinforced SMC composites in automotive applications, which is why car manufacturers including Volkswagen have already shown interest in this material.

In the second part, the goal of this thesis was totally met as a tangible weight reduction of about 11% in GF reinforced SMC composites was achieved by addition of CNC in the epoxy matrix. It proofed that CNC can be used in a scalable manufacturing process as it is

used in the industry to achieve a significant weight reduction in GF reinforced SMC composites. The results also show that it is worth it to further investigate the positive effect of CNC on the mechanical properties of SMC composites. Solving major issues of the CNC introduction as inhomogeneous dispersion and agglomeration, thermal stability and a lack of large scale manufacturing processes show great potential to achieve further weight reductions in automotive SMC applications. Also, the positive effect of CNC can be investigated using other polymers than epoxy, i.e. polyester. In addition to the introduction of CNC in the SMC matrix, scalable ways of introducing CNC in the composite as coating of the reinforcements have to be developed. An approach of coating GF in the SMC production line was investigated in APPENDIX B of this thesis. Another promising future task, is to resolve the wetting and void content issues seen in the BF/epoxy composites in the presence of CNC to achieve similar light-weighting effects as seen with the GF/epoxy composites.

APPENDIX A. CALIBRATION OF THE SMC LINE

A.1 General SMC Set-Up and Operation Procedure

This appendix describes the step-wise procedure of setting up and operating the "Fin and Fram SMC line". First, a general approach is outlined to provide an overview about the necessary steps to successfully run the SMC line. Subsequently, each step is described in-depth in a separate section in this appendix including all needed actions as well as common mistakes which must be avoided.

The procedure can be subdivided in 5 steps:

1.) Calculating the Set-Up parameters:

    The numeric set-up parameters are calculated based on the desired parameters of the final composite plate (e.g. dimensions, fiber content, etc.) using an Excel-spreadsheet template.

2.) Calibration of the SMC line before the run:

    The calculated parameters have to be set at the SMC line to achieve the desired results.

3.) Preparation of the resin:

    The preparation of the resin should be carried out after the SMC set-up due to the risk of too early gelling or curing.

4.) Running the SMC line:

After all the preparations are completed, the SMC machine can be run. This includes pouring the resin, starting the conveyor belt and the fiber chopper as well as collecting the compound.

5.) Cleaning of the SMC machine and used tools:

Thorough cleaning of the SMC line is required immediately after each run to avoid curing and sticking of the resin within the machine. Otherwise, the SMC line cannot be set up properly for the next run and the desired results cannot be achieved.

A detailed description of each step is given in the following sections.

A.2 Calculation of the Set-Up Parameters of the SMC Line

It is necessary to set up the SMC line based on precise calculations, to achieve the desired properties of the final SMC product, e.g. exact fiber content or outer dimensions. Therefore, an Excel spreadsheet template has been created to efficiently transfer the given input data into set-up parameters for the SMC line. The necessary input data is the desired length, width and thickness of the final SMC material given by the dimensions of the mold cavity.

Furthermore, the number of SMC layers in the mold, the fiber fraction as well as the density of the fibers and the liquid resin are required. Additionally, the length and width of the SMC sheets and the number of fiber rovings used in the SMC line must be defined upfront. For the length and width of the sheets the dimensions of the mold minus 1 inch turned out to be appropriate for molds of the size of 1 to 2 feet. This allows to place the sheets in the mold cavity although they become slightly wider in the compaction zone of the SMC line while the gaps between SMC sheets and the edge of the mold cavity are not too big.

The number of rovings has to be chosen depending on the width of the sheets to achieve a homogeneous fiber distribution throughout the whole width of the SMC sheet. For a sheet width of 10 in, at least 6 rovings are required for a uniform fiber distribution. A thin SMC sheet can be made and hold against the light to check the distribution of the fibers. Clear lines with lower fiber content (i.e. higher transparency) in the SMC direction reveal a too small number of fiber rovings.

The above mentioned input parameters are filled in the grey fields of the set-up spreadsheet which will then automatically calculate the necessary height of the doctor blades, the cutting speed set-up value and the belt speed set-up value of the conveyor belt (fields with red font). Figure A.1 shows an exemplary Set-Up Spreadsheet.

Parameters of Plate/Mold:

Length	16.5	in	-->	419.1	mm
Width	11	in	-->	279.4	mm
Height	6	mm	-->	6	mm
Number of Layers	3		-->	3	Layers
Fiber Fraction	50	%	-->	0.5	
Density of Fiber	2.54	g/cm^3	-->	0.00254	g/mm^3
Density of Resin (liquid)	1.098	g/cm^3	-->	0.0010984	g/mm^3

Parameters calculated (theoretical):

Volume of Plate	-->	702579	mm^3
Volume of one Layer	-->	234193	mm^3
Density of Plate	-->	0.00153	g/mm^3
Mass of Plate	-->	1077.49	g
Mass of one Layer	-->	359.16	g
Mass of Fibers in 1 Layer	-->	179.58	g
Mass of Resin in 1 Layer	-->	179.58	g

Set-Up-Parameters at SMC-Line

Sheet width	9	in	-->	228.6	mm
Sheet length	14.5	in	-->	368.3	mm
Height of Doctor-Blade			-->	**0.97**	mm
Case 1: Keeping Fiber flow constant -> Variation in Belt Speed					
Fiber Flow			-->	3.8	g/s
Cutting Speed - Set Value			-->	**6.4**	
Belt Speed			-->	7.793	mm/s
Belt Speed - Set Value			-->	**11.4**	
Case 2: Keeping Belt Speed constant -> Variation in Cutting Speed					
Belt Speed			-->	10	mm/s
Belt Speed - Set Value			-->	**14.5**	
Fiber Flow			-->	4.876	g/s
Cutting Speed - Set Value			-->	**8.0**	

Figure A.1: Exemplary SMC Set-Up Spreadsheet.

There are two ways to set up the SMC line to obtain a certain fiber content in the SMC sheet. In case 1, the mass flow of fibers (cutting speed) is set to a certain value and the

conveyor belt speed and its set-up value at the SMC machine are calculated accordingly through the spreadsheet. In case 2, a certain conveyor belt speed is set and the mass flow and the related cutting speed set-up value are calculated correspondingly. The spreadsheet template can be used for both cases depending on which parameter the operator wants to keep constant throughout different batches.

Before using the spreadsheet, the operator always has to make sure that the right equation is used for the relation between cutting speed set-up value and fiber flow. This relation varies with the fiber type and the number of rovings, so that the equations of the spread-sheet have to be adjusted to different types and numbers of rovings. So far, the equations for 4 and 6 rovings of GF (4800 tex) and 6 rovings BF (4800 tex) have been determined. For other combinations of fiber types and number of rovings, new equations have to be established. For this purpose, the weight of chopped fibers of a constant time span can be measured for several cutting speed set-up values. These values can be displayed in an Excel-Chart together with a best fit straight line. Also, the equation of this best fit straight line can be displayed in the options menu. This equation reveals the numeric relation between fiber flow and cutting speed set-up value for the used combination of fiber type and number of rovings and has to be used in the spreadsheet. Figure A.2 displays such a relation between fiber flow and cutting speed as well as its numeric equation.

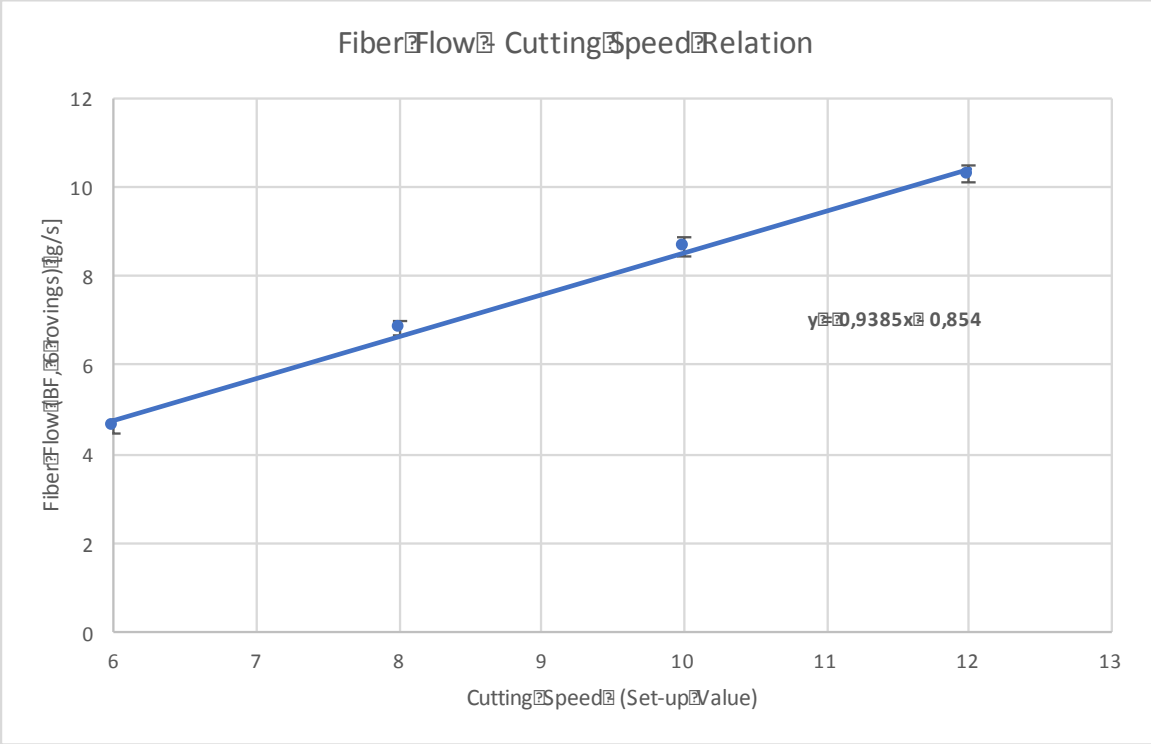

Figure A.2: Exemplary relation between fiber flow and the cutting speed set-up value for 6 rovings of BF (4800 tex).

A similar chart exists for the relation between set-up value of the conveyor belt-speed and the actual conveyor belt speed. However, this relation cannot be changed through different set-ups. Therefore, no changes in the equations for the belt speed have to be made.

After filling out the spreadsheet with the correct equation for the cutting speed and all the input data, it can be printed to easily set-up the SMC line at the shop floor. After the SMC run, the printed spreadsheet can be stuck onto the final compression molded SMC plate and serve as a label allow identification of the resulted composites.

A.3 Calibration of the SMC line

After calculating the parameters with the set-up spreadsheet, the calibration of the SMC line can be started. However, there are far more parameters to set up at the SMC line than

the three calculated parameters of the spreadsheet. All the parameters and how to set them up are described in this section.

Roving Set-Up

The fiber rovings are guided from the spools to the chopper through black pipes. It is important to distribute the rovings uniformly and symmetric on the pipes within the whole width of the attempted sheet width since this influences the distribution of the fibers within the composite. An exemplary distribution for 6 fiber rovings is shown in Figure A.3.

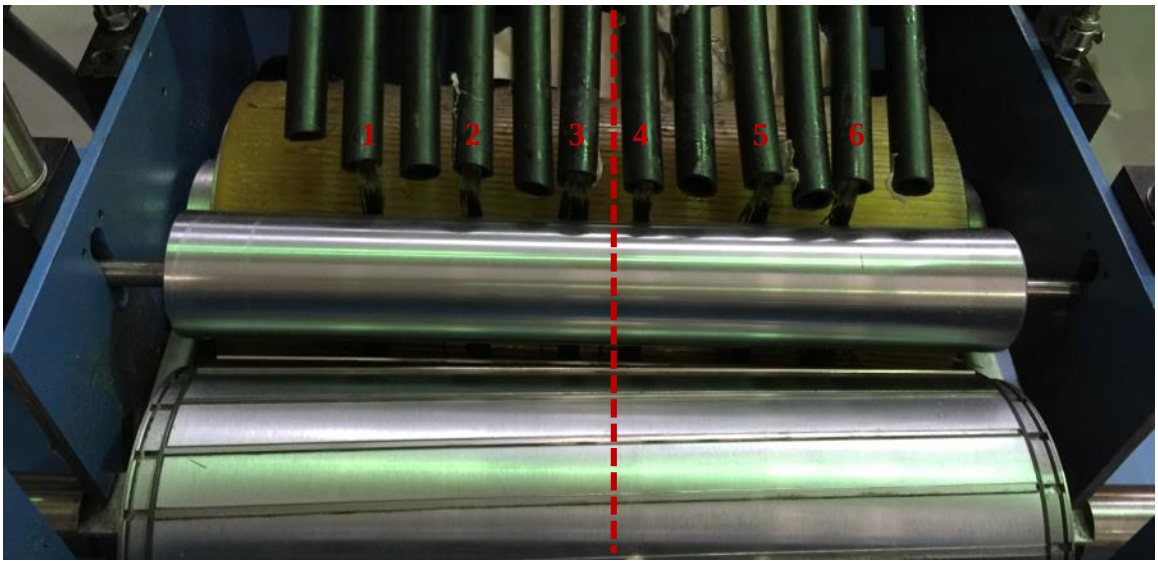

Figure A.3: Uniform roving distribution on the black supply pipes for 6 rovings set-up.

Usually, the same roving set-up can be used for the most runs. However, if a change in the number, distribution or type of fiber rovings is necessary, there are multiple ways to implement this change. The simplest way is to cut the old rovings at the shelf, turn off cutting and feed pressure at the SMC line and pull the rest of the rovings out of the pipes. Then, take the new rovings at the shelf and push them through the correct pipes bit by bit

until they reach the chopper. There, the rovings have to be threaded first between the steel and the yellow rubber roller and secondly between chopper and yellow rubber roller. Afterwards, feed and cutting pressure can be turned on again. Instead of pushing the roving by hand through the long pipes, air pressure can be used to accelerate the whole process.

If the same pipes but just a different fiber type needs to be used, the easiest way to carry out the change is to tape the beginning of the new rovings onto the old rovings at the shelf. Then, cut only the old rovings behind the tape and run the cutter until the beginnings of the new rovings were pulled completely through the pipes. Figure A.4 shows this technique for the change from basalt fiber (dark brown) to glass fiber (white).

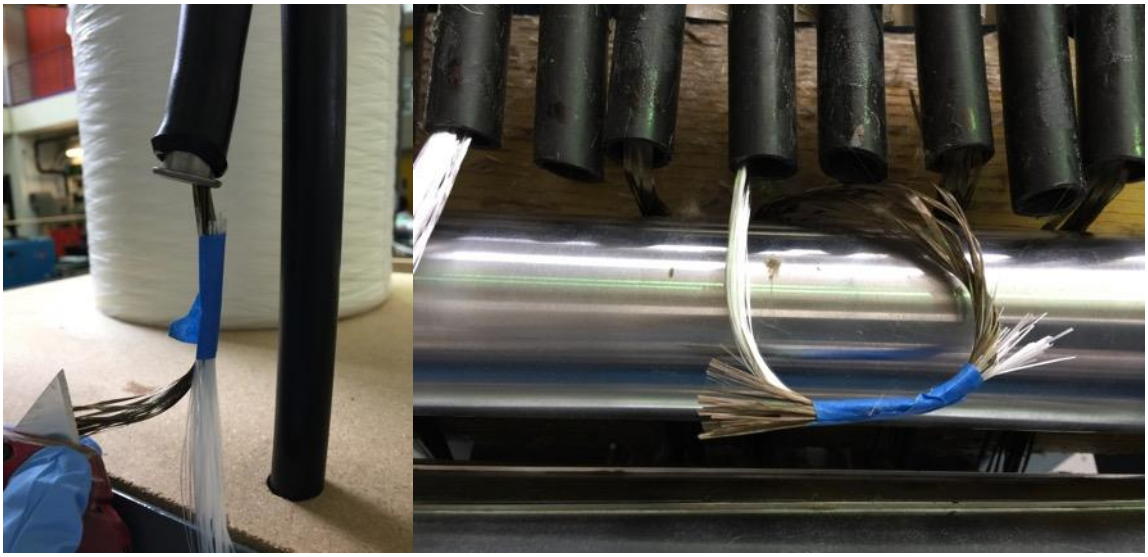

Figure A.4: Change of fiber rovings using tape and the rotating cutter of the SMC line

During the set-up of the rovings, attention should be paid to possible traps at the shelf where the rovings could get tangled up or stuck during the SMC run.

Set-Up of the Fiber Guiding Sheets

Before setting up the guiding sheets, the whole SMC line should be turned off, so that the cutter will not start running. The guiding sheets affect the width of the chopped fibers on the carrier film. Each of them is fixed with two magnets on both sides, so that they can be moved linearly up and down and from and to the center of the conveyor belt as well as pivoted. First, the upper ends with the magnets should be pushed towards the outside to avoid that chopped fibers can get to the wrong side of the guiding sheets. While doing this, attention is required to not touch the sharp cutting blades. Second, the sheets are pulled down with both hands until the lower edge is about 3 to 5 mm above the carrier film. Then, the lower edges of both guiding sheets are carefully pivoted towards the center of the conveyor belt until they have the same distance as the sheet width defined on the set-up spreadsheet. Also, they should be arranged symmetrically to the center of the conveyor belt. As a practical instrument two large rulers can be laid between conveyor belt and guiding sheets to measure their distance and their positions relative to the conveyor belt as well as to make sure that they are parallel to each other.

Set-Up of the Resin Reservoir and the Doctor Blades

After making sure that the fibers are dropped in the right space, the width and position of the resin reservoir must be adjusted accordingly to that. It works in the exact same way for both reservoirs, the upper and the lower one. On both sides of the black resin reservoir boxes, an axis protrudes with a hand screw on top of it. Loosening these screws allows to move the plastic sheets inside the reservoirs until they have the same distance as the sheet width defined on the Set-Up Spreadsheet and until they are arranged symmetrically within

the reservoir boxes. Again, a large ruler can be used as a tool for this. Afterwards, the hand screws are tightened again. The width and position of the continuous resin film (upper and lower) are hereby set.

The thickness of the resin film is set by the height of the doctor blades. As this parameter has a significant influence on the amount of resin and consequently on the fiber fraction, it has to be set up very precisely. The height of each doctor blade (upper and lower) is justified by two screws, one on each side. Turning the screw clockwise means pushing up the doctor blade, counterclockwise means to let it down. First, it is let completely down. Second, the electronic indicators are set in the according mounts and fastened with the small hand screws. Then, the small levers at the doctor blades are switched, so that the connection pins jump out and touch the electronic indicators. Subsequently, the indicators are turned on and set to zero. Finally, the screws are turned clockwise until the indicators show the correct height as calculated with the set-up spreadsheet. Figure A.5 shows the set-up of the doctorblade system.

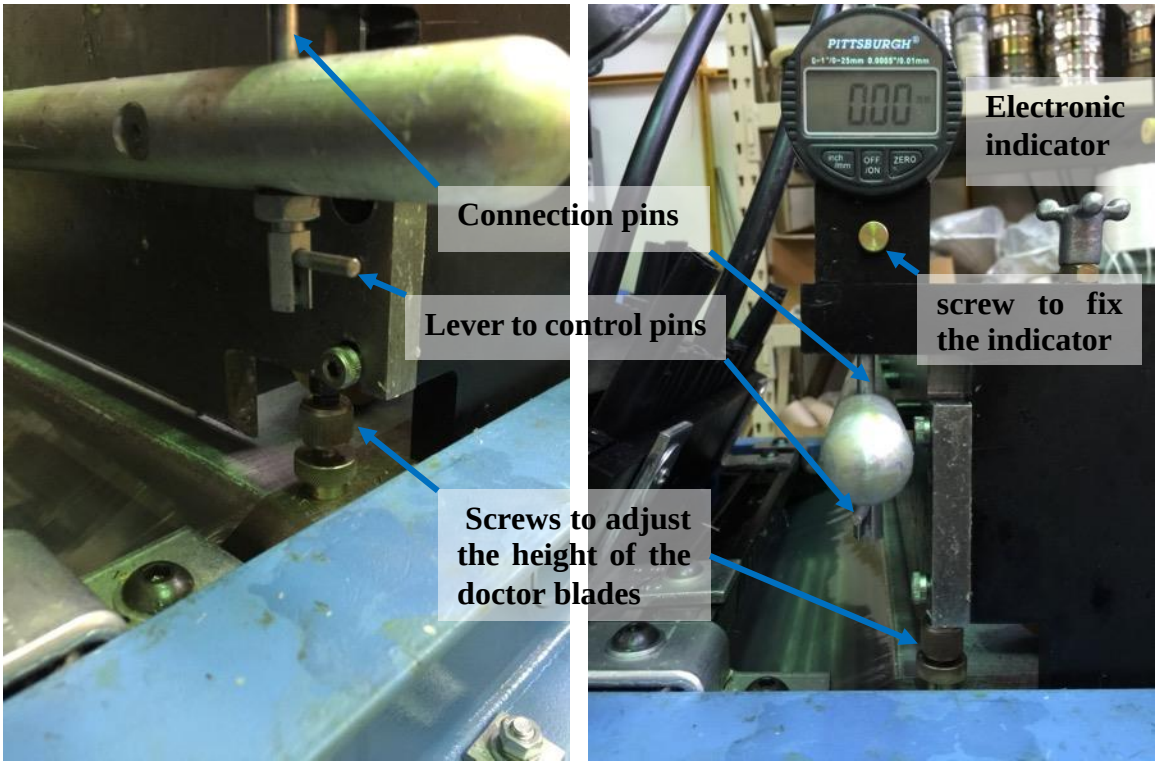

Figure A.5: Set-up of the doctor blade system with the tools needed for its calibration

Set-Up of Cutting Speed and Belt Speed

The cutting and belt speeds are set up through the panels. Pushing the arrows allows to increase or decrease the values to the calculated values of the Set-Up Spreadsheet.

Set-Up of Cutting and Feed Pressure

In general, the cutting and feed pressure should be kept as high as possible to make sure the rovings get chopped to the correct length. However, if the pressures are too high the electric motor is too weak to rotate the whole cutting system at the desired speed or to move it at all. Therefore, optimum pressures have to be found at which the system can run at the correct speed and still cut all fibers. However, this optimum varies with different cutting

speeds, number and types of rovings, which is why short tests with different pressures have to be run for new roving and speed combinations before the actual SMC run is performed. Also, before each run it should not only be checked whether the correct pressure value is set, but also whether it is turned on. This rule applies equally to all pressure set-ups.

Set-Up of Upper and Lower Belt Tension

The pressure of the upper and lower conveyor belt should be set to 60 psi. Lower pressures can cause sporadic stops of the belts, since the friction between belts and drive shafts becomes too low. Using higher pressures sets the belts under very high tension, leading to very high compaction in the compaction zone though using only small compaction parameters. Keeping the conveyor belt at 60 psi keeps the belt running all the time while it is still possible to make fine adjustments in the compaction zone.

Set-Up of Compaction Zone

The compaction zone can be set up using the three black hand wheels. One of these transversal adjustments is shown in Figure A.6. In general, the compaction should be gradually increased from the first hand wheel to the last one. At the first transversal adjustment, a small gap between the upper and lower compaction rollers is required for high fiber contents to allow the thick compound to enter the compaction zone without getting destroyed. For the second and third adjustment, it is recommended to use the highest possible compaction (move upper and lower compaction rollers together) to achieve maximum fiber wetting and to push out trapped air. However, resin squeeze-out limits the maximum applicable compaction. Thus, for every combination of fiber (type,

content, etc.) and resin (viscosity, etc.) the right compaction parameters have to be determined via trial and error.

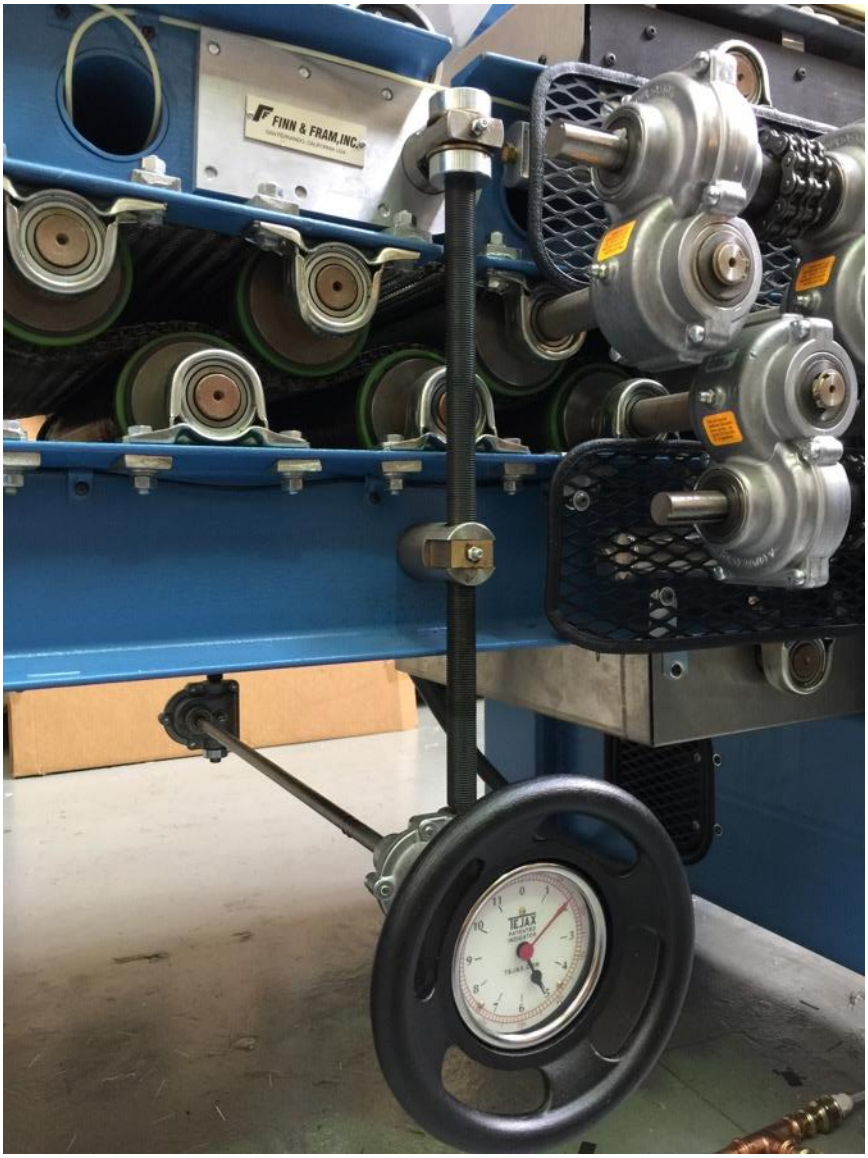

Figure A.6: One of three hand wheels for the adjustment of the compaction zone.

Set-Up of the Winder and the Winder Pressure

First, the white cardboard roll must be put completely onto the winder rod. Second, the end of the cardboard roll has to be centered and fixed with the intended aluminum part. Then,

the ends of the carrier films which are hanging out of the compaction zone can be taped onto the carton roll using three pieces of tape for the center and at both sides. Turning the big round plate of the winder clockwise puts the carrier films under initial tension.

Setting the winder pressure to a certain value and turning it on will keep the carrier film under tension while running the SMC line. A small pressure of 10 to 20 psi is sufficient for most cases and avoids too much pressure on the winded sheets and possible resin squeeze-out. If resin squeeze-out is not an existing problem, the winder pressure can be increased.

Set-Up of Carrier Films and Film Tension

For the Set-Up of the upper and lower carrier film the most important thing is that they are aligned with the conveyor belts. Most of the time they stay aligned and variances occur very rarely or only after a new roll of carrier film had been installed. In these cases, the whole roll of the carrier film must be moved in the respective direction to align it again. Then, the conveyor belt should be run for a while to make sure that the film is aligned throughout the whole SMC line. The pressure for the upper and lower film tension can be kept constant at 30 psi.

A.4 Preparation of the Resin

The preparation of the resin is not directly related to the calibration of the SMC line. However, for successful SMC runs it is important to mention that the preparation of the resin should not be started before the SMC line is completely set up. The set-up of the SMC line takes a considerable amount of time. Unexpected needs like additional cleaning, repairs or maintenance may occur and extend the set-up time. If the resin has been already

prepared before the SMC set-up is completed, it is possible that the resin will cure before the SMC line is ready to be run or the set-up is made hectically and sloppy to ensure that the gelling of the resin has not started.

A.5 Running the SMC Line

After the resin is prepared, all SMC parameters are checked one last time to make sure nothing changed while the resin was prepared. If any parameter changed, it can be set up correctly again. Otherwise, the pouring of the resin in the lower reservoir can be started directly. Afterwards, the SMC Line is ready to start. First, the conveyor belt is turned on through pushing the green start button. When the lower resin film reaches the first mark (green), the second half of the resin must be poured to the upper reservoir, so that upper and lower resin film reach the compaction zone at the same time. While one operator is pouring the upper resin, the second operator has to start the cutter as soon as the lower resin film reaches the second mark (red). Both markers are displayed in Figure A.7. Sometimes, the start of the cutter has to be supported manually to overcome the initial friction through turning the shaft of the yellow rubber roller by hand. Until all the resin is gone, the operators just have to watch for any issues in the SMC line and in case stop it and resolve the problem. After all the resin is gone, the cutter has to be stopped, but the conveyor belt keeps running until all material is collected on the winder.

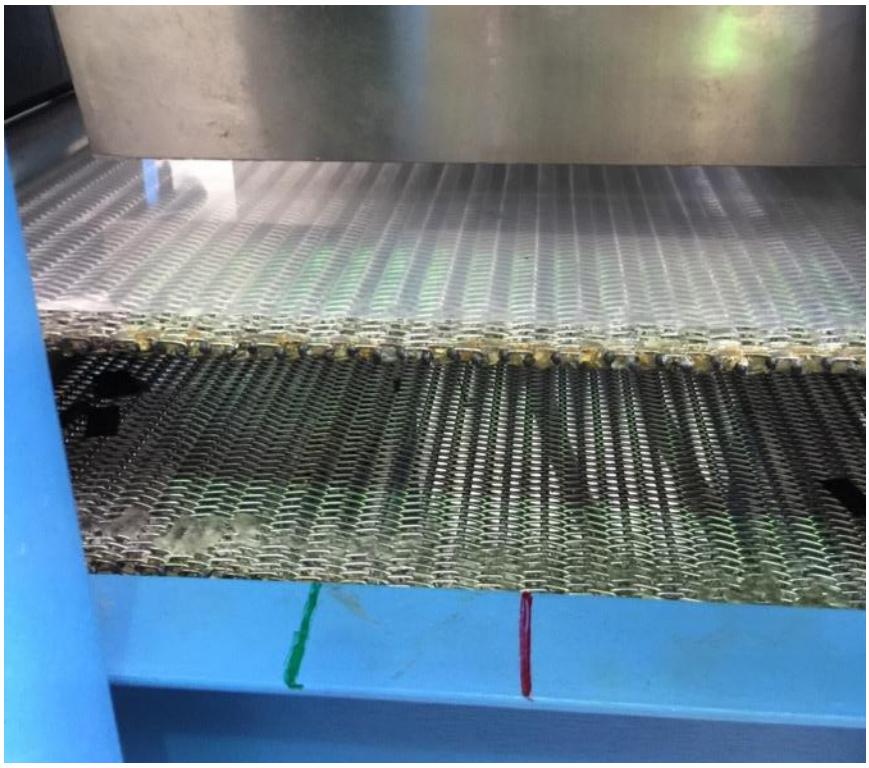

Figure A.7: Markers to start pooring the resin in the upper doctor box (green) and to start the cutter (red).

A.6 Cleaning the SMC line and the Used Tools

After the SMC run is finished, it is important to start immediately with a thorough cleaning of the SMC line. All parts of the line as well as all supporting tools which came in contact with resin have to be cleaned before the resin gets cured and stuck within the line. For this purpose, all the dirty parts can be removed and solvents such as acetone or isopropanol can be used to remove all the resin. Besides the resin, chopped fibers on, in and around the SMC line have to be cleaned up using a vacuum cleaner. This includes the cutter as well as the yellow rubber roller. The cleaning part is the last part of a SMC run. However, it has to be considered as the first necessary step for the preparation of the next successful SMC run.

APPENDIX B. PROCESS INTEGRATION OF CNC FIBER COATING IN THE SHEET MOLDING COMPOUNDS PRODUCTION LINE

B.1 Reasons for coating fibers with cellulose nanocrystals

In a previous study, it was shown that the coating of glass fibers with small amounts of cellulose nanocrystals (CNC) increases the interfacial shear strength between fiber and matrix significantly [41]. As a result of the increased interfacial adhesion and stress transfer ability, the mechanical properties are increasing as well without any weight penalty. Therefore, the coating of fibers with CNC is an opportunity to improve the properties of lightweight SMC composites significantly.

B.2 Process requirements

A small amount of water (2 %) can increase the mechanical properties of epoxy system composites, whereas larger amounts lead to the opposite effect [57]. Therefore, a physical requirement is that the fibers are dried when they get in contact with the epoxy resin. Besides this physical aspect of the process, economic aspects have to be considered as far as the automotive industry is concerned. Due to the pressure to keep the cost low and the waste to a minimum in the automotive sector, the coating process of the fibers should be time and cost efficient. Furthermore, the process must be scalable to fulfill the high-volume requirements of the automotive industry. The process in the above-mentioned fundamental study [41] was the following: chopped fiber rovings were immersed in an aqueous CNC suspension for two minutes and then they were spread on covered trays and dried for 24 h

at ambient temperature under ventilation. Adopting this lab-scale coating method for high volume production in automotive industry would have several disadvantages regarding time and cost aspects. The long drying time would lead to a long throughput time. Also, huge storage areas for the 24 h drying process of the fibers would be needed causing high storage cost. Furthermore, the usual SMC process could not be used. Common machines which chop the fibers and drop them immediately on the lower resin film could not be used since the fibers would have been already chopped, a requirement of the lab-scale coating method. Therefore, cost-intensive customized machines which can spread the coated chopped fibers on the resin film would have to be designed. Additionally, a lot of waste processes occur through the extra handling of the fibers. Consequently, a totally different approach was investigated in this study which is described in this appendix.

B.3 Development of a scalable coating process

The approach followed in this study tried to avoid all the disadvantages of the batch process using the principle of process integration. The idea was to integrate the coating and drying of the fibers as a continuous process between the storage of the roving spools and the entering point of the fibers in the SMC machine (Compare chapter 2.2.2). The electric motor of the fiber cutter in the SMC machine was used to pull the fibers continuously through a bath which contained the aqueous CNC solution followed by a drying apparat before they are finally cut and spread on the resin in the SMC machine. The basic principle was developed stepwise through several prototypes which are described in the following.

B.3.1 Coating Process Integration – Prototype 1

The principle of the first coating apparatus prototype is shown in Figure B.1. The fiber rovings from the roving spools were pulled through the whole coating appliance by the rotation of the cutter in the SMC machine. First, the rovings were led through a bath of aqueous CNC suspension. A pair of rotatable rods forced the fiber rovings to immerse completely into the suspension. Afterwards, the rovings were directed to a drying box (dimensions: 12x12x12 in^3). This box had one opened and five closed sides. Four Wagner HT1000 heat guns, each with a power of 1200 W, were installed on the sides of the box to blow hot air into it. Five rotatable pairs of rods guided the rovings 10 times from each side to the other to achieve a certain time period within the hot drying box. Finally, the fibers were pulled further until they reached the cutter and got chopped onto the lower resin layer to continue with the usual SMC process.

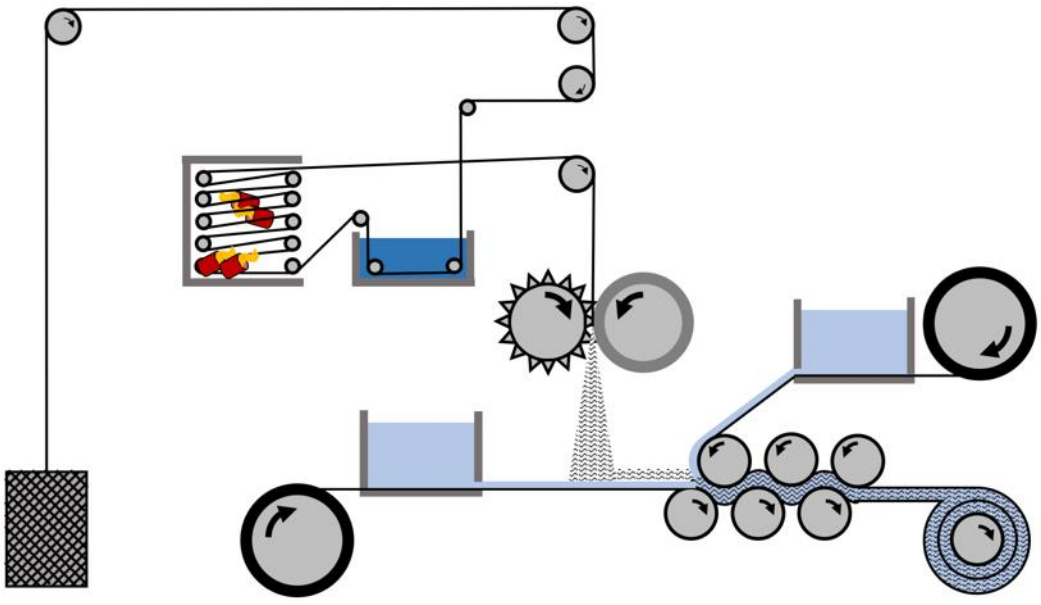

Figure B.1: Principle of the coating process integration in SMC line (Prototype 1).

However, the fibers were still noticeable wet when they came out of the heat box. The timeframe, the power of the heat guns or both were not sufficient to dry the fibers. It was visible that the chopped fibers of each roving stuck together because of the water they still contained. As a result, they did not disperse well on the resin layer after they got chopped. Because of the damage the water would cause to the epoxy matrix and because of the poor fiber spreading, this set up could not be used to manufacture usable SMC plates. Process improvements regarding timeframe, power and mode of heat transfer had to be made through the development of a second prototype.

B.3.2 Coating Process Integration – Prototype 2

The second prototype was a major modification of prototype 1. The initial bath for the aqueous CNC suspension was replaced by a second box. This box had the same dimensions as the first box (12x12x12 in^3) and had 2 open sides. It was attached to the first box (final dimensions 24x12x12 in^3) and had an integrated bath at the bottom which also contained the aqueous CNC suspension. The advantage of integrating the bath into the box is the reduction of the total area. In addition to the integrated bath, the second box contained three pairs of steel rollers which had basically two functions: The first one was to press the water out of the fibers through the weight of the rollers and the extra pressure which was applied on the solid axes of the rollers through cable ties. The second one was to conduct the heat to the fibers. The heat sources in the second box were six heat guns same as those used in the first box. Two of them were placed on the top of the box and two were placed on each of the closed sides. With the four heat guns of the first box, a total of 10 heat guns

was installed, providing a total power of 12 kW. The whole structure of prototype 2 is shown in Figure B.2.

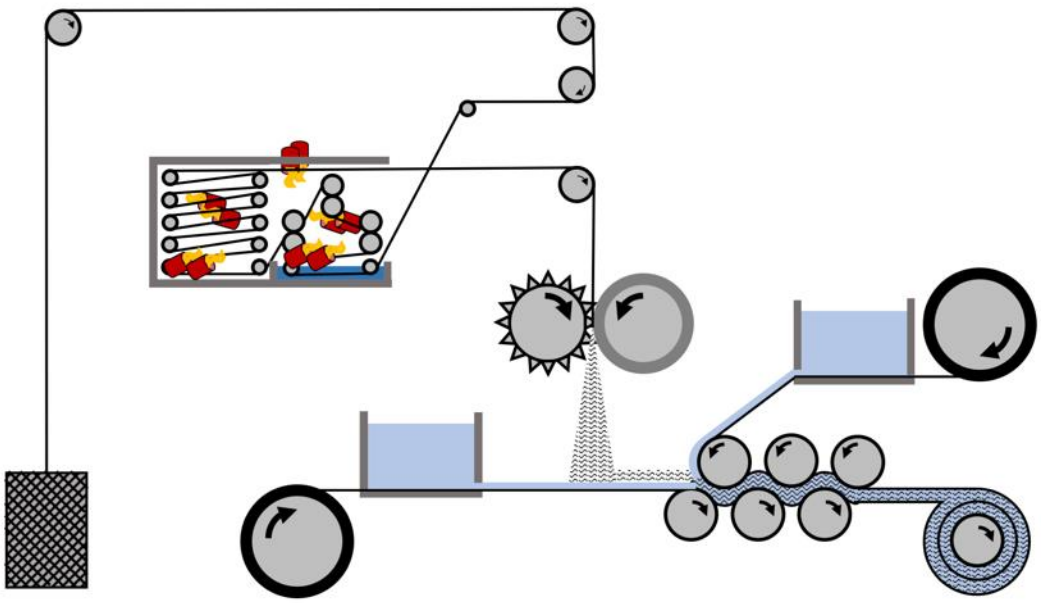

Figure B.2: Principle of the coating process integration in SMC line (Prototype 2).

The heat guns were turned on 10 minutes prior to the SMC run to heat up the three steel roller pairs. Subsequently, the process was started. First, the fibers were pulled through the bath. Then, they reached the three pairs of rollers, where they were squeezed out and heated up simultaneously. It was visible that water got squeezed out from the fiber rovings when the rovings were going through each roller set. Also, it was visible that the squeezed water evaporated on the hot surface of the rollers immediately. After the fibers had passed the three roller pairs, they went into the first box for further drying, before they were guided through the top of the second box towards the cutter of the SMC machine. Reaching the cutter, the fibers were much dryer compared to fibers entering the SMC line using the approach of prototype 1, but it was perceptible that the fiber rovings were still too wet for

making composites. However, it was observed that the fibers were significantly dryer after passing through the three pairs of squeeze-out rollers compared to when they reached the cutter. This lead to the conclusion that the fibers absorbed water in box 1. The most probable cause for this effect is that there was a high concentration of steam in box 1 since it could not escape in any direction, because of the closed sides. Based on that finding, a third prototype was developed.

B.3.3 Coating Process Integration – Prototype 3

As box 1 did rather show a negative effect on drying the fibers due to keeping the vapor inside the system it was removed for the third prototype. Only box 2 was used. As it had two open sides, the vapor could escape very easily. A disadvantage of prototype 3 was that the available time for drying was reduced compared to prototype 2 since the speed of the fibers was the same but the distance travelled was reduced. To compensate for this, extra heating power was applied on prototype 3. A total of 12 heat guns were installed to provide enough heat to completely evaporate the whole water in the short amount of time while the fibers went through the box. The whole structure of prototype 3 is shown in Figure B.3.

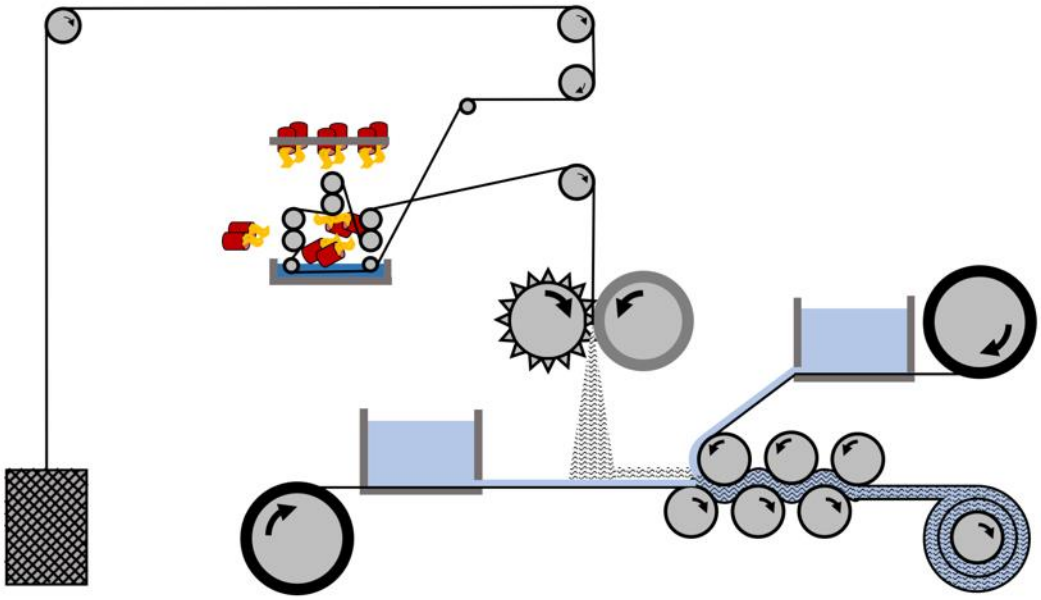

Figure B.3: Principle of coating process integration in SMC line (Prototype 3).

The procedure was basically the same as the one in prototype 2. The heat guns were turned on 10 minutes prior to the SMC run to heat up the rollers. Then, the fiber rovings were pulled through the bath and the three roller pairs, before they entered the cutter of the SMC line. The fiber rovings felt completely dry when they came out of the box. Therefore, prototype 3 was integrated to the SMC line to make compounds. However, the chopped rovings although seemed to be drier still did not disperse very well. Further investigation revealed, that the rovings were completely dry on the surface, but still wet in the interior which made the fibers stick together and not disperse very well. **Fehler! Verweisquelle konnte nicht gefunden werden.** shows the continuous SMC material coming out of the SMC machine. It is visible that the fibers of a roving stuck together as bundles.

Figure B.4: Wet fibers stuck together in continuous SMC plate coming out of the SMC line.

APPENDIX C. PUBLICATIONS BASED ON THIS RESEARCH WORK

Baaij, F.; Asadi, A.; Mainka, H.; Rademacher, M.; Thompson, J.; Moon, R. J.; Kalaitzidou, K.: Feasibility study of using basalt fibers in sheet molding compounds (SMC); Society for the Advancement of Material and Process Engineering Conference, Seattle, 2017.

Asadi, A.; Baaij, F.; Kalaitzidou, K.: Basalt fibers as a sustainable and cost-effective alternative to glass fibers in sheet molding compound (SMC). Composites Part B Engineering. Ausgabe 123, S. 210-218, 2017.

Asadi, A.; Baaij, F.; Moon, R. J.; Kalaitzidou, K.: Cellulose nanomaterials and basalt fibers: an approach towards light-weighting in sheet moulding compounds; 21st International Conference on Composite Materials, Xi'an, 2017.

Asadi, A.; Baaij, F.; Mainka, H.; Rademacher, M.; Thompson, J.; Moon, R. J.; Kalaitzidou, K.: Cellulose Nanocrystals and Basalt Fibers: An Approach toward Lightweight Sheet Molding Compounds; 32nd ASC Technical Conference, West Lafayette, 2017.

Asadi, A.; Baaij, F.; Moon, R. J.; Kalaitzidou, K.: Cellulose Nanocrystals For Lightweight Sheet Molding Compounds Composites; 17th Automotive Composite Conference & Exhibition, Novi, 2017.

REFERENCES

1. Lutsey, N.P., *Review of technical literature and trends related to automobile mass-reduction technology*. Institute of Transportation Studies, 2010.

2. An, F. and A. Sauer, *Comparison of passenger vehicle fuel economy and greenhouse gas emission standards around the world.* Pew Center on Global Climate Change, 2004. **25**.

3. Mallick, P.K., *Materials, design and manufacturing for lightweight vehicles*. 2010: Elsevier.

4. Tucker, R., *Trends in automotive lightweighting.* Metal Finishing, 2013. **111**(2): p. 23-25.

5. Cheah, L. and J. Heywood, *Meeting US passenger vehicle fuel economy standards in 2016 and beyond.* Energy Policy, 2011. **39**(1): p. 454-466.

6. Fisher, M., J. Kolb, and S. Cole. *Enhancing future automotive safety with plastics*. in *The 20th International Technical Conference on the Enhanced Safety of Vehicles (ESV), Paper*. 2006.

7. Stewart, R., *Lightweighting the automotive market.* Reinforced plastics, 2009. **53**(2): p. 14-21.

8. Lyu, M.-Y. and T.G. Choi, *Research trends in polymer materials for use in lightweight vehicles.* International journal of precision engineering and manufacturing, 2015. **16**(1): p. 213-220.

9. Brooke, L. and H. Evans, *Lighten up!* Automotive Engineering International, 2009. **117**(3).

10. Bjelkengren, C., *The impact of mass decompounding on assessing the value of vehicle lightweighting*. 2008, Massachusetts Institute of Technology.

11. Mallick, P.K., *Fiber-reinforced composites: materials, manufacturing, and design*. 2007: CRC press.

12. Takahashi, M., *Development of high strength steels for automobiles.* Shinnittetsu Giho, 2003: p. 2-6.

13. Verbrugge, M., et al. *Mass decompounding and vehicle lightweighting*. in *Materials Science Forum*. 2009. Trans Tech Publ.

14. Chawla, N. and K.K. Chawla, *Metal Matrix Composites*. 2013: Springer Science & Business Media.

15. Mahajan, G. and V. Aher, *Composite material: A review over current development and automotive application.* International Journal of Scientific and Research Publications, 2012. **2**(11): p. 1-5.

16. Wang, R.-M., S.-R. Zheng, and Y.G. Zheng, *Polymer matrix composites and technology*. 2011: Elsevier.

17. Mallick, P. and S. Newman, *Composite materials technology*. 1990: Hanser Munich etc.

18. Rosato, D.V. and D.V. Rosato, *Reinforced plastics handbook*. 2004: Elsevier.

19. Lu, J., S. Khot, and R.P. Wool, *New sheet molding compound resins from soybean oil. I. Synthesis and characterization.* Polymer, 2005. **46**(1): p. 71-80.

20. Boylan, S. and J.M. Castro, *Effect of reinforcement type and length on physical properties, surface quality, and cycle time for sheet molding compound (SMC) compression molded parts.* Journal of applied polymer science, 2003. **90**(9): p. 2557-2571.

21. Hapuarachchi, T., et al., *Fire retardancy of natural fibre reinforced sheet moulding compound.* Applied Composite Materials, 2007. **14**(4): p. 251-264.

22. Advani, S.G. and K.-T. Hsiao, *Manufacturing techniques for polymer matrix composites (PMCs)*. 2012: Elsevier.

23. Wulfsberg, J., et al., *Combination of carbon fibre sheet moulding compound and prepreg compression moulding in aerospace industry.* Procedia Engineering, 2014. **81**: p. 1601-1607.

24. Orgéas, L. and P.J. Dumont, *Sheet molding compounds.* Wiley Encyclopedia of composites, 2012.

25. Wang, J., S.Q. Shi, and K. Liang, *Comparative life-cycle assessment of sheet molding compound reinforced by natural fiber vs. glass fiber*. Journal of Agricultural Science and Technology. B, 2013. **3**(7B): p. 493.

26. Sarasini, F., et al., *Effect of basalt fiber hybridization on the impact behavior under low impact velocity of glass/basalt woven fabric/epoxy resin composites.* Composites Part A: Applied Science and Manufacturing, 2013. **47**: p. 109-123.

27. Dhand, V., et al., *A short review on basalt fiber reinforced polymer composites.* Composites Part B: Engineering, 2015. **73**: p. 166-180.

28. Lopresto, V., C. Leone, and I. De Iorio, *Mechanical characterisation of basalt fibre reinforced plastic.* Composites Part B: Engineering, 2011. **42**(4): p. 717-723.

29. Singha, K., *A short review on basalt fiber.* International Journal of Textile Science, 2012. **1**(4): p. 19-28.

30. Wei, B., H. Cao, and S. Song, *Tensile behavior contrast of basalt and glass fibers after chemical treatment.* Materials & Design, 2010. **31**(9): p. 4244-4250.

31. Mingchao, W., et al., *Chemical durability and mechanical properties of alkali-proof basalt fiber and its reinforced epoxy composites.* Journal of Reinforced Plastics and Composites, 2008. **27**(4): p. 393-407.

32. Černý, M., et al., *Partially pyrolyzed composites with basalt fibres – Mechanical properties at laboratory and elevated temperatures.* Composites Part A: Applied Science and Manufacturing, 2009. **40**(10): p. 1650-1659.

33. Moon, R.J., et al., *Cellulose nanomaterials review: structure, properties and nanocomposites.* Chemical Society Reviews, 2011. **40**(7): p. 3941-3994.

34. Moon, R.J., G.T. Schueneman, and J. Simonsen, *Overview of Cellulose Nanomaterials, Their Capabilities and Applications.* JOM, 2016. **68**(9): p. 2383-2394.

35. Brinchi, L., et al., *Production of nanocrystalline cellulose from lignocellulosic biomass: Technology and applications.* Carbohydrate Polymers, 2013. **94**(1): p. 154-169.

36. Pedrazzoli, D., A. Pegoretti, and K. Kalaitzidou, *Synergistic effect of exfoliated graphite nanoplatelets and short glass fiber on the mechanical and interfacial properties of epoxy composites.* Composites Science and Technology, 2014. **98**: p. 15-21.

37. Dorigato, A., S. Morandi, and A. Pegoretti, *Effect of nanoclay addition on the fiber/matrix adhesion in epoxy/glass composites.* Journal of Composite materials, 2012. **46**(12): p. 1439-1451.

38. Pedrazzoli, D. and A. Pegoretti, *Silica nanoparticles as coupling agents for polypropylene/glass composites.* Composites Science and Technology, 2013. **76**: p. 77-83.

39. Njuguna, J., K. Pielichowski, and J.R. Alcock, *Epoxy-Based Fibre Reinforced Nanocomposites.* Advanced Engineering Materials, 2007. **9**(10): p. 835-847.

40. Asadi, A., et al., *Introducing cellulose nanocrystals in sheet molding compounds (SMC)* Composites Part A: Applied Science and Manufacturing, 2016. **88**: p. 206-215.

41. Asadi, A., et al., *Improving the interfacial and mechanical properties of short glass fiber/epoxy composites by coating the glass fibers with cellulose nanocrystals.* Express Polymer Letters, 2016. **10**(7): p. 587-597.

42. Girouard, N., et al., *Exploiting colloidal interfaces to increase dispersion, performance, and pot-life in cellulose nanocrystal/waterborne epoxy composites.* Polymer, 2015. **68**: p. 111-121.

43. Hunston, D., et al., *Test protocol for single-fiber fragmentation test-International round robin*.

44. Rich, M., et al. *Round robin assessment of the single fiber fragmentation test*. in *Procedings of the American Society for Composites 17th Technical Conference*. 2002.

45. Feih, S., et al., *Testing procedure for the single fiber fragmentation test*. 2004, Forskningscenter Risø.

46. Awal, A., et al., *Interfacial studies of natural fibre/polypropylene composites using single fibre fragmentation test (SFFT).* Composites Part A: Applied Science and Manufacturing, 2011. **42**(1): p. 50-56.

47. Kelley, A. and W. Tyson, *Tensile properties of fiber-reinforced metals.* Journal of Mechanical and Physical Solids, 1965. **13**: p. 329-350.

48. Klein, C.A., *Characteristic strength, Weibull modulus, and failure probability of fused silica glass.* Optical Engineering, 2009. **48**(11): p. 113401-113401-10.

49. Yang, D., et al. *Measuring and modeling the cure-dependent rubbery moduli of epoxy molding compound*. in *Thermal, Mechanical and Multi-Physics Simulation and Experiments in Micro-Electronics and Micro-Systems, 2005. EuroSimE 2005. Proceedings of the 6th International Conference on*. 2005. IEEE.

50. Mallik, P.K., *Fiber-reinforced composites: materials, manufacturing and design*. 3 ed. 2007, Florida, USA: CRC Press, Taylor & Francis Group.

51. Gibson, R.F., *A review of recent research on mechanics of multifunctional composite materials and structures.* Composite Structures, 2010. **92**(12): p. 2793-2810.

52. Asadi, A., et al., *Basalt fibers as a sustainable and cost-effective alternative to glass fibers in sheet molding compound (SMC).* Composites Part B: Engineering, 2017. **123**: p. 210-218.

53. Asadi, A., et al., *Lightweight sheet molding compound (SMC) composites containing cellulose nanocrystals.* Composite Structures, 2017. **160**: p. 211-219.

54. Madhukar, M.S. and L.T. Drzal, *Fiber-matrix adhesion and its effect on composite mechanical properties: II. Longitudinal (0) and transverse (90) tensile and flexure behavior of graphite/epoxy composites.* Journal of Composite Materials, 1991. **25**(8): p. 958-991.

55. Gao, S.-L. and E. Mäder, *Characterisation of interphase nanoscale property variations in glass fibre reinforced polypropylene and epoxy resin composites.* Composites Part A: Applied Science and Manufacturing, 2002. **33**(4): p. 559-576.

56. Gao, S.L., E. Mäder, and R. Plonka, *Nanocomposite coatings for healing surface defects of glass fibers and improving interfacial adhesion.* Composites Science and Technology, 2008. **68**(14): p. 2892-2901.

57. Wu, L., S.V. Hoa, and M.T. Ton-That, *Effects of water on the curing and properties of epoxy adhesive used for bonding FRP composite sheet to concrete.* Journal of applied polymer science, 2004. **92**(4): p. 2261-2268.